

# UC San Diego

## UC San Diego Electronic Theses and Dissertations

### Title

The effects of pacing location on regional activation using epicardial electrical mapping

### Permalink

<https://escholarship.org/uc/item/0mr620rr>

### Author

Nguyen, Tammy N.

### Publication Date

2010

Peer reviewed|Thesis/dissertation

UNIVERSITY OF CALIFORNIA, SAN DIEGO

**THE EFFECTS OF PACING LOCATION ON  
REGIONAL ACTIVATION USING EPICARDIAL  
ELECTRICAL MAPPING**

A Thesis submitted in partial satisfaction of the requirements  
for the degree Master of Science

in

Bioengineering

by

Tammy N. Nguyen

Committee in charge:

Professor Jeffrey Omens, Chair  
Professor Andrew McCulloch, Co-Chair  
Professor Francisco Villarreal  
Professor Karen Christman

2010

Copyright

Tammy N. Nguyen, 2010

All rights reserved.

The Thesis of Tammy N. Nguyen is approved, and it is  
acceptable in quality and form for publication on  
microfilm and electronically:

---

---

---

Co-Chair

---

Chair

University of California, San Diego

2010

# TABLE OF CONTENTS

Signature Page .....	iii
Table of Contents .....	iv
List of Figures .....	vi
List of Tables .....	ix
Abstract .....	x
Chapter 1: Background .....	1
1.1 Cardiac Physiology .....	1
1.1.1 Cardiac Anatomy .....	1
1.1.2 Cardiac Electrophysiology .....	4
1.2 Heart Disease and Congestive Heart Failure .....	5
1.3 Cardiac Resynchronization Therapy .....	8
1.4 Clinical Significance .....	11
1.5 Local Electrogram Signals .....	11
1.6 Isochronal Mapping .....	12
1.7 Project Aims .....	12
Chapter 2: Materials and Methods .....	14
2.1 Surgical Preparation and Pacing Protocol .....	14
2.2 Study Design .....	16
2.3 Experimental Measurements and Data Acquisition .....	18
2.3.1 Hemodynamics .....	18
2.3.2 Electrical Activation Recording .....	19
2.4 Determination of the Local Activation Sequence .....	24
2.5 Converting Unipolar Signals into Bipolar Signals .....	27
2.6 Rough Mapping of Raw Activation Times .....	29
2.7 Three-Dimensional Electrode Reconstruction .....	30

2.8	The Assumptions of Isochronal Mapping.....	31
2.9	Contour Isochronal Mapping .....	31
2.10	Geometrically Fit Epicardial Activation Maps .....	33
Chapter 3: Results .....		36
3.1	Local Electrograms and Activation Times .....	36
3.1.1	Different Modalities for Determining Activation Time.....	37
3.1.2	Positive and Negative Deflections in Local Electrograms .....	38
3.1.3	Unipolar to Bipolar Signals .....	39
3.1.4	Filtered Signals .....	40
3.1.5	Automatic Activation Time Determination Accuracy .....	42
3.2	Epicardial Excitation in Normal Heart .....	43
3.3	Epicardial Excitation in Tachycardia-Induced Heart Failure .....	44
3.4	Epicardial Excitation in Tachycardia-Induced HF with an Infarct.....	46
Chapter 4: Discussion .....		49
4.1	Local Activation Determination .....	49
4.2	Effects of Myocardial Infarcts on Local Activation .....	50
4.3	Purkinje System .....	51
4.4	Noisy Local Electrograms .....	52
4.5	Limitations .....	53
Chapter 5: Conclusions .....		55
Appendix A: Isochronal Maps .....		57
Appendix B: Isochronal Maps in <i>Continuity</i> Instruction Manual.....		82
Appendix C: Matlab Script for Determining Local Activation Times .....		95
References .....		111

# LIST OF FIGURES

Figure 1: Longitudinal cross-section of the heart showing the major components [1].....2

Figure 2: Typical fiber angle measurements are taken in successive sections from histology (open circles) and are estimated using Diffusion Tensor Magnetic Resonance Imaging (open circles) [3]. .....3

Figure 3: (Left) Graphical depiction of the placement of recording/pacing electrodes. The location of the atrial pacing electrodes is signified by a red diamond, RV apex electrodes by a green diamond, and LV endocardial/epicardial electrodes by blue diamonds. LV electrodes as 1) Anterior Base, 2) Anterior Apex (or Anterior BS), 3) Lateral, 4) Posterolateral, and 5) Coronary Sinus. (Right) Schematic diagram of a plunge electrode consisting of two insulated transformer wires inserted in a needle. ....15

Figure 4: The electrode sock consists of 24 electrodes. The grey circles represent the individual electrode positions and the red circles represent the pacing sites....20

Figure 5: Schematic representation of the electrode sock on the heart. The sock was situated around the heart, in contact with the epicardial surface. The 24 electrodes primarily sit on the LV wall of the heart. The RV did not contain any electrodes. The first anterior column of electrodes was placed along the LAD. ....21

Figure 6: The higher resolution electrode sock is comprised of 128 electrodes; 32 electrodes go into each connectors, which then connects into a 132-channel amplifier system. The electrode sock is fabricated by attaching 128-electrodes to a nylon sock. ....22

Figure 7: Steps for making epicardial local activation time maps.....25

Figure 8: Visualization verification of the calculated activation time allows for user to note and omit noise channels from map output. ....26

Figure 9: Unipolar and bipolar electrode locations; unipolar electrode positions are red, bipolar electrode positions are green, the inner diameter is the apex, and the outer diameter is the base.....28

Figure 10: Compares unipolar and bipolar signals. ....28

Figure 11: (Left) Tessellated unipolar 3D coordinates form a smooth convex surface. Triplets of adjacent unipolar signals form triangle to ensure surface is convex. ....	29
Figure 12: (Left) Activation times of epicardial pacing at the posterior coronary sinus. The earliest activated site is close to the site of pacing. As the position between the initial pacing site and the electrode increases, the activation time increases. (Right) Endocardial pacing at the posterior coronary sinus reveals shorter times than the epicardial pacing.....	30
Figure 13: 2D representation of the sock shows the electrode location represented by the bigger black circles and the pacing locations as the smaller black circles...	32
Figure 14: The resulting 2D ‘contourf’ plot fits the data input into the matrix.....	32
Figure 15: The 2D representation of the 128-electrode sock and resulting ‘contourf’ plot below.....	33
Figure 16: Flowchart describing the steps to creating an isochronal map in a problem-solving environment for multi-scale modeling. ....	34
Figure 17: Cross-sectional view of the mesh which contains 7 circumferential elements, 3 apex-to-base elements, 28 nodes, and 21 elements. ....	34
Figure 18: Sample 3D isochronal map developed in Continuity.....	35
Figure 19: Using the maximum negative slope overall and the maximum slope of the biggest peak is the only method that reveals timing difference in local activation. This confirms that this is, in fact, probably the best determining factor. ....	37
Figure 20: Negative and positive deflections from the 128-electrode sock.....	38
Figure 21: The RMS error associated with the activation times calculated from bipolar signals is high than the activation times calculated from unipolar signals. ....	39
Figure 22: Compares isochronal maps created from unipolar and bipolar electrodes....	40
Figure 23: Activation time dispersion resulting from filtering signals.....	41
Figure 24: (Top) 2-dimensional isochronal map averaged over multiple beats (Bottom) 2-dimensional isochronal map, from filtered electrode signals, averaged over multiple beats. Notice that the filtered isochronal maps results in a map with more smooth time transitions. ....	41



Figure 25: Comparing automatically calculated activation times to the golden standard. ....	42
Figure 26. The average activation time dispersion calculated from the 128-electrode sock. ....	44
Figure 27: Activation time dispersion resulting from epicardial pacing in heart with heart failure. ....	45
Figure 28: Activation time dispersion comparing biventricular and single left ventricular pacing in hearts with tachycardia-induced heart failure. ....	45
Figure 29: Epicardial activation maps in hearts with tachycardia-induced heart failure. ....	46
Figure 30: Activation time dispersion resulting from epicardial pacing in heart with heart failure and a myocardial infarct on the lateral wall. ....	47
Figure 31: Activation time dispersion comparing biventricular and single left ventricular pacing in hearts with tachycardia-induced heart failure and a myocardial infarct. ....	48
Figure 32: Isochronal maps comparing isochronal maps from ENDO and EPI posterior coronary sinus pacing reveal that endocardial pacing does not always restore synchrony better than epicardial pacing. ....	48
Figure 33: The local electrograms from the second chronic dog, Ripley, show a significant number of noisy electrode channels where 33 out of 128 electrodes (over 25%) are noisy. ....	52
Figure 34: 2D isochronal maps for the activation time determined for one beat, averaged over multiple beats, and filtered signals averaged over multiple beats. ...	53

## LIST OF TABLES

Table 1: NYHA functional classification of heart failure [11]. .....	7
Table 2: Outline of the 9 Canine studies utilizing an electrode sock array to measure epicardial activation. Yellow cells show that Dogs 7-9 are the focus on the analysis because they utilized the 128-electrode sock with the new amplifier system, yielding signals sufficient for analysis.....	17
Table 3: Runs documentation for studies with the 128-electrode sock. ....	23
Table 4: Average and maximum activation times from the sock electrodes. ....	43

ABSTRACT OF THE THESIS

**THE EFFECTS OF PACING LOCATION ON  
REGIONAL ACTIVATION USING EPICARDIAL  
ELECTRICAL MAPPING**

by

Tammy N. Nguyen

Master of Science in Bioengineering  
University of California, San Diego, 2010

Professor Jeffrey Omens, Chair

Professor Andrew McCulloch, Co-Chair

Cardiac resynchronization therapy (CRT) is an effective intervention for patients with heart failure but has a 30% non-responder rate due to a lack of predictive, mechanism-based objective criteria for patient selection. In order to fully optimize

treatment outcomes, computational models can be used to predict molecular, biomechanical, and electrophysiological mechanisms of cardiac function. The methods presented in this thesis provide an efficient technique to estimate epicardial activation time parameters and thus will prove useful as the electrophysiological input for predictive patient-specific computational model development. By developing three-dimensional isochronal maps, the sequence of ventricular activation in normal hearts, hearts with heart failure, hearts with myocardial infarcts, and hearts with ventricular dyssynchrony, such as left bundle branch block (LBBB), can be visualized. Through the use of a 128-electrode sock array, it is confirmed that the local activation time is most efficiently calculated using the time of the maximum negative derivative averaged over multiple beats. Automatic determination of the activation times proved to be comparable to manual determination (the standard). It is also seen that filtering signals causes data loss and should be avoided if possible. The calculated activation times are then input into an anatomical fit geometry of the heart to create an epicardial isochronal activation map in Continuity. Inspection of these maps reveals that endocardial pacing does not always restore more ventricular synchrony when compared to epicardial pacing, specifically in the presence of tachycardia-induced heart failure and a myocardial infarct.

# **CHAPTER 1: BACKGROUND**

## **1.1 Cardiac Physiology**

### ***1.1.1 Cardiac Anatomy***

The heart is a muscular organ that contracts regularly and continuously, pumping blood to the body and lungs. The heart is comprised of 4 chambers: the right and left atria, and the left ventricle (LV) and right ventricle (RV). The right side of the heart collects deoxygenated blood, in the right atrium, and pumps it through the right ventricle into the lungs where carbon dioxide can be exchanged with oxygen (through diffusion).

The left side of the heart collects oxygenated blood from the lungs into the left atrium and through the left ventricular out to the rest of the body. The heart valves essentially help maintain unidirectional blood flow in the heart by opening and closing based on the pressure difference across the valve. The atrioventricular (AV) valves are located between the atria and the ventricles. When the blood pressure in an atrium exceeds the pressure in the ventricle due to ventricular contraction, the AV valves between the atrium and ventricle closes blood freely flows into the pulmonary trunk from the right ventricle and into the aorta from the left ventricle.

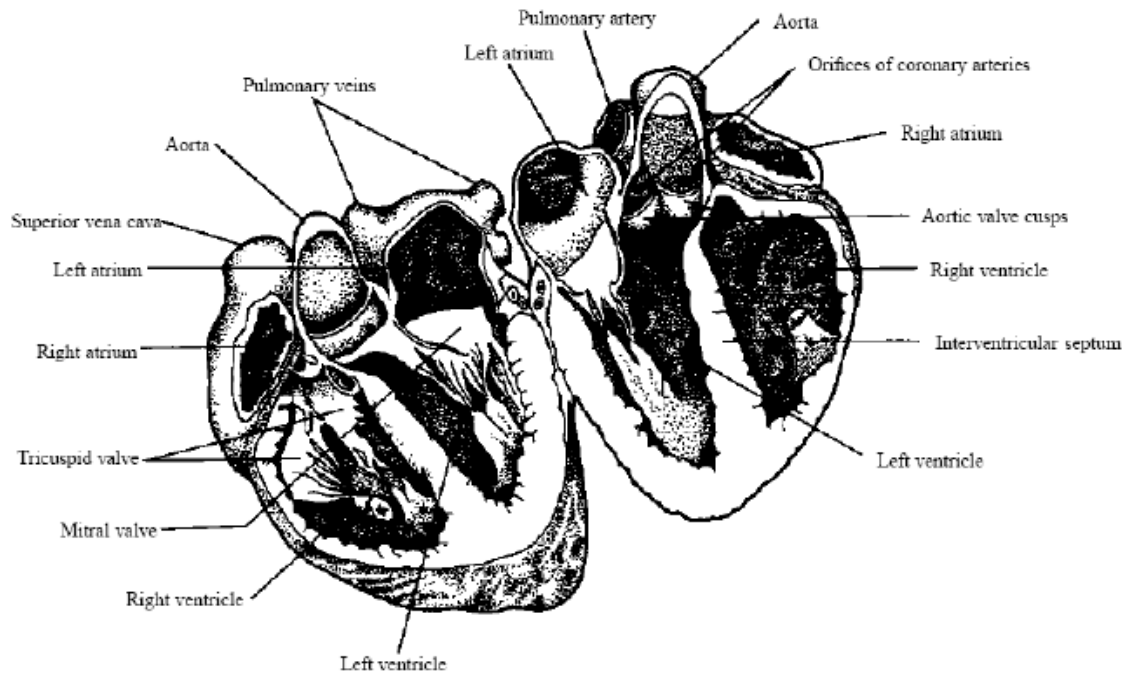


Figure 1: Longitudinal cross-section of the heart showing the major components [1].

The cardiac ventricular tissue exhibits a highly-coupled three-dimensional (3D) muscle fiber architecture, which has a profound impact on the electrical and mechanical

functions in the heart. In order to better understand how these structure effect the electrical and mechanical functions, it is necessary to quantitatively describe the cellular architecture and the connective tissue associated with the ventricles. In depth observations of the microstructure of the myocardial tissue reveals discrete layers of myocardial muscle fibers organized into a complex arrangement called laminae or sheet consisting of 3 to 4 layers of myofibers [2]. The myocardial sheets are connected by loose connective tissue. This well-defined structure of fibers and sheets allows the myocardial muscles to work in a mechanically optimal process to pump blood efficiently to the body.

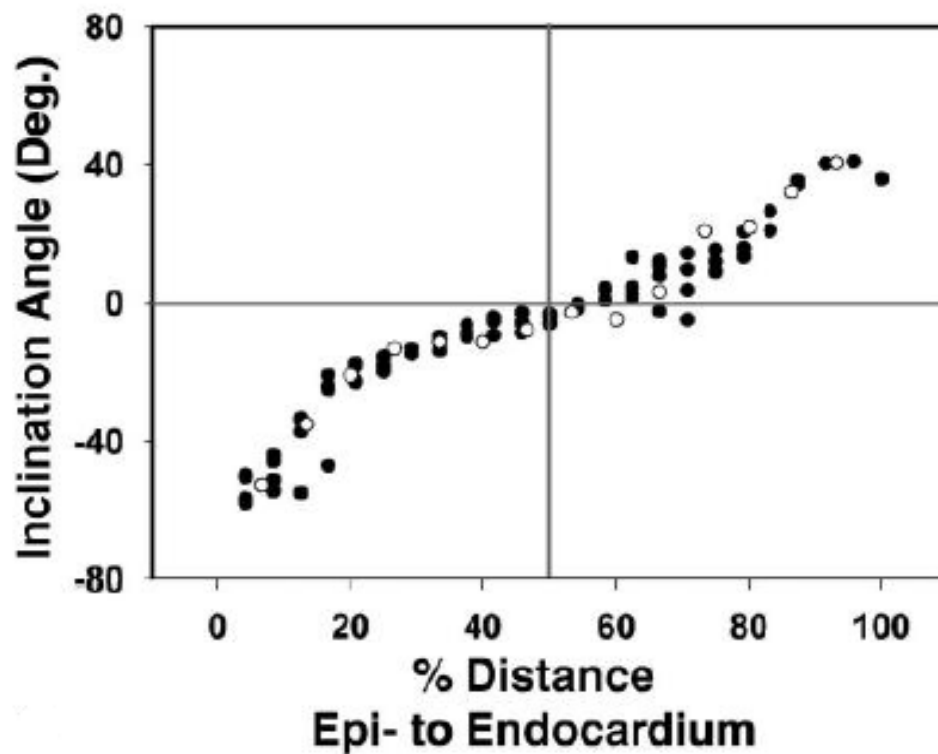


Figure 2: Typical fiber angle measurements are taken in successive sections from histology (open circles) and are estimated using Diffusion Tensor Magnetic Resonance Imaging (open circles) [3].

Gross dissections and histology measurements reveal that there is a transmural variation of fiber orientations [4-6]. The fiber angles, measure from the horizontal plane, increase nearly linearly as a function of transmural depth from  $-60^\circ$  at the epicardium to  $0^\circ$  at the mid-wall and  $+60^\circ$  at the endocardium (Figure 2). Investigators have demonstrated the ventricular fiber structure has a significant influence on cardiac electromechanics and is, thus, critical in understanding cardiac function in both healthy and diseased hearts.

### ***1.1.2 Cardiac Electrophysiology***

Cardiac muscle, when triggered by depolarization of the plasma membrane, undergoes contraction as the gap junctions between cardiac myocytes allow action potentials to propagate from one cell to another. The pumping action is a result of electricity flow through the heart. The heart's natural pacemaker, the sino-atrial (SA) node, sends out regular electrical impulses to the atria, causing both atria to contract in unison and pump blood into the ventricles. The electrical impulse is then conducted to another region of specialized cardiac muscle tissue, a relay point called the AV node. The impulses are delayed for about 0.1 seconds before spreading through the walls of the ventricles, causing them to contract and pump out the blood. The delay ensures that the atria completely empty before the ventricles contract. Once the electrical impulse passes the AV node, it enters the interventricular septum where the conduction system fibers, known as the bundle of His, separate into right and left bundle branches, which enter the wall of both ventricles and make contact with Purkinje fibers that allow rapid conduction of impulses throughout the ventricles. Purkinje fibers form conducting pathways called



bundle branches, conducting the signals to the apex of the heart along and throughout the ventricular walls. The diffuse distribution of Purkinje fibers and their ability to rapidly conduct electrical impulses cause simultaneous depolarization of all ventricular myocytes and ensure a single coordinate contraction of the heart. This entire cycle lasts about 0.8 seconds.

In a normal and healthy heart, the electrical impulses generated from the SA node propagates in a way such that depolarization of ventricular muscle cells always occurs from the endocardium to the epicardium. Depolarization and contraction of ventricular muscle cells spread from apex towards the base. Optimal cardiac function requires a proper and synchronous sequence of activation, although the activation sequence of the myocardium is inhomogeneous and may vary between individuals.

If the electrical activity of the heart is disrupted, for example by a disturbance in the heart's natural rhythm known as an arrhythmia, the heart's overall ability to sufficiently pump blood is compromised and can cause serious repercussions. Patients with dyssynchronous heart failure have altered activation sequences and conduction defects, such as left bundle branch block (LBBB) and right bundle branch block (RBBB). Ventricular contraction dyssynchrony may lead to impairment of ventricular systolic function.

## **1.2 Heart Disease and Congestive Heart Failure**

Heart disease stands are the leading cause of death among Americans. To date, it is prevalent in over 5.7 million Americans with over 290,000 deaths annually [7]. It stands as the leading cause of hospitalization for both men and women of age 65 or above

in the United States [8]. Healthcare costs associate to heart disease are estimated to exceed \$35 billion annually [9]. CHF is expected to pose as a serious public health problem with the population aging as well as modern lifestyles involving unhealthy diets and physical inactivity.

Congestive heart failure (CHF), or heart failure, is a condition where the heart is unable to sufficiently pump blood to the body as a consequence of abnormality in cardiac structure, rhythm, function, or conduction [10]. Congestive heart failure may be caused by narrowed arteries (coronary artery disease), a history of heart attack, high blood pressure, heart valve disease, disease of the heart muscle (cardiomyopathy), heart defects present at birth (congenital heart defects), or infections of the heart valves and/or heart muscle (endocarditis and/or myocarditis). A large number of patients with CHF have comorbidity related to the underlying cardiac defect or its cause in addition to the consequences of heart failure. The comorbidity nature of CHF makes management and treatment highly complex. Generally, decreased efficiency in pump function of the heart in CHF patients results in reduced blood flow and reduced cardiac output causing exercising difficulties, fatigue, and dizziness. Furthermore, neurohormonal activation often occurs to increased blood volume by retaining water in the kidneys to compensate for the reduced efficiency of cardiac function. Excess salt and water, cause by high blood and fluid pressure backed up behind the heart, may enter the lungs and other body tissues causing shortness of breath and edema.

The New York Heart Association (NYHA) has outlined functional classification reflecting the severity of the CHF condition based on the degree to which physical activity is limited (Table 1).

Table 1: NYHA functional classification of heart failure [11].

<b>NYHA Class</b>	<b>Symptoms</b>
<b>I</b>	No symptoms of activities and no limitation in ordinary physical activity.
<b>II</b>	Mild limitation during ordinary activity.
<b>III</b>	Marked limitation during less-than-ordinary activities. Comfortable only at rest.
<b>IV</b>	Severe limitation. Symptoms occur at rest.

CHF may arise from dysfunction of either the left or right ventricle. It is also typically classified as either systolic or diastolic dysfunction depending on whether the abnormality is caused by contraction or relaxation of the heart. Systolic dysfunction is characterized by reduced ventricular contractility, ventricular dilation, diminished ejection fraction and stroke volume, and increased end-diastolic volume or pressure as a compensation for reduced stroke volume. Diastolic dysfunction often occurs in patients with hypertension and hypertrophy. Myocardial contractility, diastolic volume and ejection fraction appear normal in these patients; however, there is an upward shift in the pressure-volume curve, causing an increase in end-diastolic pressure in the left ventricle since the heart can no longer withstand normal diastolic volumes due to the inability of the ventricle to relax. CHF is typically accompanied by progressive cardiac remodeling, in which the structure and function of the heart are altered in an attempt to compensate for the pressure or volume overload and/or cardiac injury. In the long run, this maladaptive remodeling causes impairment of cardiac function and irreversible injuries. Treatments for CHF patients include medications that address CHF symptoms and promote myocardial remodeling, implantable cardiovascular defibrillators (ICDs)

designed to prevent sudden death due to arrhythmias, surgery, and transplantation [10, 12-17].

### **1.3 Cardiac Resynchronization Therapy**

Cardiac resynchronization therapy (CRT) is an established treatment for patients with heart failure, a prolonged QRS duration, and impaired left ventricular function. This therapy involves multisite pacing to the right and left ventricles, and thus is also known as biventricular pacing. By pacing both sides of the left ventricle, the pacemaker can resynchronize a heart that is not contracting synchronously, which occurs in roughly 25-50% of heart failure patients. Intraventricular conduction delay causes asynchrony of the contraction of the ventricles, leading to discoordinate wall motion and lower efficiency in the pumping function of the heart.

CRT devices contain at least two leads, one in the RV and another to pace the LV. It is common for patients in sinus rhythm to have a lead in the RA to facilitate synchrony with atrial contraction. Optimal cardiac function can be achieved by altering the timing between the atrial and ventricular contraction, as well as the timing between the septum and LV, and the location of the LV pacing site.

CRT performed on such patients has been shown to reduce mortality, restore synchrony, and improve symptoms and functional performance [18-21]. The American College of Cardiology/American Heart Association/Heart Rhythm Society guidelines recommend CRT patients with end-stage drug refractory HF of New York Heart Association (NYHA) class III or IV severity, depressed left ventricular ejection fraction (LVEF  $\leq$  35%), prolonged QRS duration ( $\geq$  120 ms), and sinus rhythm as a class I

indication with level of evidence A. These conventional criteria results in a 20% to 40% non-responder rate [19, 22-24]. It was suggested that electrical dyssynchrony represented by prolonged QRS intervals is not necessarily related to mechanical dyssynchrony, which may explain the prevalence of non-responding patients [24-26].

During biventricular pacing, the RV and LV may be stimulated either simultaneously or sequentially. Biventricular pacing stimulus is most commonly delivered at the RV apex and the LV epicardial surface. This LV stimulation site was a variable in this study and the goal was to determine which LV pacing location and whether epicardial or endocardial stimulus was optimal. In practice, the most common location of LV paving laterally or posterolaterally on the epicardium. Lambiase et al. showed that patients with heart failure and ventricular conduction delays had a slow conduction zone within the LV [27]. Pacing the LV from an area with faster conduction compared to other LV sites increased the hemodynamic gain and was accompanied by a reduction in both LV activation time and QRS width.

It has been shown that during simultaneous biventricular pacing from RV apex and a site on the lateral LV epicardium, an initial LV endocardial breakthrough site occurs in the mid or apical LV septum. This breakthrough site originates from the RV pacing site. The time it takes from the right activation wavefront to cross the septum and reach the LV is nearly the same time it takes the wavefront originating from the LV pacing site to break from the epicardium into the endocardium (30-60ms). This results in two near simultaneous LV endocardial breakthrough sites, one in the septum and the other in the lateral region. The RV stimulus is primarily located on the endocardium whereas the LV stimulus typically spread at the epicardium and myocardium. Once the

RV stimulus reaches the LV endocardium, it propagates from the septum toward the anterior and then the lateral LV region. At the same time, it crosses the intramyocardial layers, reaching the epicardium after a variable delay and propagates in the same direction of the endocardial front, but much more slowly. The endo- to epicardium activation gradient is noted in the septoanterior LV region. From the LV pacing site, activation soon spreads over the epicardium, radially toward both the anterior and posterior regions. At the same time, the wavefront breaks into the endocardium and propagates in the same directions within the inner layers. The epi- to endocardium activation gradient is created in the lateral and posterolateral LV regions (the site of LV stimulus). The stimulus activation wavefronts typically collides at the anterosuperior region of the LV, where an area of slow conduction is often located.

Biventricular pacing reduces and can abolish the inter- and intraventricular electrical asynchrony, with a significant reduction of both biventricular and LV activation times as reflected by a reduction of QRS duration.

Recent data from Lambiase indicated that simultaneous pacing from the LV endocardium and endocardial RV apex elicited the largest increase in hemodynamic function, the shortest LV endocardial activation time, and the narrowest QRS complex [27]. This observation is consistent with data from Garrigue et al. who demonstrated that LV endocardial paving led to a significantly greater hemodynamic improvement and narrower QRS complex compared with LV epicardial pacing [28]. The exact three-dimensional electrical and mechanical characterization during this novel approach still needs to be defined. The three-dimensional electrical characterization is the focus of this thesis.

## **1.4 Clinical Significance**

There is no doubt that CRT has revolutionized treatment for patients with LV dysfunction and a broad QRS complex, however, CRT is an expensive treatment with possible risks so patient selection must be performed carefully. Current patient selection criteria for CRT, such as QRS duration of more than 120ms, peak oxygen utilization during exercise, and a decrease in left ventricular end-systolic volume, often fail to distinguish responders from non-responders and suggest a critical need for a more well-define set of criteria reflecting the mechanism of CRT.

Currently, 30% of the population do not benefit clinically from device implantation. Furthermore, it is not known if, even in those that appear to respond, whether or not they are experiencing maximal benefit. The exact reason for a lacking response is unclear, but may be due to factors such as minimal preimplant dyssynchrony, inadequate lead placement, scar burden, and also device settings. In recent years, considerable effort has been devoted to improving patient selection. Due to heterogeneity in disease patterns, electrical activation, timing of segmental contraction, and extent of LV remodeling, a “one setting fits all” methodology is inadequate. A more complex patient-specific model may be a more optimal way for patient selection.

## **1.5 Local Electrogram Signals**

Both unipolar and bipolar electrode configurations have been used by various investigators to record epicardial electrical activity [29-35]. Controversy exist as to which is the optimal configuration for determining the time of local cardiac activation. Bipolar leads have one positive and one negative pole whereas unipolar leads only have one true

pole (the positive pole). Unipolar electrodes have the ability to record adequate signals without intimate tissue contact, an omnidirectional field of view, and well-established and generally accepted criteria exist for determining the time of local activation [32, 36]. However, because the amplitudes of unipolar electrograms are primarily composed of global activity, it is possible that low local activity could be obscured. By nature, unipolar signals are more dispersed compared to bipolar signals. Conversely, the signals from bipolar electrodes are less sensitive to distant activation, no directional sensitivity, and have a lack of well-established criteria for the determination of local activation time.

## **1.6 Isochronal Mapping**

Isochronal mapping of cardiac activation has been used to study the spread of activation in the heart, to identify the mechanism of atrial and ventricular arrhythmias, to localize conduction disorders, and to guide ablative surgeries. In order to obtain epicardial isochronal maps, it is necessary to measure local times of activation times over the epicardial surface of the heart at a sufficient spatial and temporal resolution [37]. These local activation times could be put into a model and utilized to predict the outcome of CRT.

## **1.7 Project Aims**

The overall aim of this thesis is to develop methods for examining the effects of pacing location on the epicardial activation sequence in the heart. In order to do so, it is necessary to develop a method to create geometrically fit epicardial location activation maps. Three-dimensional mapping of this electrical local activation offers a better



understanding to the optimal pacing protocol for a patient with cardiac dyssynchrony. In order to predict and optimize outcomes of CRT in individual patients, methods for generating detailed three-dimensional finite element models of a failing human heart need to be developed.

Accurate isochronal maps can be developed with confidence assuming that the input local activation times are accurate. In literature, the time of the maximum negative derivative is taken to be the time of activation in unipolar signals and the time of the maximum amplitude is taken to be the time of activation in bipolar signals. Local activation times will be determined by comparing manual and automatic algorithms. Manual determination of activation times is the gold standard, however requires a lot of time, thus automatic algorithms should be used if they can produce highly correlated results when compared to the manual algorithm. Isochronal maps will be constructed from unipolar and bipolar signals, and from unfiltered and filtered signals.

After the optimal criteria for isochronal map development is determined, maps will be constructed using a bicubic fit geometry and linearly fit activation times in a 21 element mesh. A better understanding of the spread of activation in hearts with heart failure can be achieved by examining these epicardial maps. More specifically, 2 questions pertaining to epicardial ventricular synchrony can be answered: (1) Will endocardial pacing restore more epicardial ventricular synchrony than epicardial pacing in hearts with heart failure and a myocardial infarct, and (2) Will biventricular pacing restore more epicardial ventricular synchrony than single LV pacing?

## **CHAPTER 2: MATERIALS AND METHODS**

### **2.1 Surgical Preparation and Pacing Protocol**

Six adult mongrel dogs (19-25 kg) (three with the 24-electrode sock and six with the 128-electrode sock) were anesthetized with intravenous propofol (6mg/kg) and mechanically ventilated with isoflurane (0.5% - 2.5%) and medical oxygen (2 l/min) to maintain a surgical plane of anesthesia. A limb lead surface electrocardiogram (ECG) was used to monitor global electrical events of the heart's conduction. The heart was exposed through a median sternotomy and a left thoracotomy at the fourth intercostal space. The pericardium was opened, allowing for the heart to be suspended in a pericardial cradle.

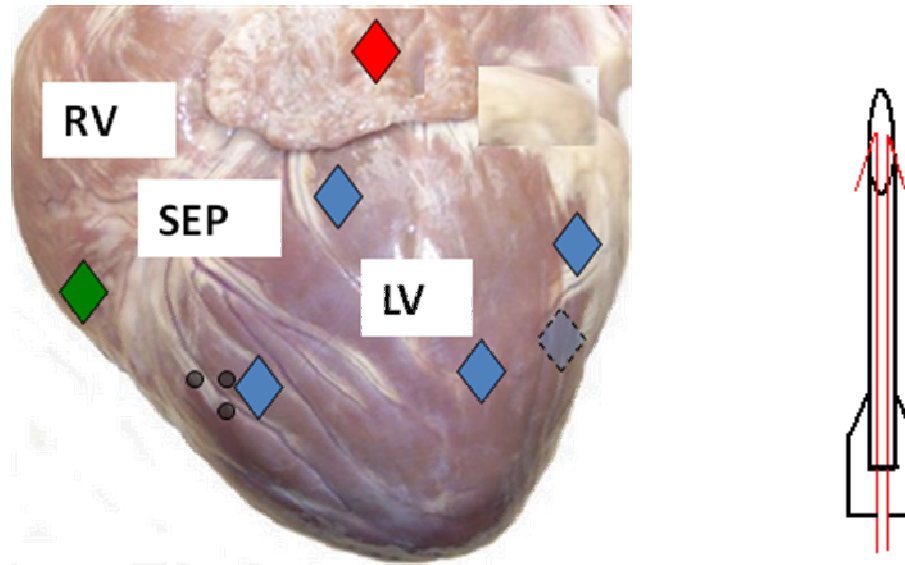


Figure 3: (Left) Graphical depiction of the placement of recording/pacing electrodes. The location of the atrial pacing electrodes is signified by a red diamond, RV apex electrodes by a green diamond, and LV endocardial/epicardial electrodes by blue diamonds. LV electrodes as 1) Anterior Base, 2) Anterior Apex (or Anterior BS), 3) Lateral, 4) Posterolateral, and 5) Coronary Sinus. (Right) Schematic diagram of a plunge electrode consisting of two insulated transformer wires inserted in a needle.

Eleven plunge electrodes were placed on both the right and left ventricles at epicardial (EPI) and endocardial (ENDO) sites. These bipolar electrodes were used to measure the timing of local electrical activation (recording mode) as well as to deliver an electrical stimulus (pacing mode). On the RV free wall one plunge electrode was positioned at the apex of the RV. The remaining ten plunge electrodes were positioned at five sites, one at the endocardium and the other at the epicardium, on the LV free wall. The specific sites were: 1) anterior near the base 2) anterior near the apex of the LV (defined as 1/3 the distance from apex to base), 3) lateral free wall, 4) posterolateral wall, 5) posterior near the coronary sinus Figure 3. In addition to the plunge electrodes, either a 24 bipolar electrode sock array or a 128 unipolar electrode sock array was placed over the ventricles to record electrical events, and thus to develop epicardial isochronal maps.

Normal electrical conduction was maintained by stimulating atrial electrodes using a square-wave constant voltage stimulator at a rate 20% above intrinsic heart rate (typically 100-110bpm) in order to suppress the normal sinus rhythm. For each ventricular site the pacing parameters were prescribed as:

1. Voltage 10% above threshold
2. Duration (i.e. pulse width) of 8 ms
3. Rate 20% above sinus rhythm

Asynchronous activation was achieved in the following ways:

1. AV sequential pacing of the LA and RV apex at a fixed delay (AV delay ~40 ms)
2. AV sequential pacing of LA and a LV site (AV delay ~40 ms)
3. Radio frequency (RF) ablation of the left bundle branch, thus inducing LBBB.

## **2.2 Study Design**

A total of 9 canine studies were performed: 3 acute dogs with the 24-electrode sock, 3 acute dogs with the 128-electrode sock, 1 acute test dog with the 128-electrode sock and the new amplifier system, and 2 chronic dogs with the 128-electrode sock and the new amplifier system (Table 2). Of the 9 canine studies, 3 are analyzed for the focus of this study because they utilize the 128-electrode sock array with the new amplifier system, yielding electrograms that are sufficient for analysis.

Table 2: Outline of the 9 Canine studies utilizing an electrode sock array to measure epicardial activation. Yellow cells show that Dogs 7-9 are the focus on the analysis because they utilized the 128-electrode sock with the new amplifier system, yielding signals sufficient for analysis.

<b>Dog #</b>	<b>Electrode Sock</b>	<b>Signals Sufficient for Analysis</b>	<b>Heart Failure Model</b>	<b>Single LV Pacing</b>	<b>BiV Pacing</b>
1	24-electrodes		<i>Acute</i> LBBB	x	x
2	24-electrodes	x	<i>Acute</i> Ventricular Dyssynchrony	x	x
3	24-electrodes	x	<i>Acute</i> Ventricular Dyssynchrony	x	x
4	128-electrodes		<i>Acute</i> Ventricular Dyssynchrony	x	x
5	128-electrodes		<i>Acute</i> Ventricular Dyssynchrony	x	x
6	128-electrodes		<i>Acute</i> Ventricular Dyssynchrony	x	x
7	128-electrodes	x	-	x	
8	128-electrodes	x	Myocardial Infarct <i>Chronic</i> Tachycardia -Induced HF <i>Acute</i> Ventricular Dyssynchrony	x	x
9	128-electrodes	x	<i>Chronic</i> Tachycardia -Induced HF <i>Acute</i> Ventricular Dyssynchrony	x	x

In the chronic dogs (Dogs 8 and 9), the heart was paced for 4 weeks to obtain tachycardia-induced heart failure. In dog 8, the blood supply was interrupted on the epicardial lateral wall (myocardial infarct).

In both the chronic and acute dogs, the following was performed during the terminal portion of the study. LV pacing was performed in sequence with a normal activation (i.e. atrial pacing) and in the presence of electrical asynchrony. In dog 1, electrical asynchrony was induced by disruption of left bundle branch in which an RF

ablation catheter was used. In the remaining dogs, a simulated model of cardiac dyssynchrony was used. This model involves sequential pacing of the atria and RV apex. RV apex pacing have been shown to produce similar activation patterns that result in a widening of the QRS complex and a reduction in pump function. For each LV site, epicardial and endocardial electrodes were stimulated in an alternating fashion. Overall the pacing protocol can be outlined as the following:

1. Atrial: Left Atrial (LA) pacing
2. Single LV: LA + Left Ventricular (LV) sequential pacing at 5 ventricular sites (first EPI, then ENDO)
3. Asynchrony: LA + RVA pacing
4. Biventricular: LA + RVA + LV pacing at 5 ventricular sites (first EPI, then ENDO)

For each pacing run global hemodynamics and electrical events were sampled and digitally recorded using Windaq acquisition software. The study was concluded with a Propofol overdose (60 mg/kg IV), and inflow occlusion was maintained to avoid cardiac overdistention and hypoxic or hyperkalemic cardiac arrest. The heart was fixed by coronary perfusion with gluteraldehyde at an average LV end-diastolic pressure from the atrial runs.

## **2.3 Experimental Measurements and Data Acquisition**

### ***2.3.1 Hemodynamics***

Basic hemodynamic data were obtained through the study. Left ventricular pressure (LVP) was measured with a Konigsberg micromanometer placed in the left

ventricular chamber via an apical purse string suture. End-Diastolic pressure (LVEDP) was determined by peak of the R-wave of the ECG. The maximum rise of LV pressure,  $dP/dt_{max}$ , was calculated by numerical differentiation of LVP. Aortic pressure (AoP) was obtained from a short 8Fr fluid filled catheter inserted in the left subclavian artery and connected to a pressure transducer. A Doppler flow probe was positioned around the ascending aorta to define the onset and conclusion of ejection. Stroke Volume (SV) was calculated by numerical integration of the aortic flow (QAo) trace during the time interval of ejection. Left ventricular volume (LVV) was determined via a 7 Fr Baan conductance catheter advanced into the LV cavity via the left common carotid artery.

### ***2.3.2 Electrical Activation Recording***

Two types of electrode socks were used to obtain data: (1) a low resolution sock with 24 bipolar electrodes, and (2) a high resolution sock with 128 unipolar electrodes. The sock was designed to ensure good contact with the heart while avoiding hemodynamic compromise. Electrograms from the epicardial electrodes were simultaneously recorded together with the pacing electrodes. By analyzing the signals obtained from the electrode sock, isochronal maps can be developed in order to better understand the cardiac electrical activation sequence in asynchronous hearts.

#### **2.3.2.1 24-Electrode Sock**

The low resolution sock is comprised of 24 bipolar button electrodes and constructed to fit comfortably around the heart; each button contains electrodes suitable for bipolar recordings between members of the pair. A schematic diagram of the sock array electrodes and the location is shown in Figure 4. The electrodes are arranged in 5

rows covering as much of the left ventricle as possible. The position of the 24 electrodes are represented by the grey circles; the first, second, and third anterior columns contains 5 electrodes each, the first lateral column contains 4 electrodes, the first posterior column contains 2 electrodes, and the second posterior column contains 3 electrodes. The red circles represent the position of the 5 epicardial and endocardial pacing electrodes located at: (1) the bead set, (2) base anterior, (3) lateral, (4) posterolateral, and (5) posterior coronary sinus. Due to the limited number of electrodes, the sock was placed around the heart with the electrodes primarily located on the left ventricular wall because this epicardial surface is the main area of interest (Figure 5). During the studies, the first row of electrodes was positioned along the left anterior descending coronary artery (LAD) for consistency. The low resolution 24-electrode sock was only utilized in the first 3 acute dogs. For the remaining dog studies, a higher resolution 128-electrode sock was used. For bipolar electrograms, the maximum amplitude is taken to be the time of activation [38].

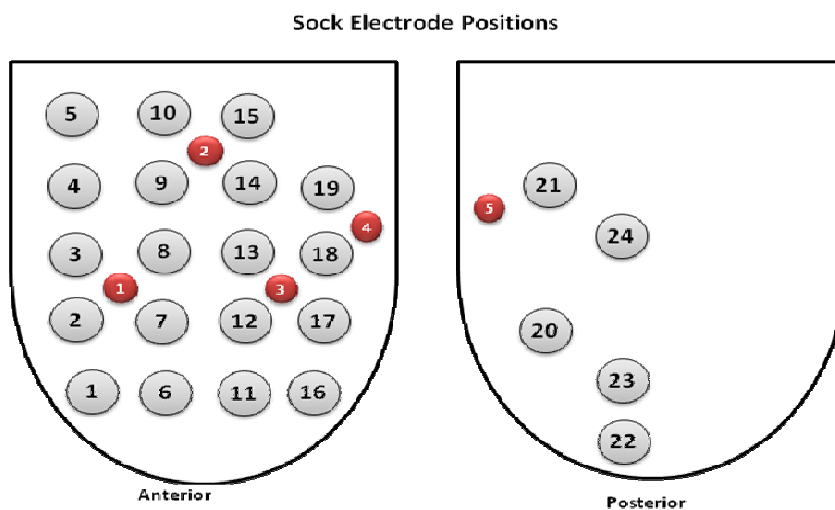


Figure 4: The electrode sock consists of 24 electrodes. The grey circles represent the individual electrode positions and the red circles represent the pacing sites.



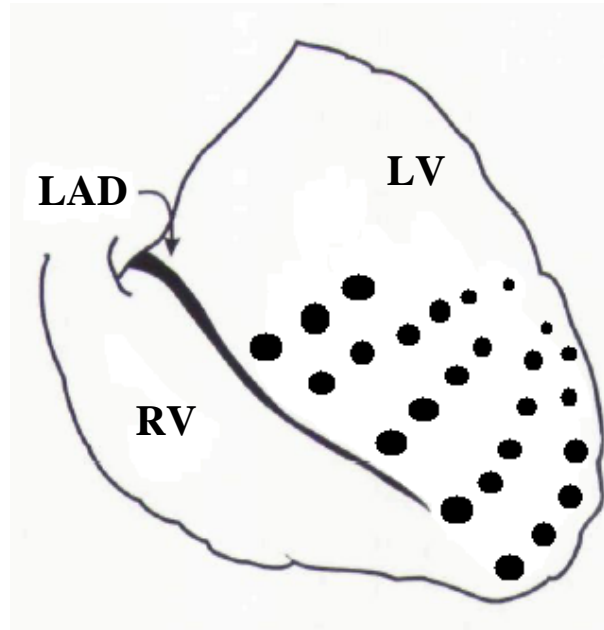


Figure 5: Schematic representation of the electrode sock on the heart. The sock was situated around the heart, in contact with the epicardial surface. The 24 electrodes primarily sit on the LV wall of the heart. The RV did not contain any electrodes. The first anterior column of electrodes was placed along the LAD.

### 2.3.2.2 128-Electrode Sock

The higher resolution sock has 128 unipolar electrodes and covers both the RV and LV surfaces. The 128-electrode sock was used in dogs 3-9. However, the amplifier that was used in dogs 3-6 resulted in very poor signals that exhibited a waveform capturing overall noise. Due to the poor signal resulting from the old amplifier system, a new custom-made amplifier system was created for the purposes of recording more useful electrode data. The data analysis system for the 128-electrode sock consisted of custom-made a 132-channel digital amplifier. Electrograms were recorded at a bandwidth of 0.01 – 500 Hz for the first chronic dog and 0.01 – 100 Hz for the second chronic dog, all at a 1000Hz sampling frequency.

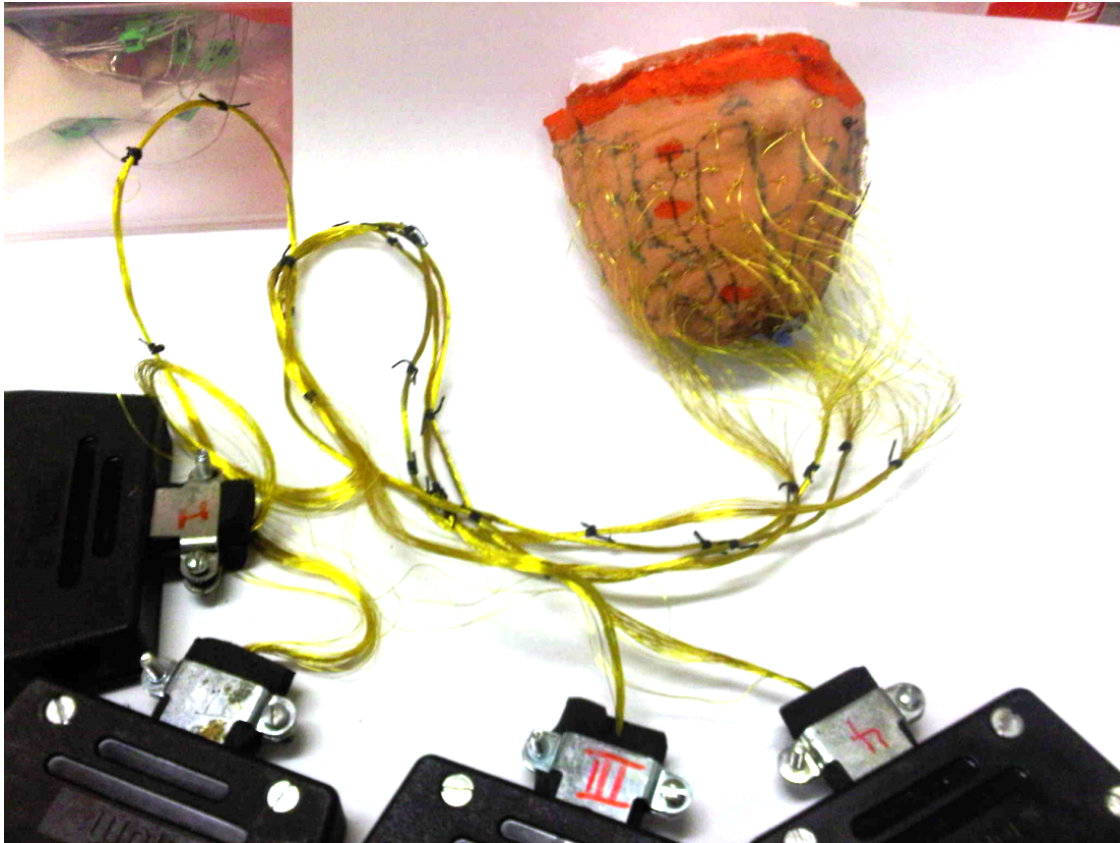


Figure 6: The higher resolution electrode sock is comprised of 128 electrodes; 32 electrodes go into each connectors, which then connects into a 132-channel amplifier system. The electrode sock is fabricated by attaching 128-electrodes to a nylon sock.

For the 128 electrode sock array in dog 7 and dog 8, only channel 51 was noisy and omitted. In the dog 9 however, on average over 17% of the electrodes (over 22 out of the 128 electrodes) are noisy. The noisy channels vary between each run and may be due to the contact of the electrode sock with the heart. It is feasible to assume that the result may be due to excess blood inhibiting contact of the sock with the heart.

Table 3: Runs documentation for studies with the 128-electrode sock.

<b>Dog ID</b>	<b>Run</b>	<b>Pacing Protocol</b>
Beagle	9	<b>Atrial</b>
Beagle	10	Single LV Epi Vent. Anterior Base
Beagle	12	Single LV Epi Pacing Bead Set
Beagle	14	Single LV Epi Vent. Posterior Wall
Dog 2 - Obi	4	<b>Atrial</b>
Dog 2 - Obi	5	<b>LBBB</b>
Dog 2 - Obi	6	BiV Endo Posterior CS
Dog 2 - Obi	7	BiV Epi Posterior CS
Dog 2 - Obi	8	BiV Endo Lateral
Dog 2 - Obi	10	BiV Epi Lateral
Dog 2 - Obi	11	BiV Endo Anterior Base
Dog 2 - Obi	12	BiV Epi Anterior Base
Dog 2 - Obi	13	BiV Endo Anterior Mid-Ventricle
Dog 2 - Obi	14	BiV Epi Anterior Mid-Ventricle
Dog 2 - Obi	15	Single LV Epi Anterior Mid-Ventricle
Dog 2 - Obi	18	Single LV Epi Posterior CS
Dog 2 - Obi	19	Single LV Epi Ant Next to Scar
Dog 3 - Ripley	1	<b>Atrial</b>
Dog 3 - Ripley	2	<b>LBBB</b>
Dog 3 - Ripley	3	BiV Endo Posterior CS
Dog 3 - Ripley	4	BiV Epi Posterior CS
Dog 3 - Ripley	5	BiV Endo Ant Next to Scar
Dog 3 - Ripley	6	BiV Epi Ant Next to Scar
Dog 3 - Ripley	7	BiV Endo Anterior Base
Dog 3 - Ripley	8	BiV Epi Anterior Base
Dog 3 - Ripley	9	BiV Endo Anterior Mid-Ventricle
Dog 3 - Ripley	10	BiV Epi Anterior Mid-Ventricle
Dog 3 - Ripley	11	BiV Endo Bead Set
Dog 3 - Ripley	12	BiV Epi Bead Set
Dog 3 - Ripley	13	Single LV Epi Bead Set
Dog 3 - Ripley	14	Single LV Epi Anterior Mid-Ventricle
Dog 3 - Ripley	15	Single LV Epi Anterior Base
Dog 3 - Ripley	16	Single LV Epi Ant Next to Scar
Dog 3 - Ripley	17	Single LV Epi Posterior CS
Dog 3 - Ripley	18	<b>Atrial</b>

For the unipolar electrograms from the 128-electrode sock, the time of most rapid deflection, demonstrated to reflect cell depolarization, has been used in epicardial mapping to indicate the occurrence of depolarization of tissue adjacent to the recording electrode [19, 30]. Blanchard demonstrated that the magnitude but not the timing of the fastest down stroke in the unipolar electrogram was affected by superposition of potentials due to distant and local electrical activity [39].

## **2.4 Determination of the Local Activation Sequence**

A method has been developed to visualize the local activation sequence in canine hearts utilizing the electrode sock arrays. The algorithm follows the series of steps as shown in Figure 7. The activation sequence was determined through the analysis of local electrograms recorded from the heart (from both the 24-electrode and 128-electrode sock). For consistency, the compression in the Windaq Waveform Browser was set 5,000 samples per second.

In an attempt to analyze multiple beats and take the average activation time over 3-5 beats, the ECG is loaded the user must select the reference times for each beat. For atrial runs, the reference is the beginning of the QRS complex. For paced runs, the reference is the time of ventricular stimulus artifact. It is not apparent where this ventricular stimulation occurs; the time of the atrial stimulus is more apparent, thus the reference time was selected to be the beginning of the atrial stimulus and add the AV delay time (typically 40 msec) to obtain the proper time for the ventricular stimulus. Once the beats are selected, the algorithm calculates the local activation times depending on selection criteria.

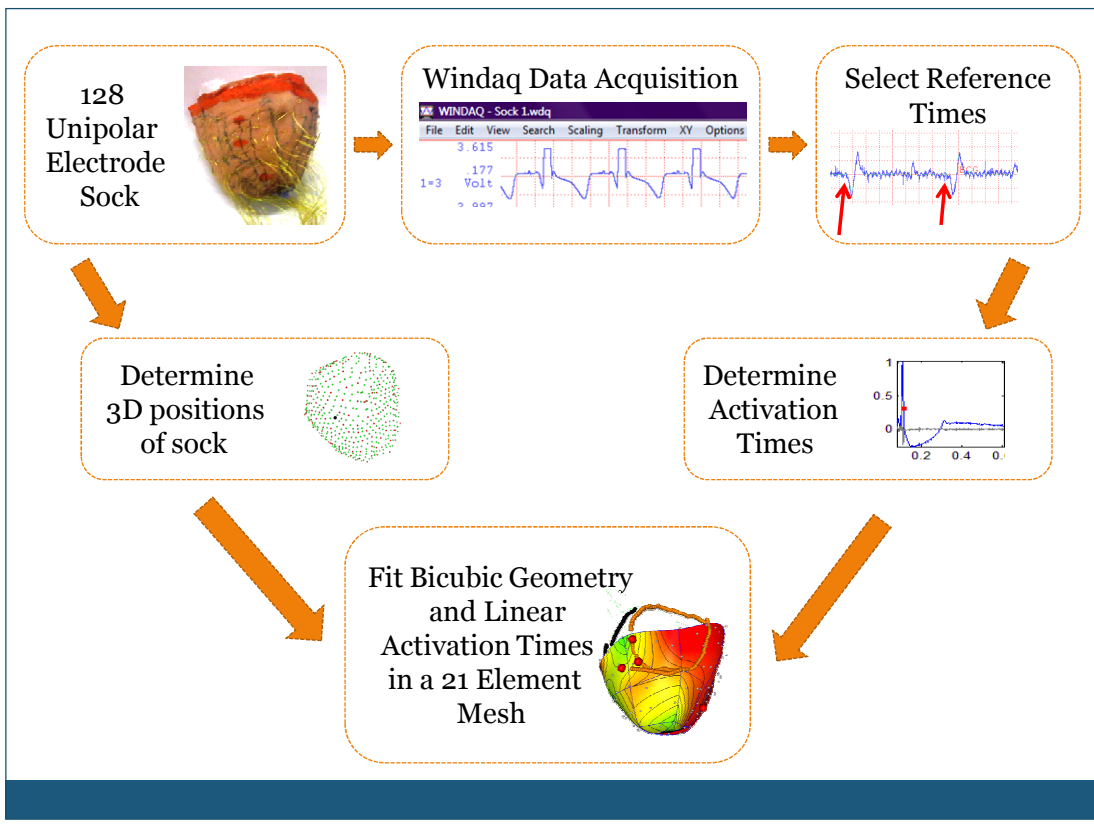


Figure 7: Steps for making epicardial local activation time maps.

The process of determining local activation times is not a trivial one and it is widely acknowledged that interpreting such waveforms may be very difficult as errors can arise for various reasons; a more prominent error arising from deflections in the waveforms produced by distant electrical activity making the local activity hard to distinguish [40-46].

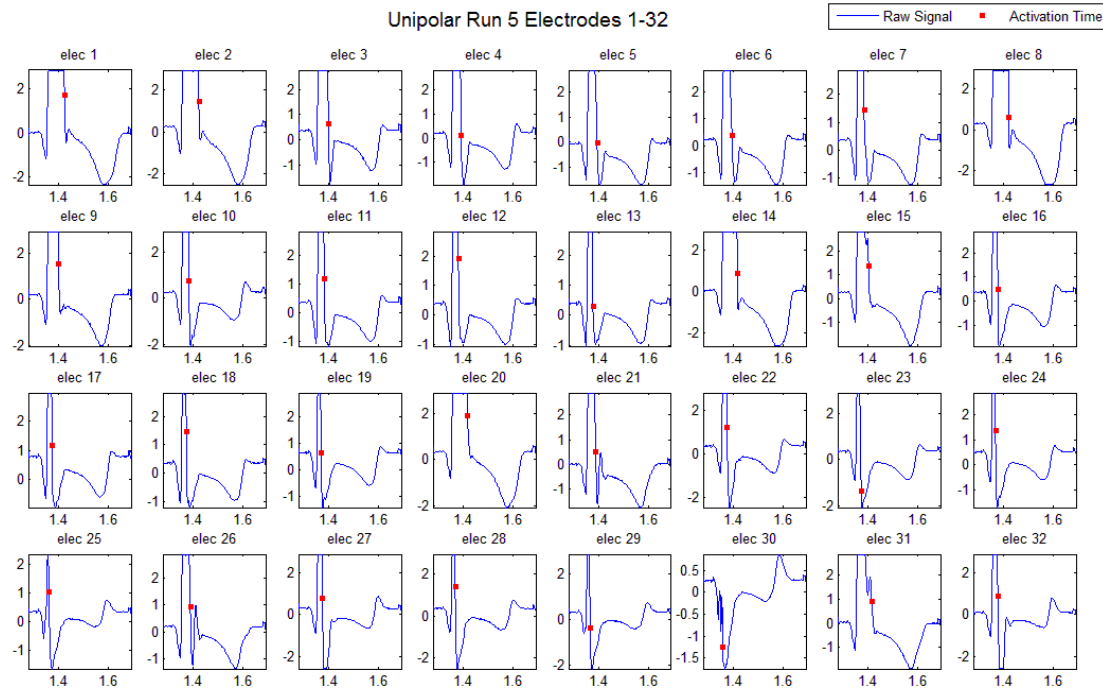


Figure 8: Visualization verification of the calculated activation time allows for user to note and omit noise channels from map output.

Qualitative methods to determine the time of local activation depend on factors including morphology, relative amplitudes, and timings of deflections, requiring a high degree of judgment and experience [40-42, 45]. Qualitative methods are more objective and facilitate estimation of error. For unipolar electrograms, the maximum negative derivative has been shown to be the best indication of local activation. The comparable indication in bipolar electrograms is the time of peak amplitude. Furthermore, unipolar signals can be converted into bipolar signals. For bipolar signals, the time of max amp is taken to be the time of local activation. For verification purposes, the script plots activation times with a red dot for user verification (Figure 8).

It is clear that without a “gold standard” for measuring electrograms, maps of electrical activation remain relative measurements. The standard of the local activation time is determined by manually inspecting the electrocardiograms. The standard of activation is the reference against which possible test of optimal methodology for determining activation are compared. The times automatically calculated by the algorithm for both unipolar and bipolar signals can be compared to this golden standard. With a R-squared correlation coefficient of 0.91, it is acceptable to use this automatic calculated value to be the time of local activation.

## **2.5 Converting Unipolar Signals into Bipolar Signals**

The unipolar potentials of two adjacent electrodes were subtracted to produce a bipolar potential at a location between the two unipolar electrodes. The peak amplitude of the bipolar signal is used as an indication of local activation. Unipolar signals are converted into bipolar signals by tessellating the electrode sock surface which creates a collection of triangles that fills the plane with no overlaps and no gaps. Each triangle has 3 corresponding pairs. From these pairs, differences are calculated to determine the bipolar signal. The bipolar signal location is theoretically located at the midpoint between the two unipolar signals. The tessellation procedure ensures that triangles form a smooth surface and that triangles had adjacent vertices. The 128 unipolar signals were converted into 374 bipolar signals.

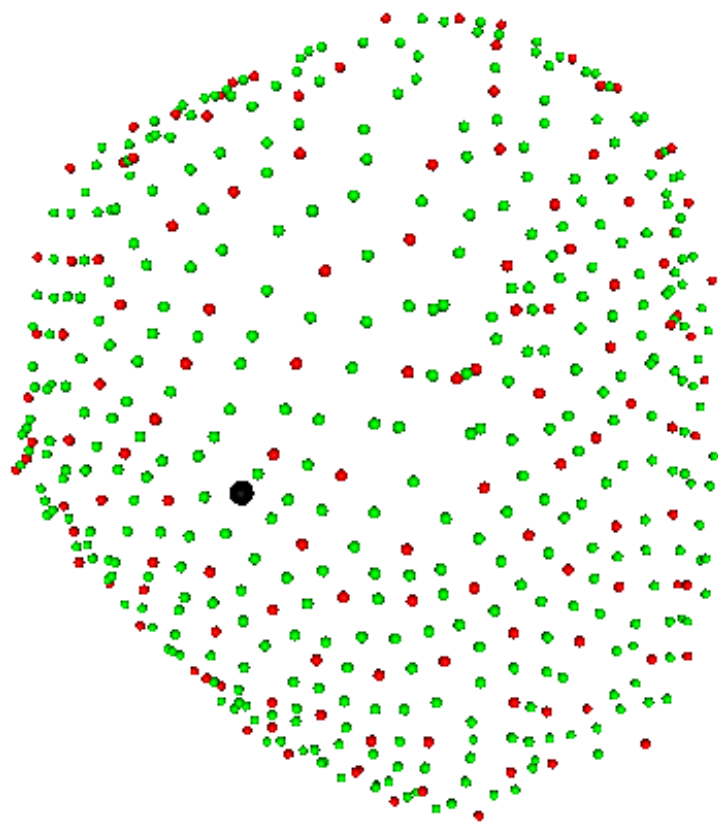


Figure 9: Unipolar and bipolar electrode locations; unipolar electrode positions are red, bipolar electrode positions are green, the inner diameter is the apex, and the outer diameter is the base.

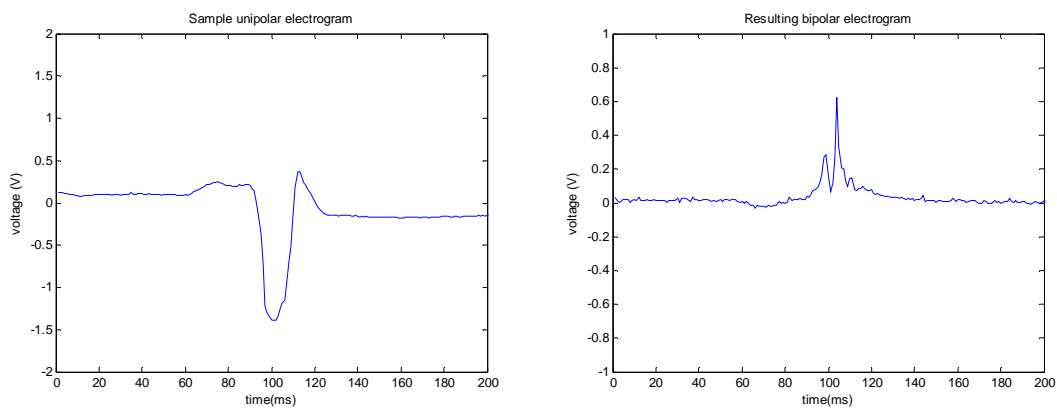


Figure 10: Compares unipolar and bipolar signals.



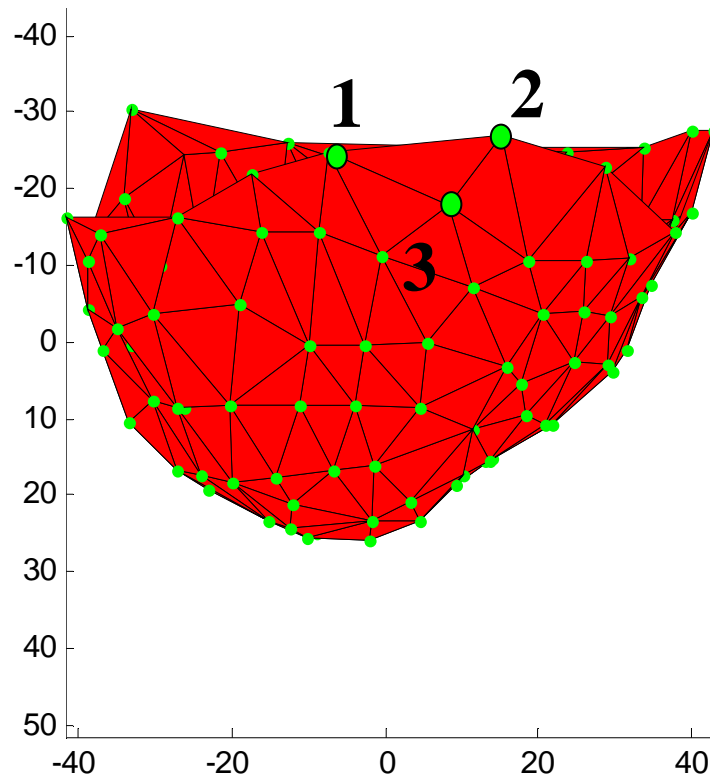


Figure 11: (Left) Tessellated unipolar 3D coordinates form a smooth convex surface. Triplets of adjacent unipolar signals form triangle to ensure surface is convex.

## 2.6 Rough Mapping of Raw Activation Times

In the preliminary stages, the activation times can be plotted on a 2-dimensional representation of the sock whereby, the calculated activation times are simply printed on the rough location on the electrode sock (Figure 12). However, this is time-consuming and was only done for the 24-electrode sock. These preliminary maps revealed the earliest site of activation fairly close to the site of pacing, agreeing with the predicted outcome. At this point, further efforts were put into creating more detailed isochronal maps for visualization.

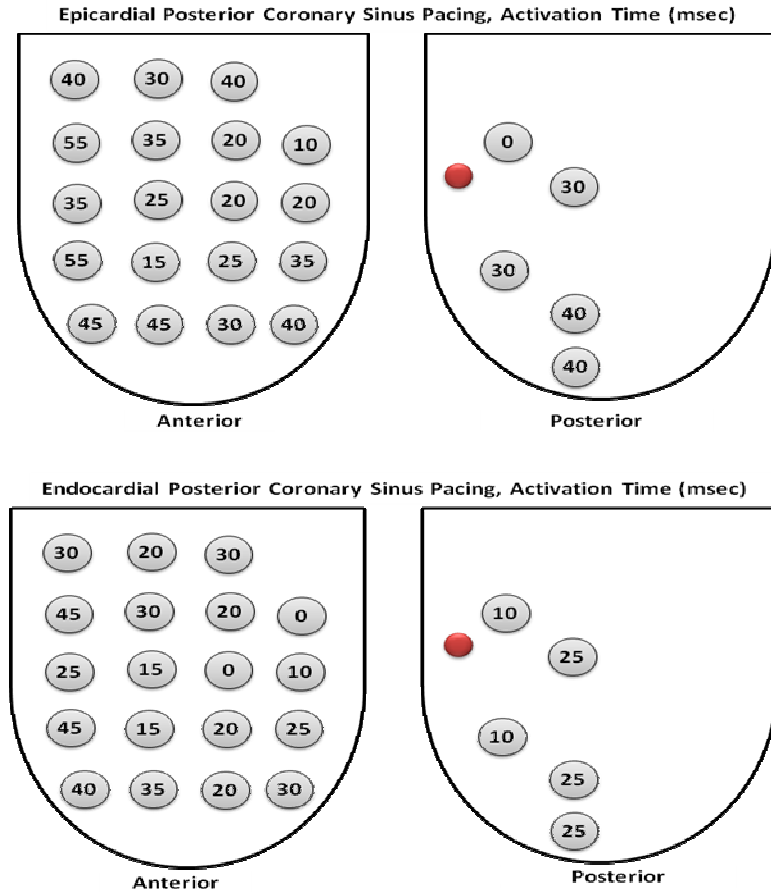


Figure 12: (Left) Activation times of epicardial pacing at the posterior coronary sinus. The earliest activated site is close to the site of pacing. As the position between the initial pacing site and the electrode increases, the activation time increases. (Right) Endocardial pacing at the posterior coronary sinus reveals shorter times than the epicardial pacing.

## 2.7 Three-Dimensional Electrode Reconstruction

The x, y, and z coordinates of the electrodes are required to make a visually realistic three-dimensional display of local activation times. To do so, there are two feasible options: (1) create an idealized set of coordinates using simple geometric structures, or (2) obtain a set of coordinates by reconstructing points using the real heart ex-vivo. The latter forms a more reasonable structure, recreating the actual geometry more accurately.

Utilizing a measurement arm, the following precise 3D coordinates were determined: recording electrodes on sock, pacing locations, and desired fiducial markings (including the left anterior descending artery (LAD) and marker surface beads). By pulling the electrode sock ex-vivo over the fixed and casted canine heart in the same location it is presumed to be located at in-vivo during the study, approximate 3D positions can be determined.

## **2.8 The Assumptions of Isochronal Mapping**

Isochronal mapping assumes that: (1) the electrode locations can be determined with acceptable accuracy, (2) a single, discrete activation time exists at each electrode location, and (3) the electrode sites are spaced closely enough to interpolate activation times at any point between electrode sites with acceptable accuracy [37].

## **2.9 Contour Isochronal Mapping**

Two-dimensional maps can be produced to represent the epicardium with reasonable results. In Matlab, 2D maps were created using the ‘contourf’ function which displays isolines calculated from a matrix of inputted activation times and fills the areas between the isolines using constant colors.

A filled contour plot displays isolines calculated from a matrix and fills the areas between the isolines using constant colors corresponding to the current figure’s colormap. For isochronal mapping purposes, the matrix is a 6 x 21 matrix representing the 2D electrode sock surface. This can be performed for both the 24-electrode (Figure 13 and Figure 14) and 128-electrode sock (Figure 15).

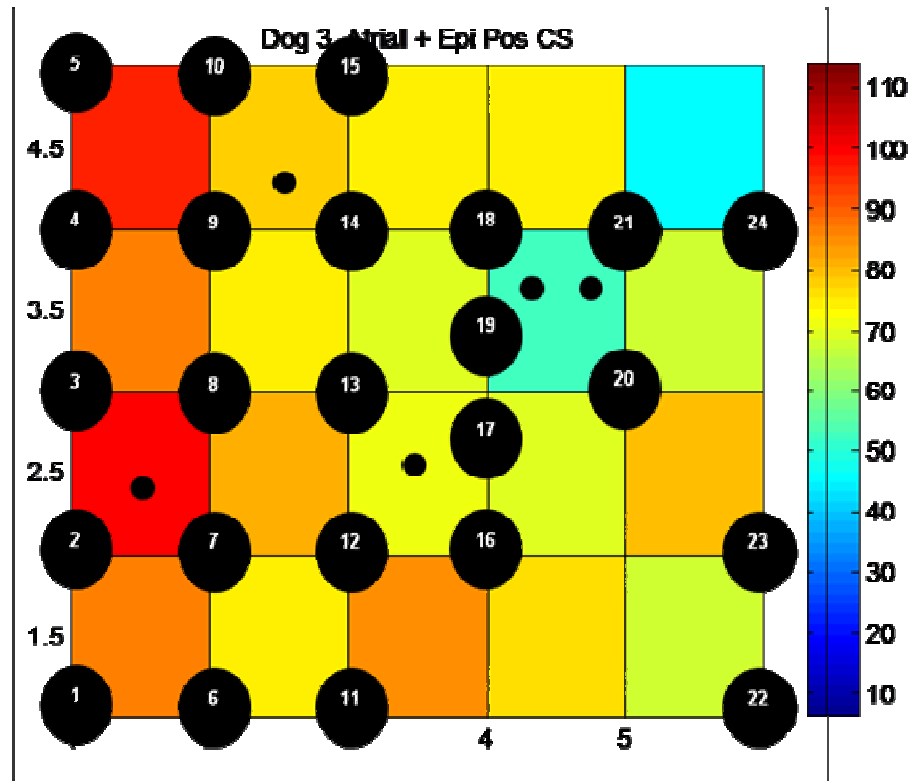


Figure 13: 2D representation of the sock shows the electrode location represented by the bigger black circles and the pacing locations as the smaller black circles.

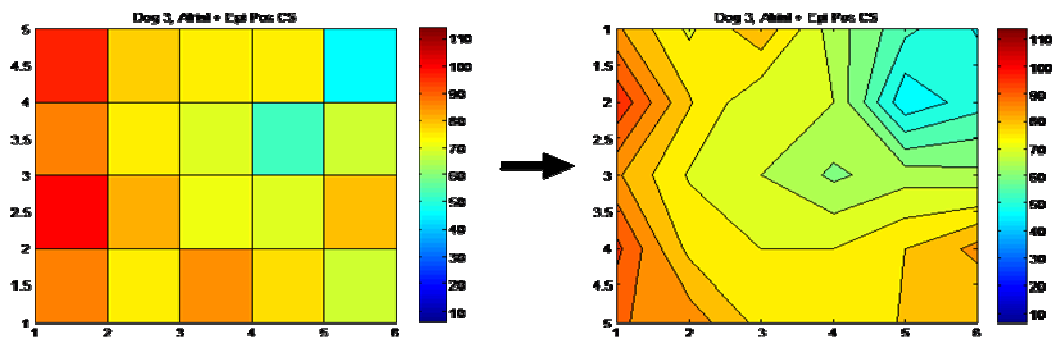


Figure 14: The resulting 2D 'contourf' plot fits the data input into the matrix.

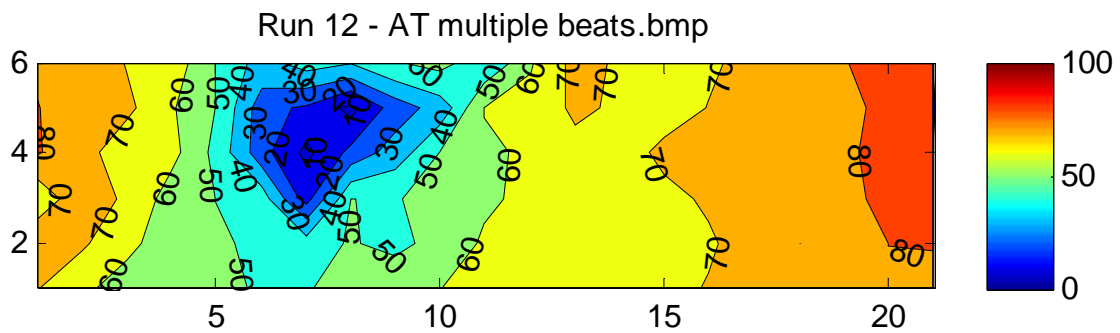
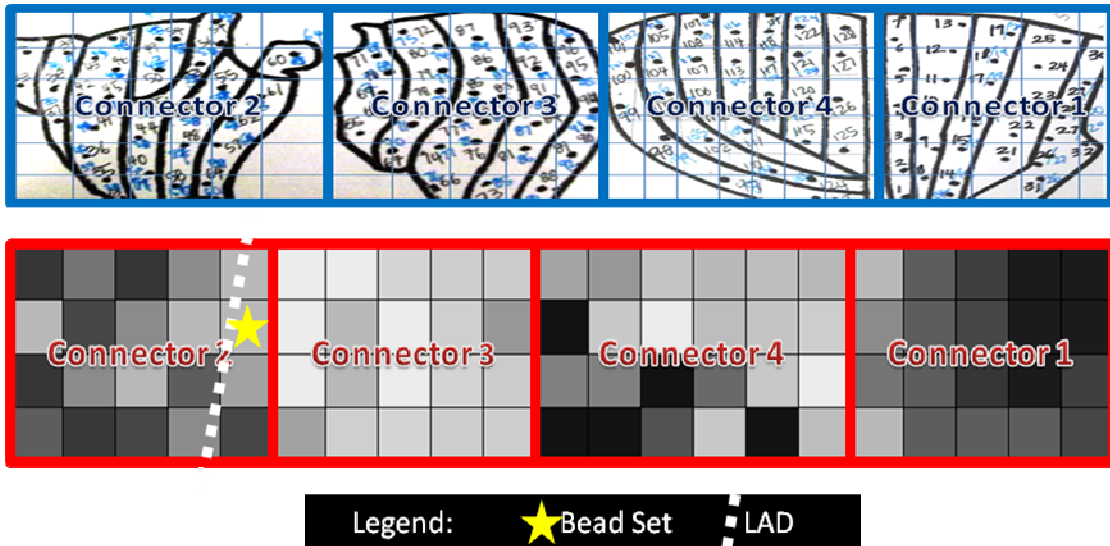


Figure 15: The 2D representation of the 128-electrode sock and resulting 'contour' plot below.

## 2.10 Geometrically Fit Epicardial Activation Maps

To do comparisons between different dogs, it is more beneficial to make a geometrically fit epicardial activation map. The basic flowchart for fitting geometries and activation times is outlined in Figure 16. First, it is necessary to import the 3D coordinates of the electrodes and the corresponding activation times. An initial mesh is made from the Cartesian points on the electrode sock consisting of 28 nodes and 21 elements. Next, the specific geometry and subsequently the activation times are fit with

bicubic fields using a least squares algorithm with an average error of  $6.5 \pm 1.7$  for unipolar signals and  $15.7 \pm 3.6$  for bipolar signals (**Error! Reference source not found.**). The activation field meshes can be rendered for visualization.

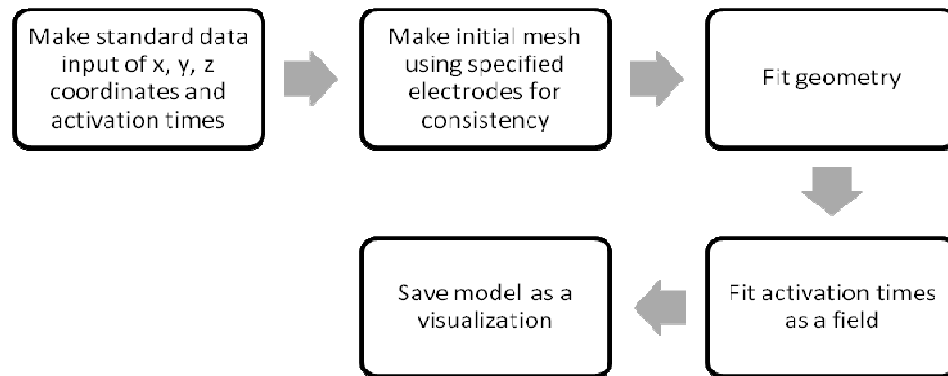


Figure 16: Flowchart describing the steps to creating an isochronal map in a problem-solving environment for multi-scale modeling.

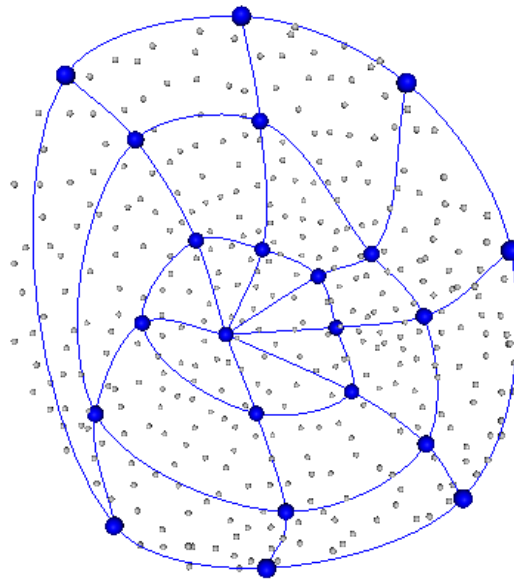


Figure 17: Cross-sectional view of the mesh which contains 7 circumferential elements, 3 apex-to-base elements, 28 nodes, and 21 elements.

The 3D positions can be loaded into the model to make an initial mesh. The fixed points in the mesh are: (1) the 4 bordering points between the RV and LV at the base and apex, (2) the apex, and (3) the base. These markers will serve as a platform to compare epicardial isochronal maps from different dogs. The initial mesh has 7 circumferential elements and 3 apex-to-base elements (Figure 17).

Once the initial mesh is constructed, the elements file needs to be defined to properly connect the nodes to make the elements. At this point, the geometry can be fit and subsequently the activation times. The activation times are fit into a field which can be rendered resulting in isochronal maps such as the one in Figure 18.

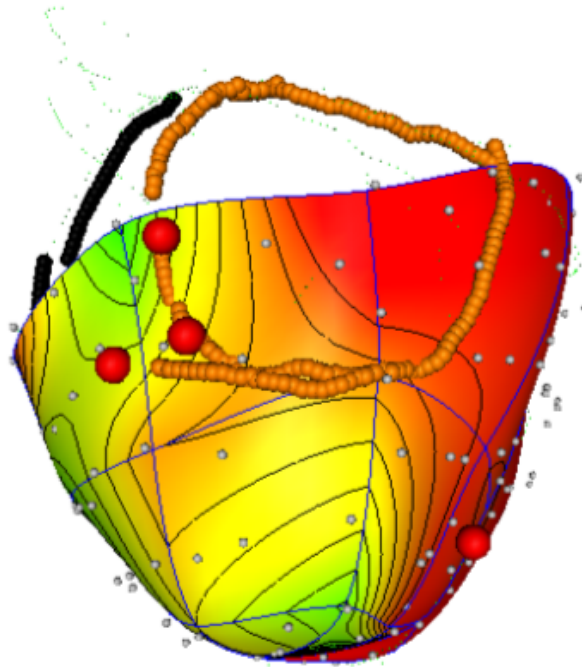


Figure 18: Sample 3D isochronal map developed in Continuity.

## **CHAPTER 3: RESULTS**

### **3.1 Local Electrograms and Activation Times**

Prior to developing epicardial activation maps, it is necessary to find the optimal measure of local activation. To do so, a few different measures were compared. First, the activation time was determined using different modalities (i.e. the maximum negative derivative, the maximum amplitude, the initial onset, etc.). Thereafter, comparison of maps with manipulated signals was compared: unipolar vs. bipolar signals and filtered vs. unfiltered signals.

This optimal measure was used to create maps for a dog with a normal heart and acute simulated cardiac dyssynchrony, a heart with chronic tachycardia-induced heart



failure, and a heart with chronic tachycardia-induced heart failure and a myocardial infarct.

### 3.1.1 Different Modalities for Determining Activation Time

Various qualitative methods exist for determining the time of local activation, some of which depend on factors including morphology, relative amplitudes, and timings of deflections. For unipolar electrograms, the maximum negative derivative has been shown to be the best indication of local activation [29, 30, 32, 36, 44, 47].

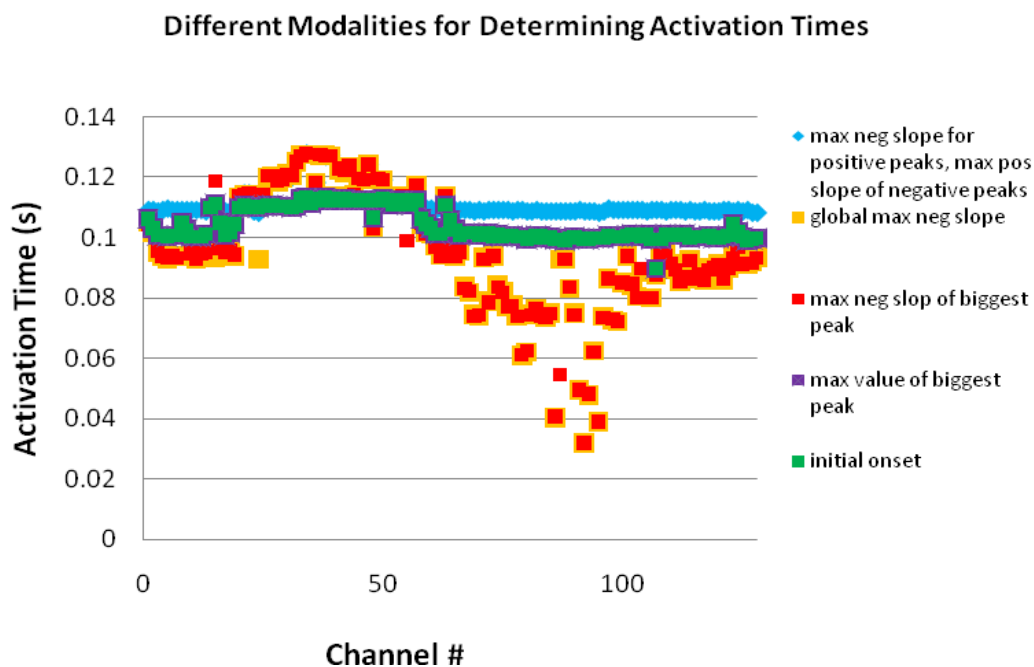


Figure 19: Using the maximum negative slope overall and the maximum slope of the biggest peak is the only method that reveals timing difference in local activation. This confirms that this is, in fact, probably the best determining factor.

Figure 19 shows the timing differences of utilizing different modalities for determining the local activation times. The only modality that revealed significant differences in activation times is the maximum negative slope. The maximum negative derivative will be used throughout this thesis.

### 3.1.2 Positive and Negative Deflections in Local Electrograms

The larger deflection of the electrograms exhibited a pattern where the negative deflection typically had earlier activation times and the positive deflection had later activation times (Figure 20). After careful examination, the earlier activation times (negative deflection) resulted from the electrodes lying on the RV and the later activation times (positive deflection) resulted from the electrodes lying on the LV. The deflection morphology of the electrograms may result of the direction in which the wave front approaches the electrode.

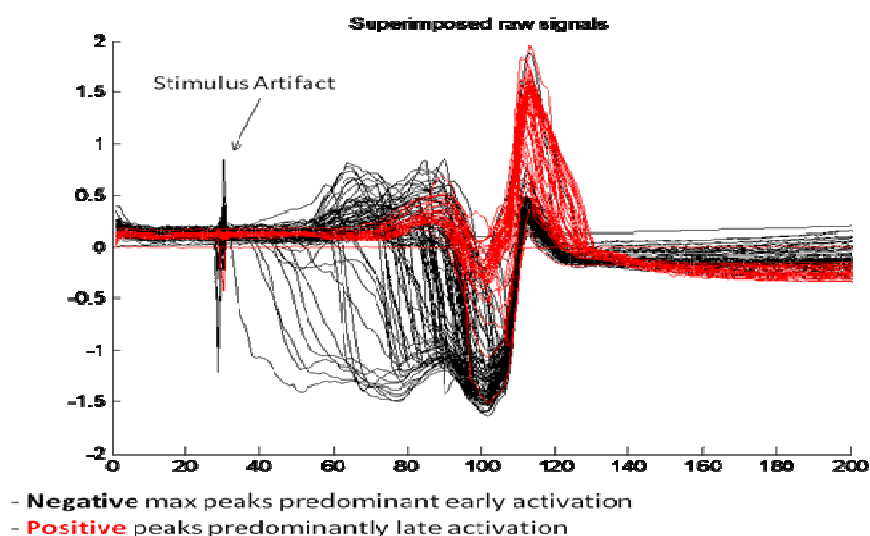


Figure 20: Negative and positive deflections from the 128-electrode sock.

### 3.1.3 Unipolar to Bipolar Signals

The unipolar signals were converted into bipolar signals, whereby, the maximum amplitude was taken to be the local time of activation. It is unclear as to whether analysis of unipolar signals or bipolar signals is optimal as there are benefits of each. Although the converting the unipolar signals into bipolar signals increases the resolution from 128 unipolar electrodes to over 300 bipolar electrodes, the error associated with bipolar activation time fitting in Continuity resulted in a RMS error higher ( $19.3 \pm 6.5$ ) than that from unipolar activation time fitting ( $6.5 \pm 1.7$ ). Analysis of bipolar signals are less sensitive to distant activations [38] and appears to produce epicardial isochronal maps with distinct isochronal lines indicating the precise site of pacing (

Figure 22). The amplitudes of unipolar electrograms are primarily composed of global activity, thus it is possible that low local activity could be obscured.

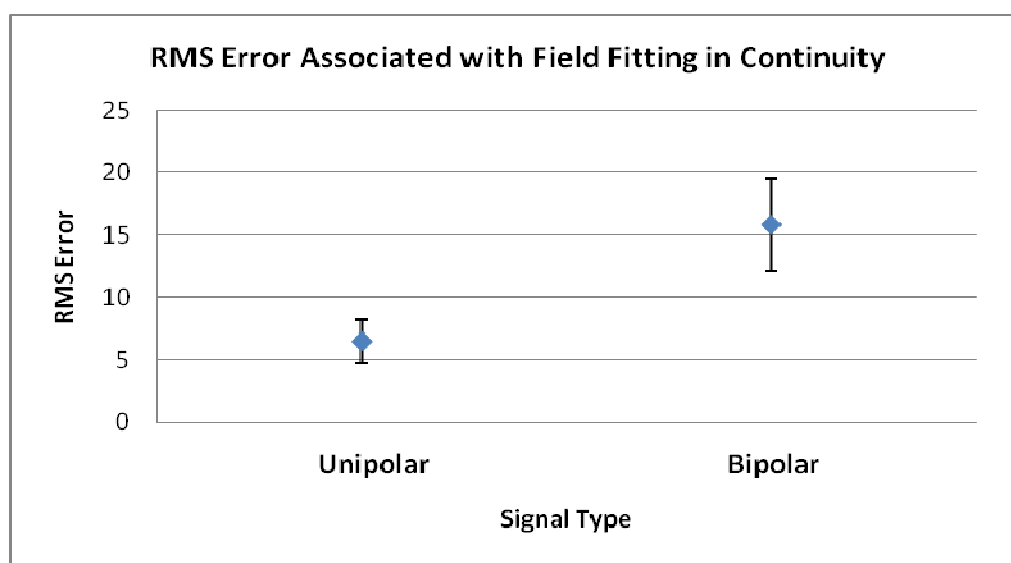


Figure 21: The RMS error associated with the activation times calculated from bipolar signals is high than the activation times calculated from unipolar signals.

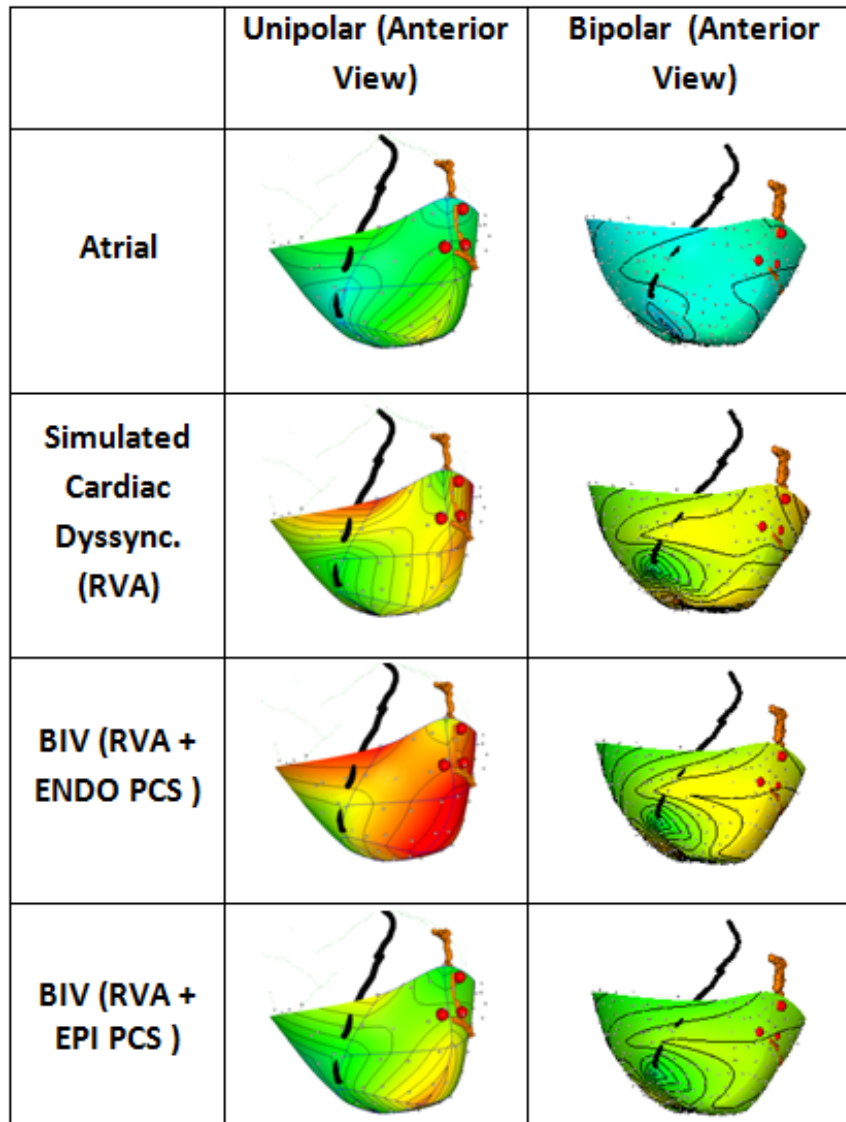


Figure 22: Compares isochronal maps created from unipolar and bipolar electrodes.

### 3.1.4 Filtered Signals

Filtering signals may have two possible results: (1) noise is filtered out, or (2) the resolution of the electrode mapping system is compromised. Here, a case is presented indicating that filtering the signals may, in fact, reduce the noise and result in desirable isochronal maps.

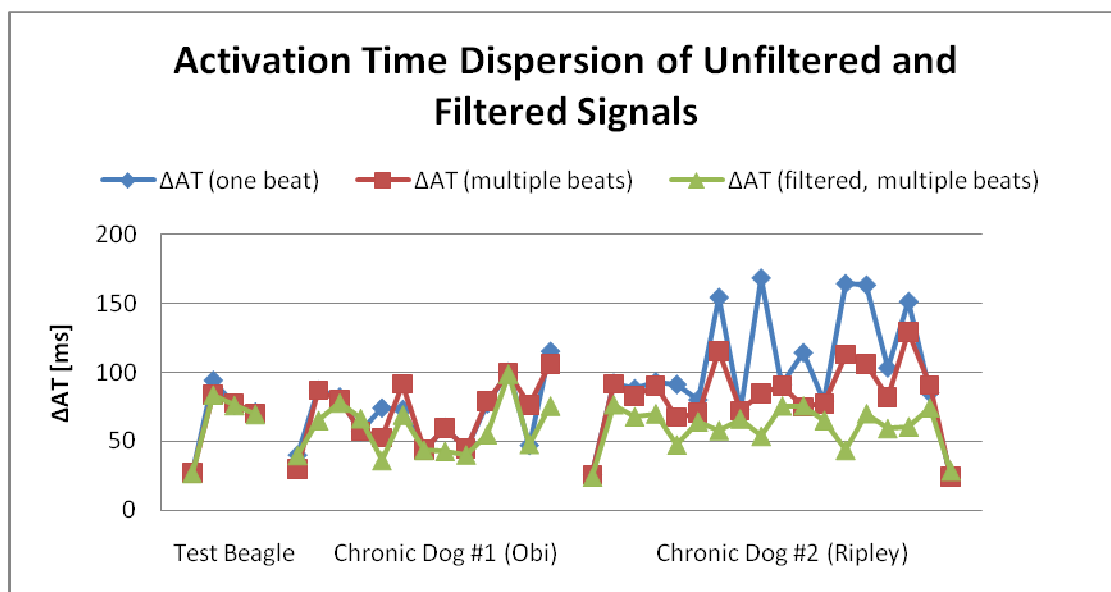


Figure 23: Activation time dispersion resulting from filtering signals.

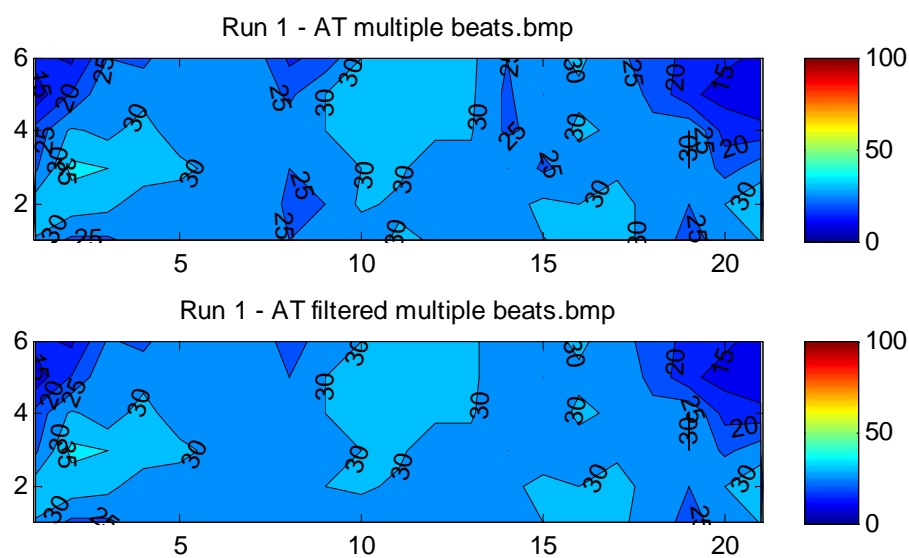


Figure 24: (Top) 2-dimensional isochronal map averaged over multiple beats (Bottom) 2-dimensional isochronal map, from filtered electrode signals, averaged over multiple beats. Notice that the filtered isochronal maps results in a map with more smooth time transitions.

### 3.1.5 Automatic Activation Time Determination Accuracy

It is clear that determining the local activation time manually is extremely time consuming and should be avoided if possible. Manual determination of the location activation is performed by inspecting each local electrogram and visually noting the time of activation (depolarization of the ventricle.) For the 24-electrode sock, this is acceptable. For the 128-electrode sock, however, this should not be performed except under the circumstances that one would like to check the validity of the data.

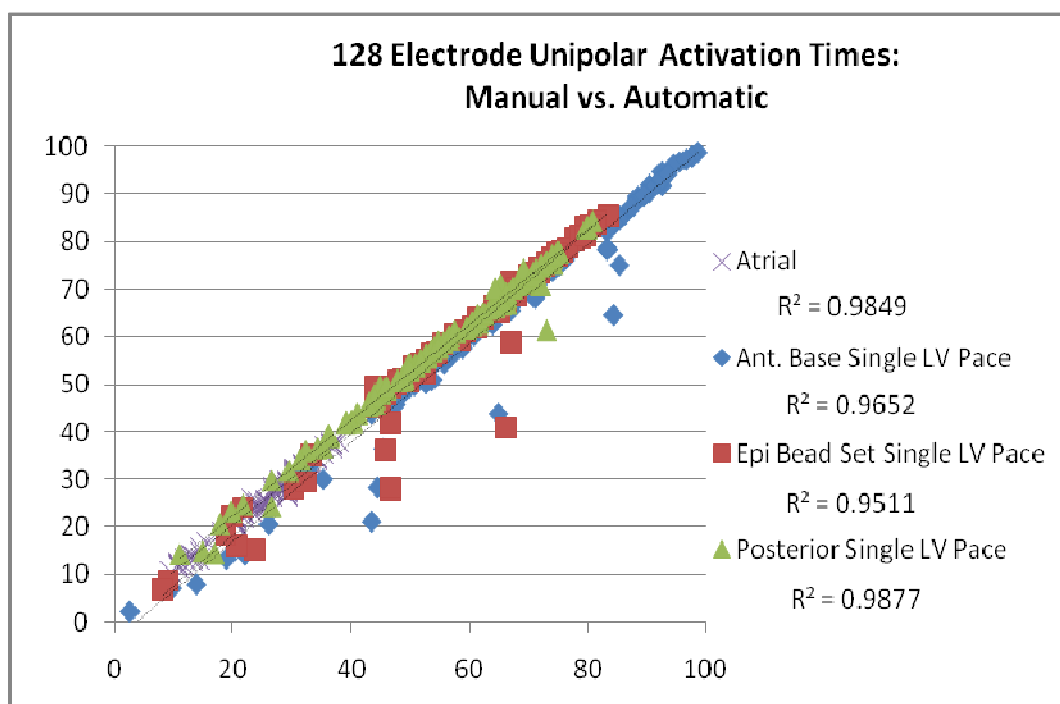


Figure 25: Comparing automatically calculated activation times to the golden standard.

To gain some perspective, for a study with 20 runs using the 128-electrode sock, manual determination would require the user to go through 2,560 individual electrograms. Figure 25 shows that the automatic algorithm is a comparable method to the manual algorithm for determining local activation times. With R-squared values

greater than 0.95, the correlation is high and thus, it is safe to assume that the automatic algorithm for determining local activation times is an accurate method which produces reliable activation times.

### 3.2 Epicardial Excitation in Normal Heart

By inspection of these activation time maps, the epicardial pacing runs have longer activation times than that of the endocardial pacing runs. The average activation time (AT) for epicardial runs is longer than that of the endocardial runs and the time of the latest activation (max AT) for the epicardial runs is greater than or equal to that of the endocardial runs. This preliminary result is parallel with what may be expected. Since the endocardium is the innermost layer of tissue that lines the chambers of the heart, pacing at these sites may lead to faster activation of the heart [48-50]. This data is summarized in the table 10. This is not the case in heart failure and myocardial infarct hearts, however, and will be discuss in the following sections 3.3 and 3.4.

Table 4: Average and maximum activation times from the sock electrodes.

<b>Location of Pacing Site</b>	<b>Average AT (ms)</b>	<b>Max AT (ms)</b>
<b>Endo post cor sinus</b>	23	45
<b>Epi post cor sinus</b>	32	55
<b>Endo postlateral</b>	14	40
<b>Epi postlateral</b>	36	60
<b>Endo lateral</b>	17	40
<b>Epi lateral</b>	54	80
<b>Endo bead set</b>	24	80
<b>Epi bead set</b>	57	80

When comparing total ventricular activation times after a LBBB simulation which prolongs the QRS duration and thus the total activation time, endocardial biventricular

pacing brings the total activation time down closer to that of an atrial run. Thus, it appears as though biventricular pacing from the endocardium is optimal for restoring function when there is left ventricular dyssynchrony. Biventricular pacing reduces electrical asynchrony, with a significant reduction in activation time dispersion.

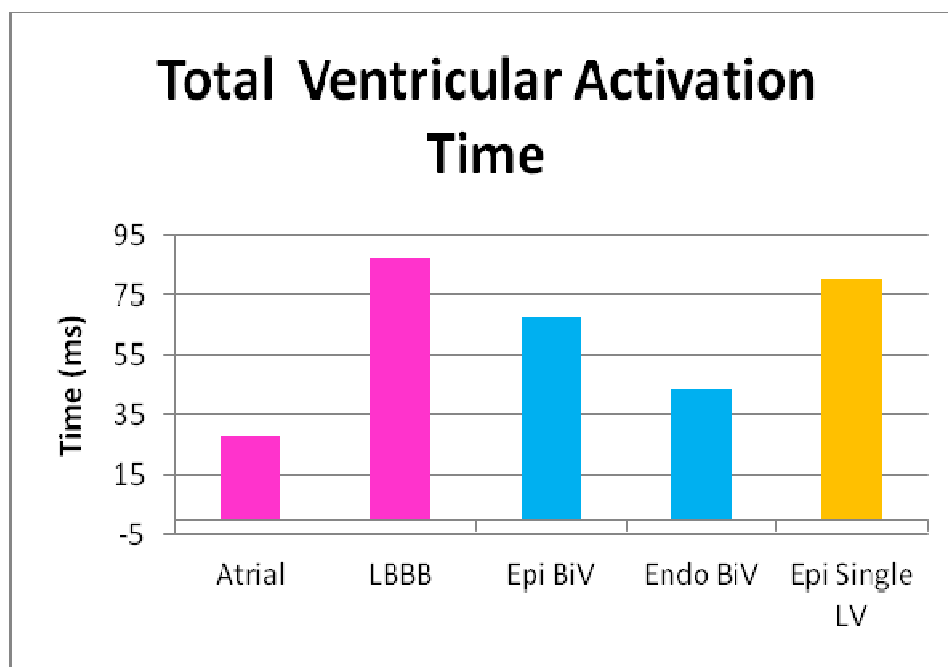


Figure 26. The average activation time dispersion calculated from the 128-electrode sock.

### 3.3 Epicardial Excitation in Tachycardia-Induced Heart Failure

More ventricular synchrony is characterized by shorter activation time dispersion ( $\Delta$ AT [ms]). In the case of heart failure (Figure 27), epicardial and endocardial biventricular pacing produced similar results in ventricular synchrony in 4/5 sites. Biventricular pacing restores more ventricular synchrony than single LV pacing (Figure 28).



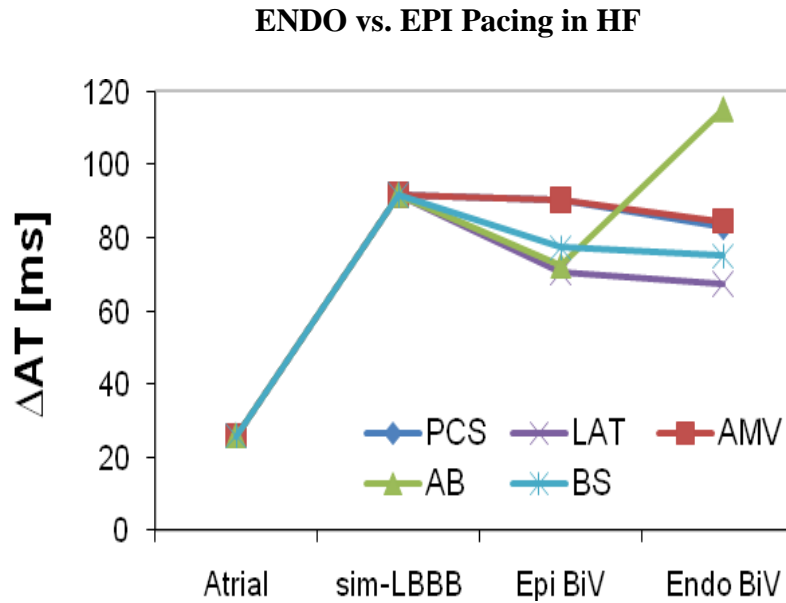


Figure 27: Activation time dispersion resulting from epicardial pacing in heart with heart failure.

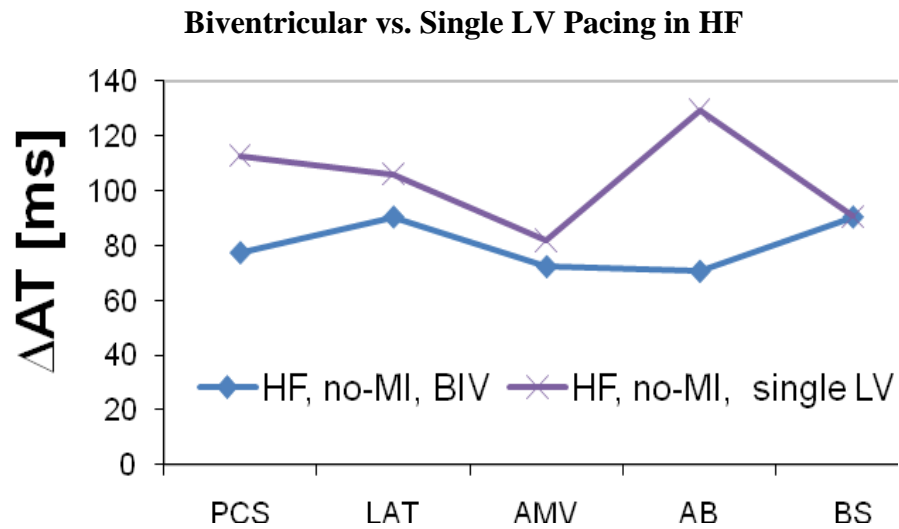


Figure 28: Activation time dispersion comparing biventricular and single left ventricular pacing in hearts with tachycardia-induced heart failure.

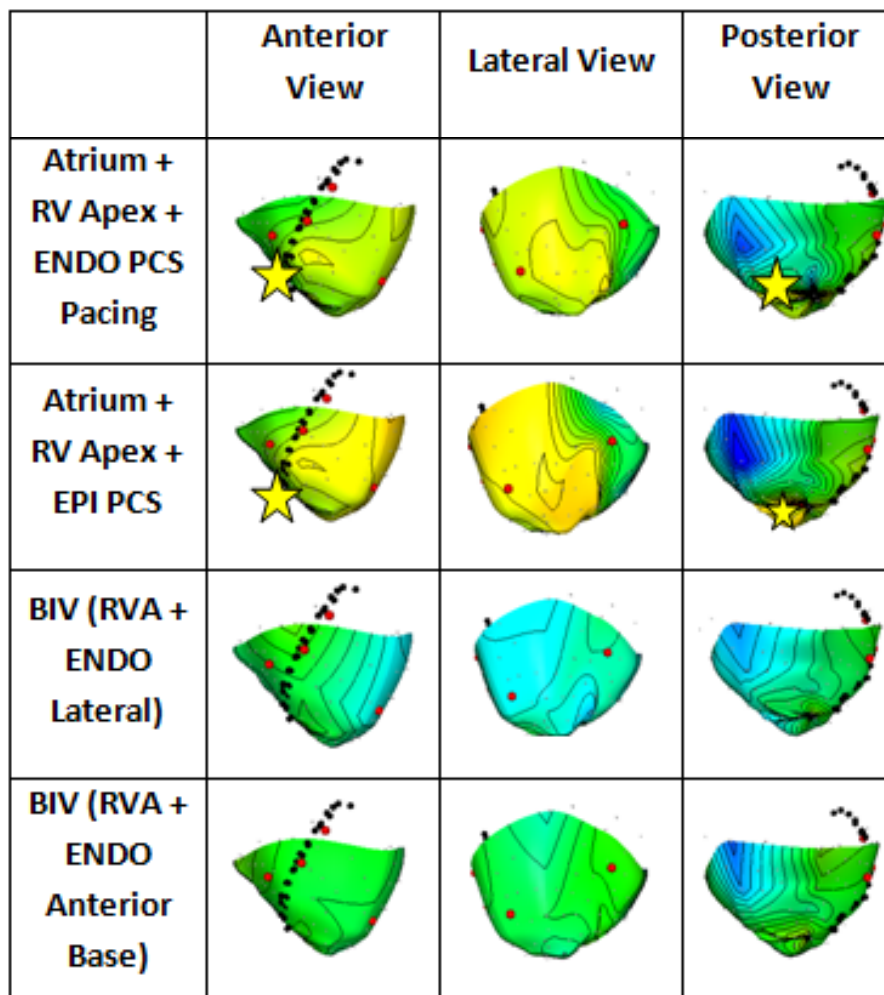


Figure 29: Epicardial activation maps in hearts with tachycardia-induced heart failure.

### 3.4 Epicardial Excitation in Tachycardia-Induced HF with an Infarct

Previously, it had been thought that endocardial pacing always resulted in more ventricular synchrony than epicardial pacing [27, 28, 50, 51]. This is the case because transmural conduction from the endocardium to the epicardium is faster than conduction along the epicardium. However, as seen in Figure 30, endocardial pacing does not always seem to create more ventricular synchrony. Again, more ventricular synchrony is

characterized by shorter activation time dispersion ( $\Delta AT$  [ms]). In the case of heart failure with a myocardial infarct (Figure 30), endocardial pacing is better than epicardial pacing except at the posterior coronary sinus pacing site. Our hypothesis is that epicardial pacing is better at the posterior coronary sinus pacing site because that is where the endocardial myocardial infarct is. Figure 32 shows the epicardial maps. The posterior coronary sinus appears to be the latest site of activation in all the runs, except when the posterior coronary sinus is paced indicating that this may be the infarct site.

In normal hearts, biventricular pacing results in more ventricular synchrony than single ventricular pacing [18, 20, 28]. The data here shows that a hearts with a myocardial infarct and tachycardia-induced heart failure, however, become more synchronous after single LV pacing

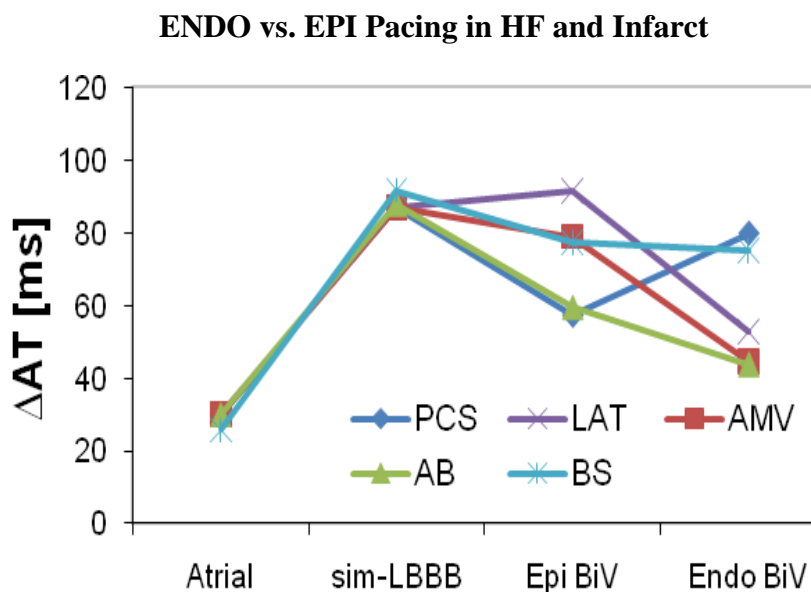


Figure 30: Activation time dispersion resulting from epicardial pacing in heart with heart failure and a myocardial infarct on the lateral wall.

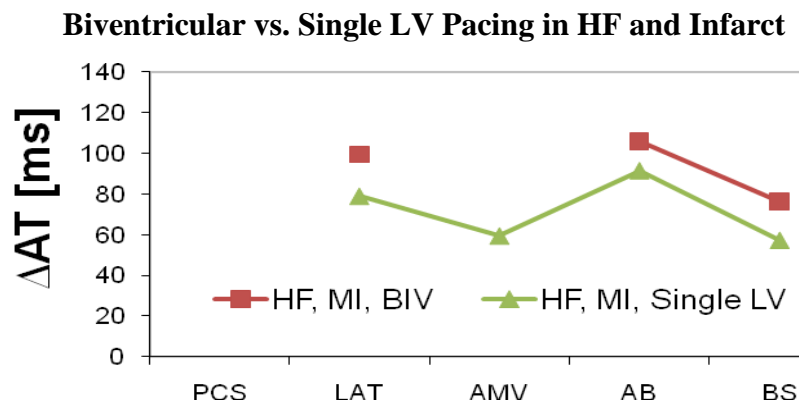


Figure 31: Activation time dispersion comparing biventricular and single left ventricular pacing in hearts with tachycardia-induced heart failure and a myocardial infarct.

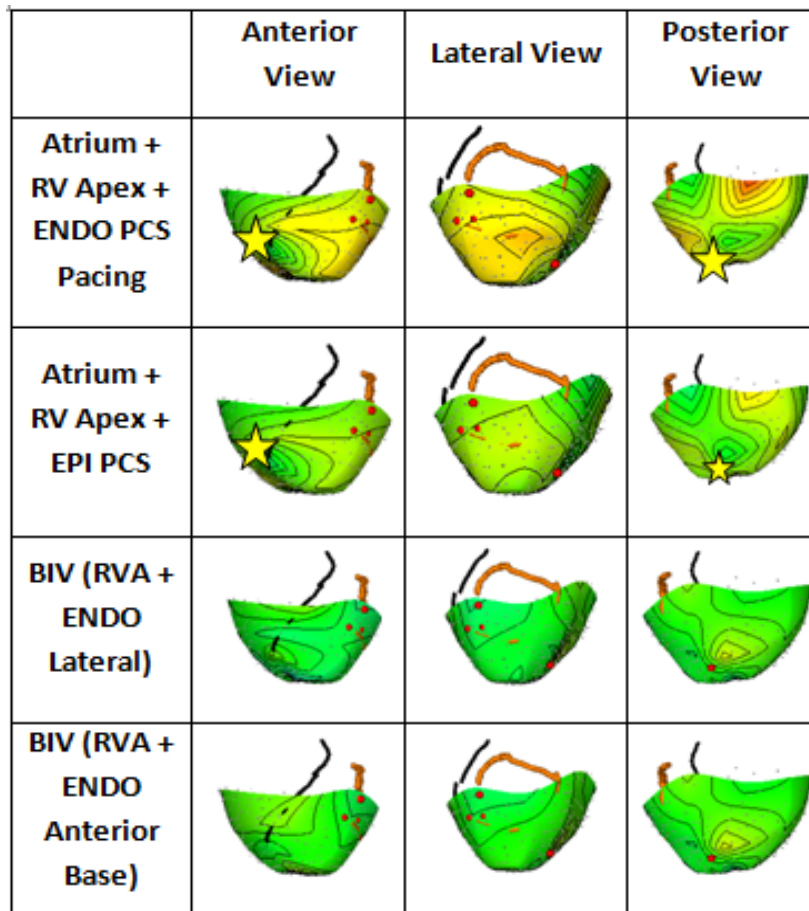


Figure 32: Isochronal maps comparing isochronal maps from ENDO and EPI posterior coronary sinus pacing reveal that endocardial pacing does not always restore synchrony better than epicardial pacing.

## **CHAPTER 4: DISCUSSION**

### **4.1 Local Activation Determination**

The determination of local activation time can be best calculated using the maximum negative derivative averaged over multiple beats (between 5 – 20 beats) of either unfiltered unipolar or bipolar electrograms. There are advantages of both unipolar and bipolar signals. Analysis of unipolar signals may offer more insight into the global activity, however, low amplitude local activity could be obscured. Analysis of bipolar

electrograms produces isochronal maps with more resolution locally, shown by distinctive closely spaced isochronal lines indicating the site of pacing.

## **4.2 Effects of Myocardial Infarcts on Local Activation**

Isochronal mapping has proven to be effective in characterizing potential distributions on the epicardial surface of the heart [52]. By inspection of epicardial activation time maps in normal hearts, endocardial pacing restores more ventricular synchrony than epicardial pacing. Recent data from Lambiase indicated that simultaneous pacing from the LV endocardium and endocardial RV apex elicited the largest increase in hemodynamic function, the shortest LV endocardial activation time, and the narrowest QRS complex [27]. The contrary is true for hearts with heart failure and myocardial infarcts. In the presence of heart failure, it is observed that endocardial pacing did not create more ventricular synchrony than epicardial pacing. In fact, for the anterior base pacing site, epicardial pacing ( $\Delta AT=72.2\text{ms}$ ) creates more ventricular electrical synchrony than endocardial pacing ( $\Delta AT=115.1\text{ms}$ ). In the presence of heart failure and a myocardial infarct on the lateral epicardium, it is observed that endocardial pacing creates more ventricular synchrony, except when the heart is paced at the posterior coronary sinus pacing site. When the heart was paced at the coronary pacing site, epicardial pacing ( $\Delta AT=57.5\text{ms}$ ) creates more electrical synchrony than endocardial pacing ( $\Delta AT=79.8\text{ms}$ ). Our hypothesis is that epicardial pacing is better at the posterior coronary sinus pacing site because that is where the endocardial myocardial infarct is. A myocardial infarct is an interruption of blood supply due to the occlusion of a coronary artery close to the epicardial surface, blocking the blood supply through the

smaller branches leading into the endocardium. A myocardial infarct may have a more damaging effect on the endocardium as a result of this, thus, the endocardium of the location of the myocardial infarct may not be able to activated properly and conduct [53].

### **4.3 Purkinje System**

There has been controversy as to whether the Purkinje System is activated during LV pacing. In these studies, the Purkinje system is not inactivated, thus, when the epicardium is paced, the activation should slowly conduct in a retrograde direction into the Purkinje system and thereafter conduct quickly through the Purkinje network back out to the epicardium. When the endocardium is paced, the activation should quickly conduct through the Purkinje System into the epicardium. If this does in fact happen, it should result in a few things: (1) Epicardial pacing should have a site of earlier activation compared to endocardial pacing (a smaller minimum activation time), and (2) endocardial pacing should have a smaller activation time spread than epicardial pacing indicating that the Purkinje Network is activated quicker and thus the entire epicardium is activated quicker. If the Purkinje system is not activated, the phenomenon of endocardial pacing exhibiting shorter activation time dispersion can be explained by the conduction occurring faster on the endocardial then spreading out transmurally to the epicardium.

## 4.4 Noisy Local Electrograms

The noisy channels vary between each run and may be due to the contact of the electrode sock with the heart. It is feasible to assume that the result may be due to excess blood inhibiting contact of the sock with the heart. For future studies, ample saline should be applied to the heart during the surgery in an attempt to eliminate undesirable local electrogram recordings.

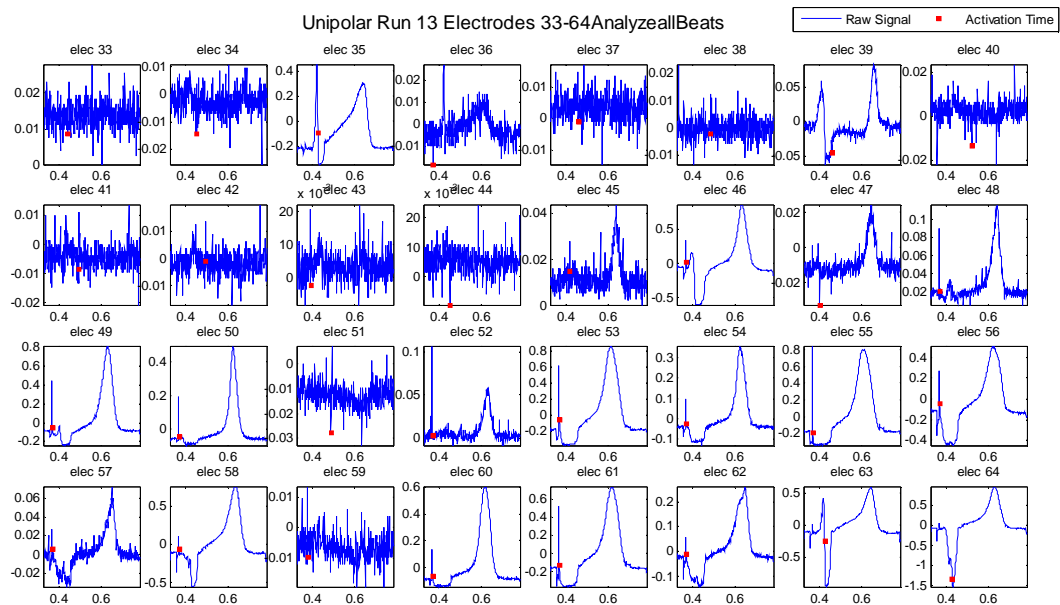


Figure 33: The local electrograms from the second chronic dog, Ripley, show a significant number of noisy electrode channels where 33 out of 128 electrodes (over 25%) are noisy.

Another aspect of Ripley's local electrograms that is worth noting is the inverted electrogram and the presence of the ventricular stimulus artifact. The ventricular stimulus may be apparent only in Ripley because this animal was paced at higher voltages.

Although it is true that these noise signals can be filtered, it is uncertain as to whether filtering causes loss of data and/or an incorrect activation time. Figure 34 shows



the resulting 2D isochronal maps for the activation times determined using: (1) raw signals over one beat, (2) raw signals averaged over multiple beats, and (3) filtered signals averaged over multiple beats.

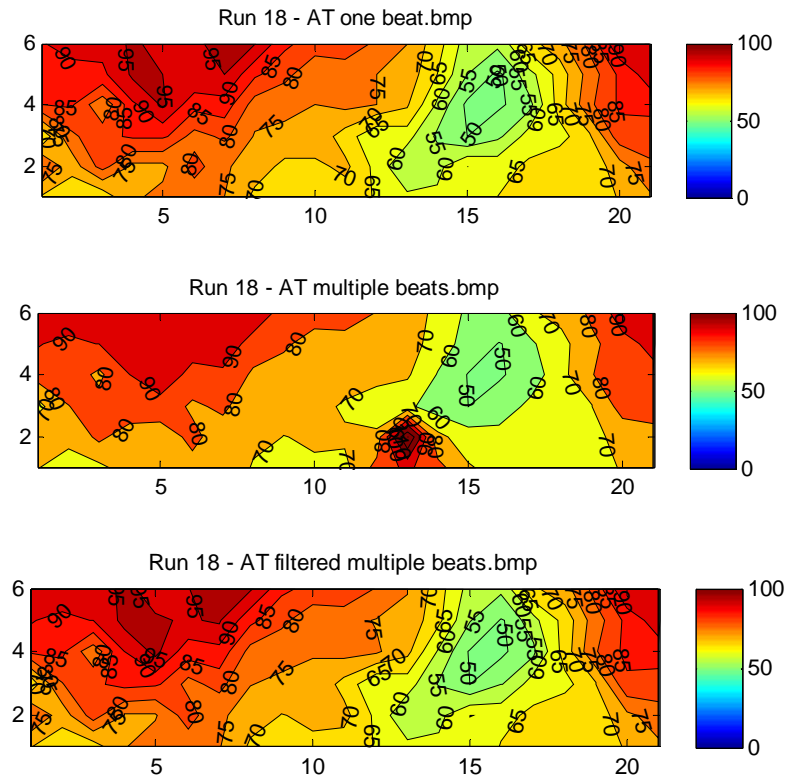


Figure 34: 2D isochronal maps for the activation time determined for one beat, averaged over multiple beats, and filtered signals averaged over multiple beats.

## 4.5 Limitations

This system is primarily for off-line analysis. It would be beneficial to visualize the 3D activation sequence in real-time to ensure that the electrode has proper contact with the epicardium of the heart so that detailed electrophysiology models can be developed in Matlab. Currently the 3D display cannot be done in real-time since activation data needs to be calculated.

It would be interesting to be able to input these epicardial activation times into Continuity and predict endocardial activation times. This would require an epicardial electrode sock, which records epicardial electrocardiograms, and an endocardial balloon catheter, which measures the endocardial electrograms.

The current electrode socks are constructed with the electrodes in no particular pattern. It would be beneficial to pull a sock over a fixed heart, where then the electrodes can be manually sewn on.

Beside from the local activation times, all the other information contained in the recorded potentials is ignored. It has been suggested that this additional information can be used to estimate the direction in which an activation front passes an electrode, the location of infarcts. Depending on the limited resolution of the electrodes, minor changes in activation times may not have been detected. It may be beneficial to perform a sensitivity analysis on this data and determine the effect of sparse recording electrodes on the resulting isochronal map.

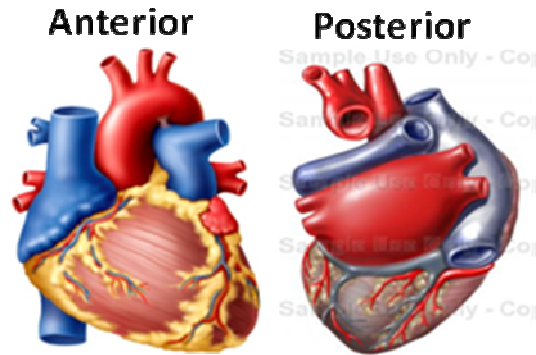
## **CHAPTER 5: CONCLUSIONS**

Characterization of the spread of electrical activation in both RV and LV has enabled a much better understanding of how CRT may potentially be applied in different patient populations presented with different activation patterns.

The method presented in this thesis provides an efficient technique to estimate epicardial activation time parameters and thus will prove useful as the electrophysiological input for predictive patient-specific computational model development. By developing three-dimensional isochronal maps, the sequence of

ventricular activation in normal hearts, hearts with heart failure, hearts with myocardial infarcts, and hearts with ventricular dyssynchrony (such as left bundle branch block) can be visualized. Through the use of a 128-electrode sock array, it is confirmed that the local activation time is most efficiently calculated using the time of the maximum negative derivative averaged over multiple beats for unipolar signals and the maximum amplitude for bipolar signals. Automatic determination of the activation times proved to be comparable to manual determination (the standard). It is also seen that filtering signals causes a lost data and should be avoided if possible. The calculated activation times are then input into an anatomically fit geometry of the heart to create an epicardial isochronal activation map in a multi-scale modeling software. Inspection of these maps reveals that endocardial pacing does not always restore more ventricular synchrony when compared to epicardial pacing and that biventricular pacing doesn't always restore more ventricular synchrony when compared to single LV pacing, typically in the presence of tachycardia-induced heart failure and a myocardial infarct.

## APPENDIX A: ISOCHRONAL MAPS



Anterior and posterior view of the heart. The socks are visualized in this orientation.

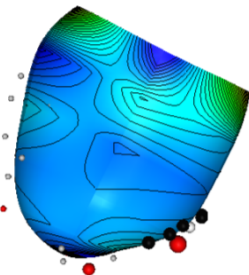
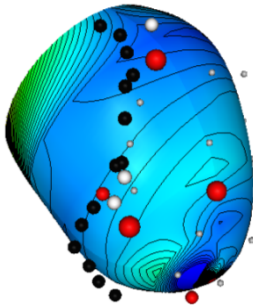
### Acute Dog #2: 24-Electrode Bipolar Sock, Simulate LBBB, Single LV Pace

---

#### Atrial Pacing

Anterior View

Posterior View

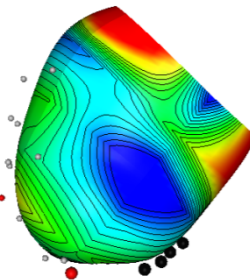
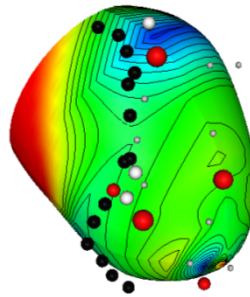


#### Simulated LBBB

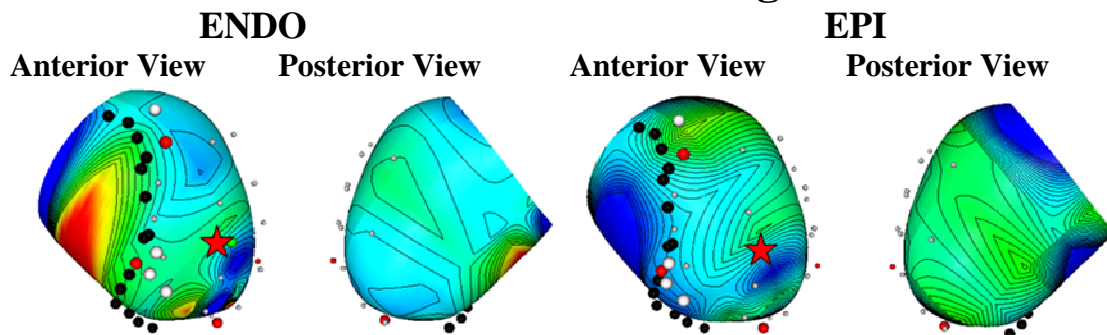
(Atrium + RV Apex)

Anterior View

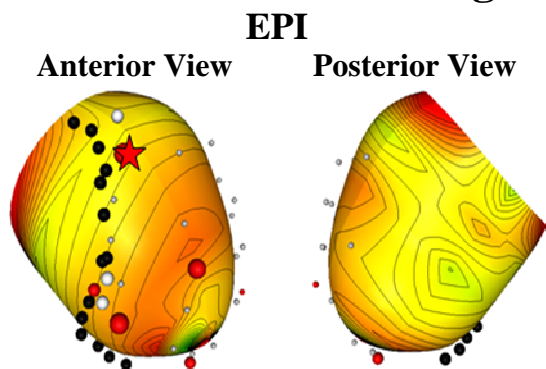
Posterior View



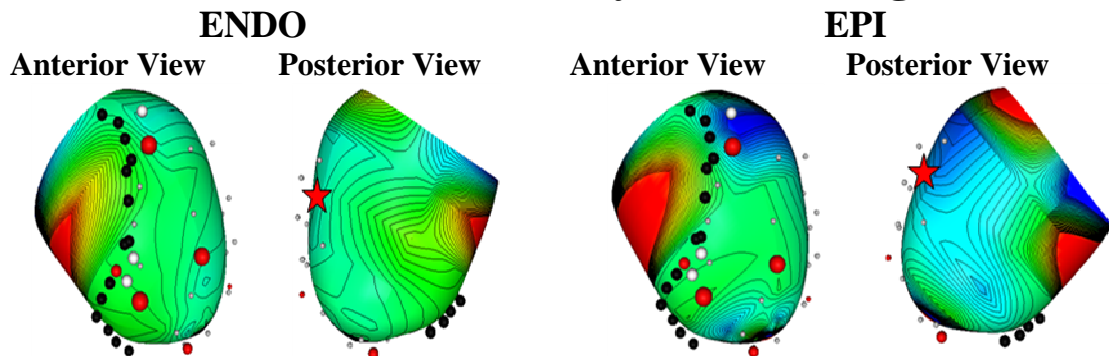
## Lateral Wall Pacing



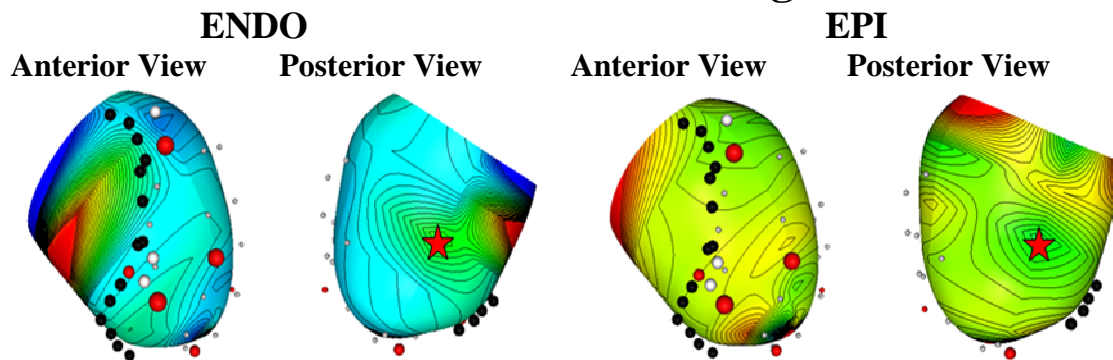
## Anterior Base Pacing



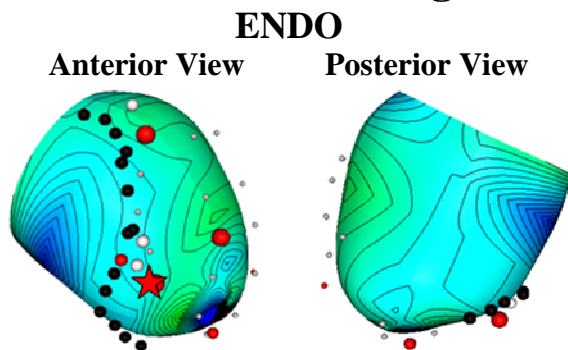
## Posterior Coronary Sinus Pacing



## Posterolateral Pacing



## Bead Set Pacing



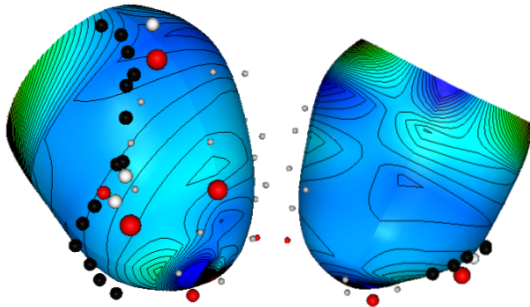
## Acute Dog #3: 24-Electrode Bipolar Sock, Simulate LBBB, Single LV Pace

---

### Atrial Pacing

Anterior View

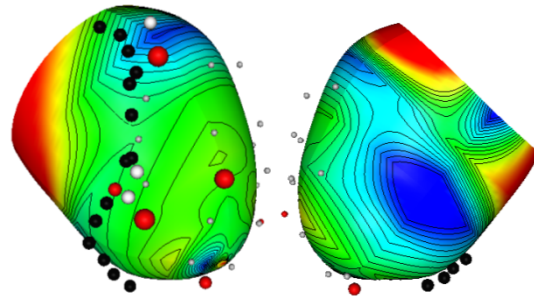
Posterior View



### Simulated LBBB (Atrium + RV Apex)

Anterior View

Posterior View



### Atrium + Lateral Wall Pacing

ENDO

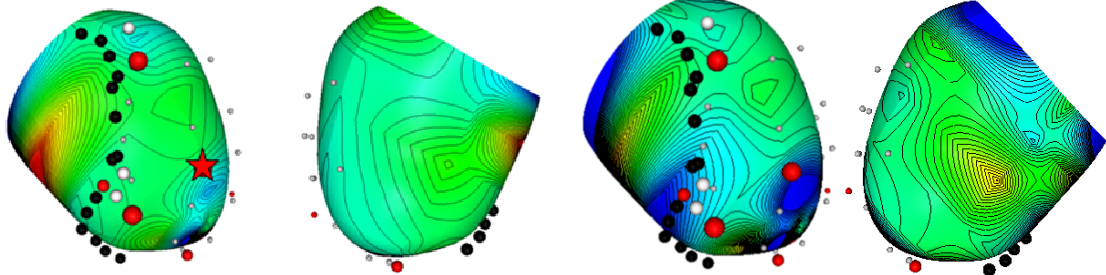
EPI

Anterior View

Posterior View

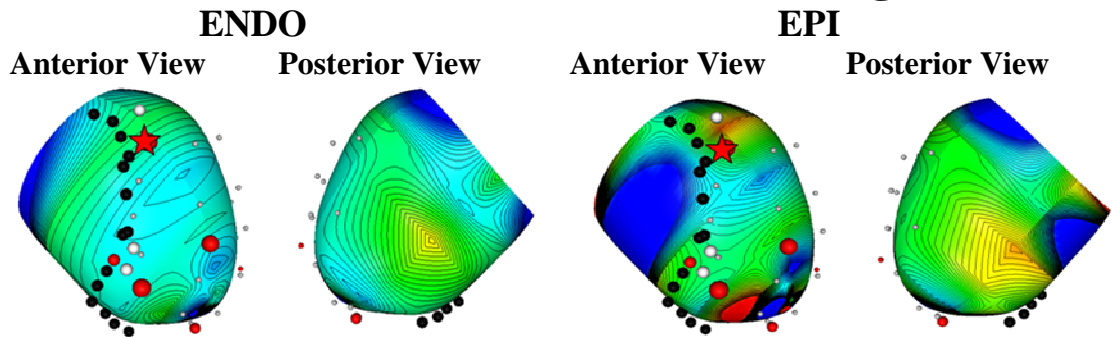
Anterior View

Posterior View

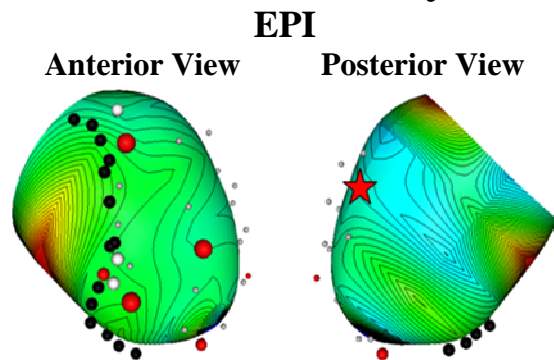




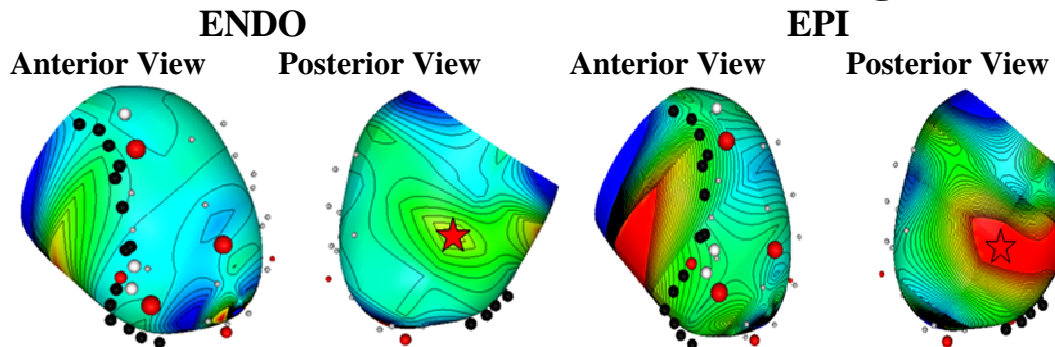
## Atrium + Anterior Base Pacing



## Atrium + Posterior Coronary Sinus Pacing



## Atrium + Posterolateral Pacing



## Atrium + Bead Set Pacing

ENDO

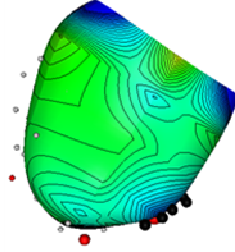
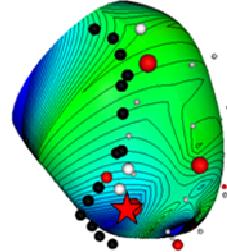
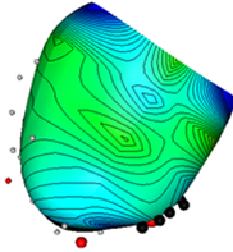
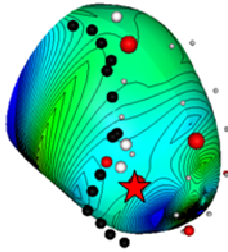
EPI

Anterior View

Posterior View

Anterior View

Posterior View

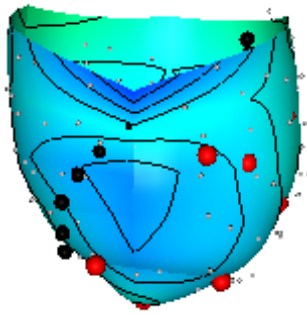


## Acute Dog #1, Test Beagle: 128-electrode Unipolar Sock, Single LV Pacing

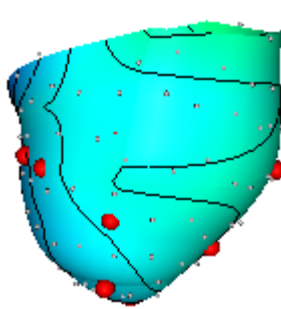
---

### Atrial Pacing

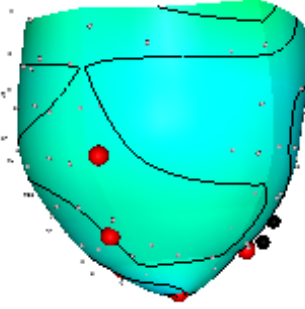
Anterior View



Lateral View

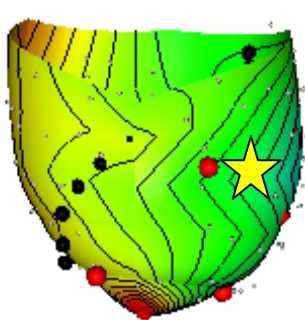


Posterior View



### Atrium + EPI Ventricular Anterior Base Pacing

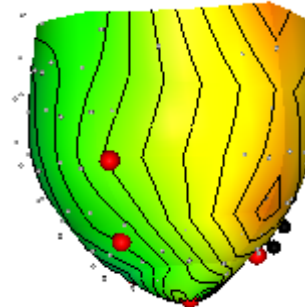
Anterior View



Lateral View

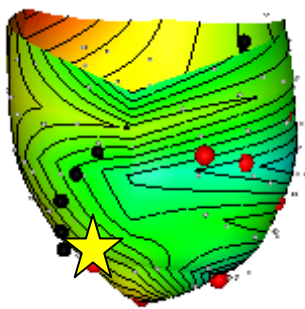


Posterior View

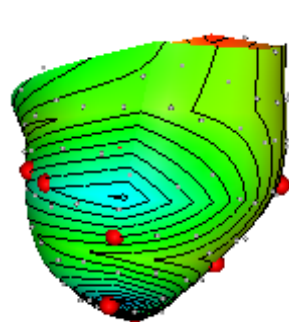


### Atrium + EPI Bead Set Pacing

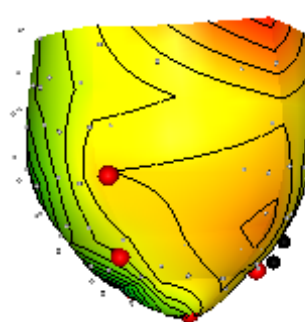
Anterior View



Lateral View

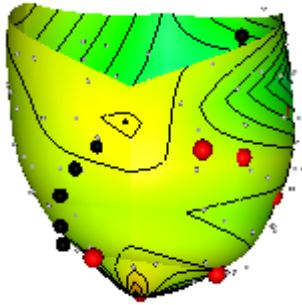


Posterior View

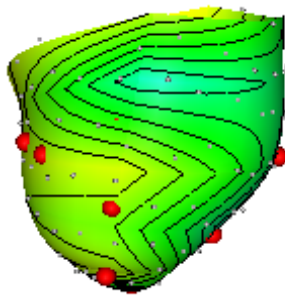


## Atrium + EPI Ventricular PCS Pacing

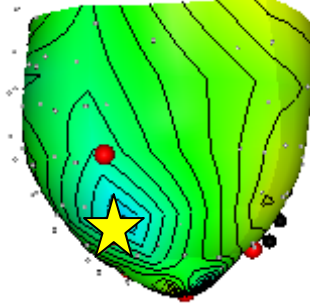
Anterior View



Lateral View



Posterior View

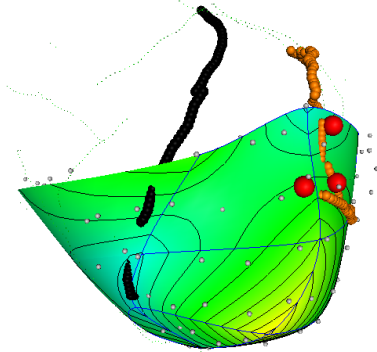


## Chronic Dog #1, OBI: 128-Electrode Sock, Unipolar Signals, Tachycardia-Induced Heart Failure with Myocardial Infarct

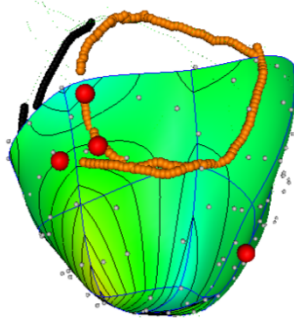
---

### Atrial Pacing

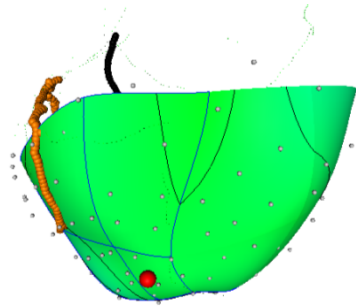
Anterior View



Lateral View

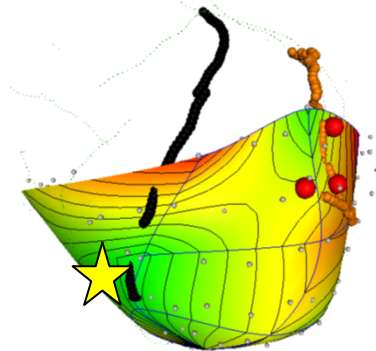


Posterior View

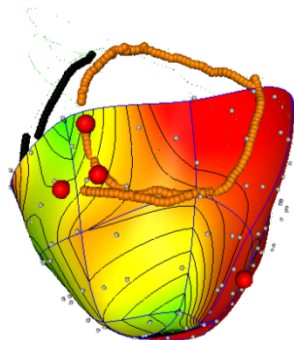


### Simulated LBBB (Atrium + RV Apex) Pacing

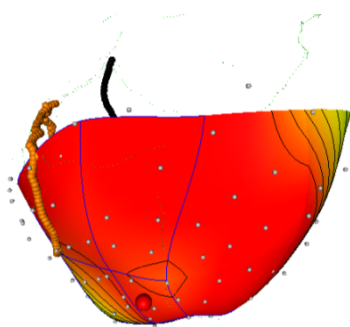
Anterior View



Lateral View



Posterior View

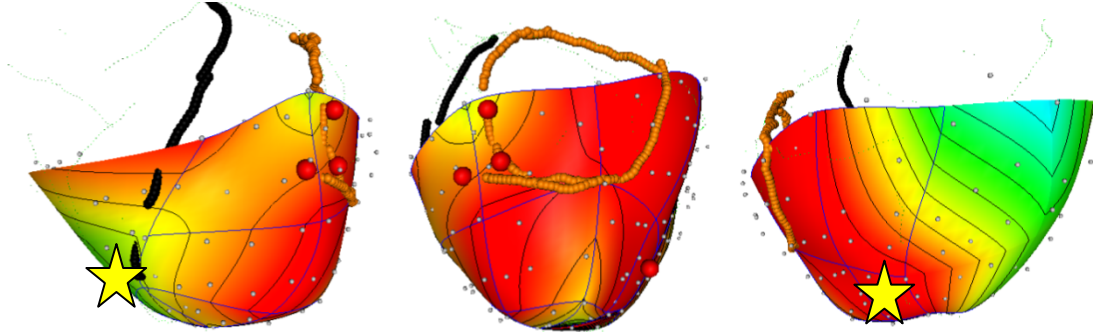


### Atrium + RV Apex + ENDO PCS Pacing

Anterior View

Lateral View

Posterior View

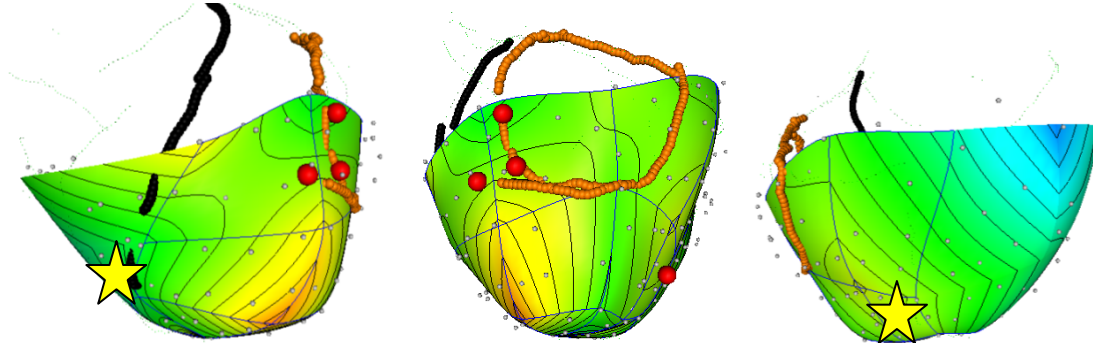


### Atrium + RV Apex + EPI PCS Pacing

Anterior View

Lateral View

Posterior View

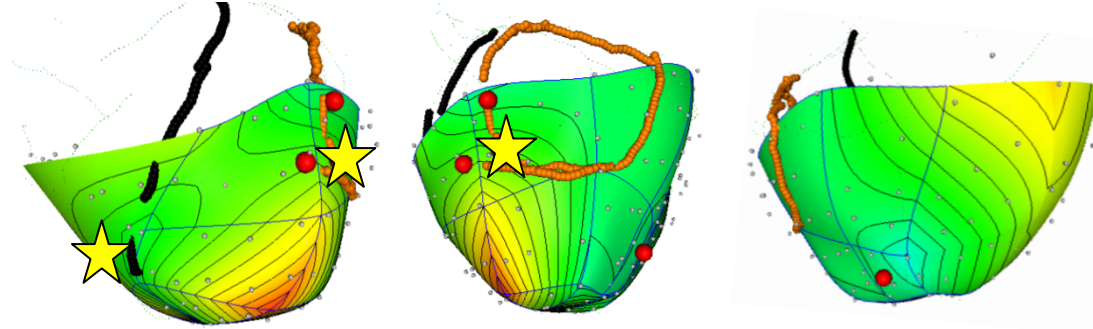


### Atrium + RV Apex + ENDO Lateral Pacing

Anterior View

Lateral View

Posterior View

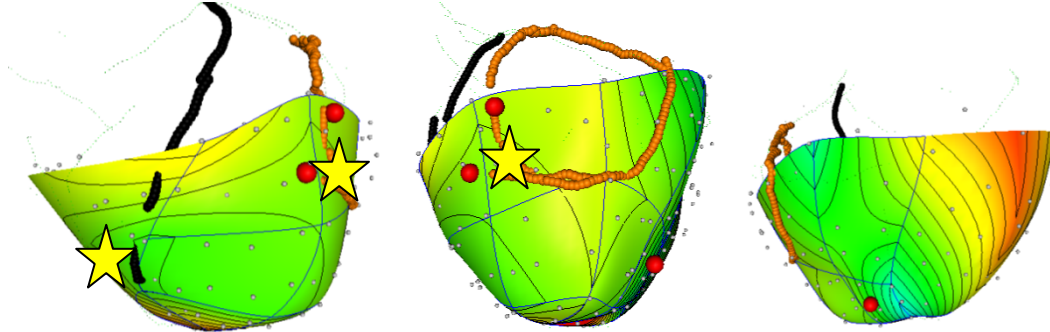


### Atrium + RV Apex + EPI Lateral Pacing

Anterior View

Lateral View

Posterior View

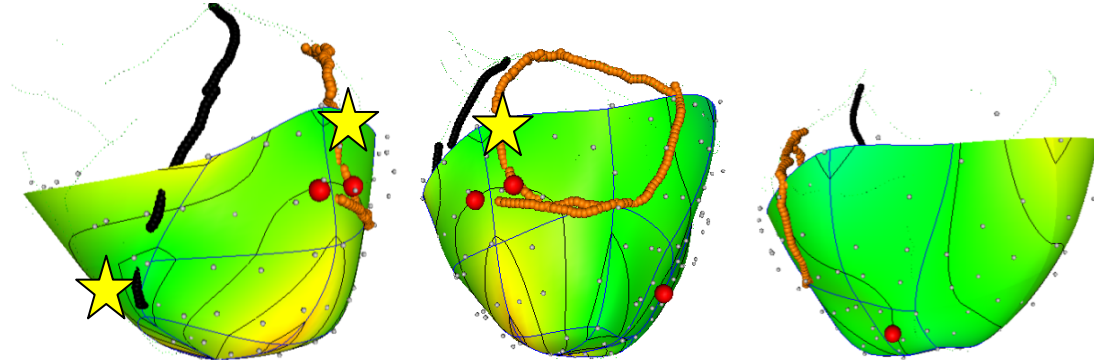


### Atrium + RV Apex + ENDO Anterior Base Pacing

Anterior View

Lateral View

Posterior View

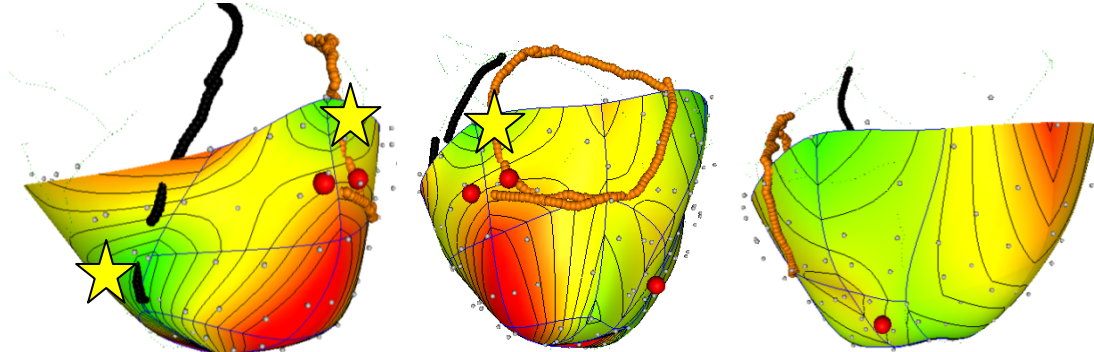


### Atrium + RV Apex + EPI Anterior Base Pacing

Anterior View

Lateral View

Posterior View

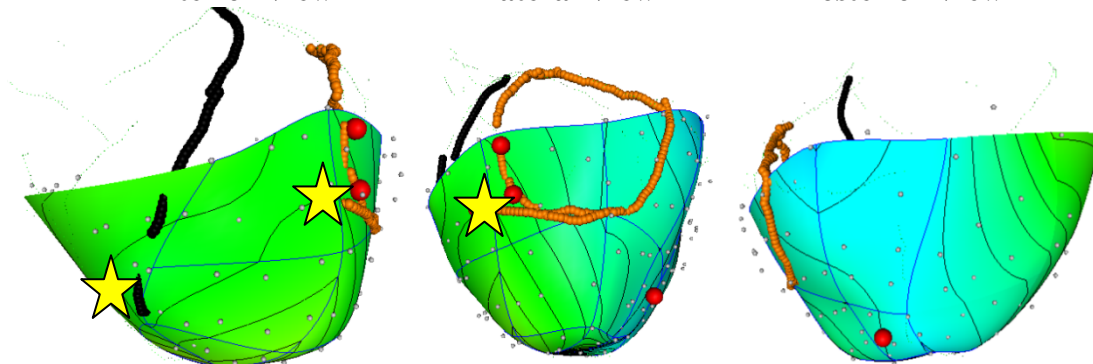


**Atrium + RV Apex + ENDO Anterior Mid-Ventricle Pacing**

Anterior View

Lateral View

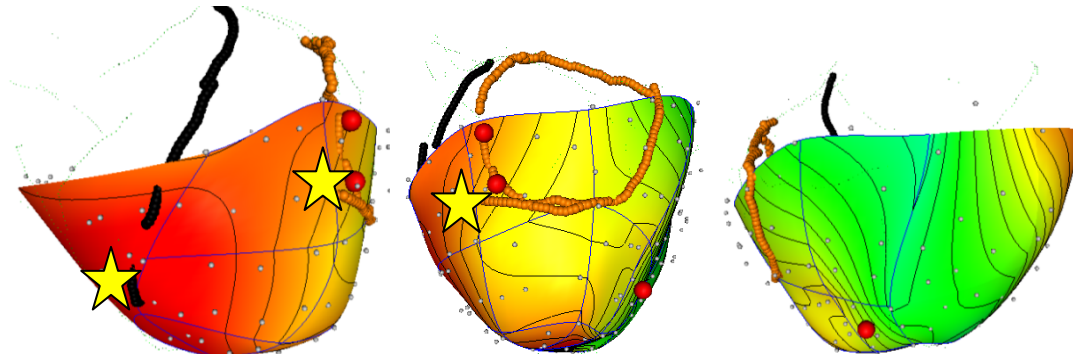
Posterior View

**Atrium + RV Apex + EPI Anterior Mid-Ventricle Pacing**

Anterior View

Lateral View

Posterior View

**Atrium + EPI Anterior Mid-Ventricle Pacing**

Anterior View

Lateral View

Posterior View





## Atrium + EPI Posterior Coronary Sinus Pacing

Anterior View

Lateral View

Posterior View

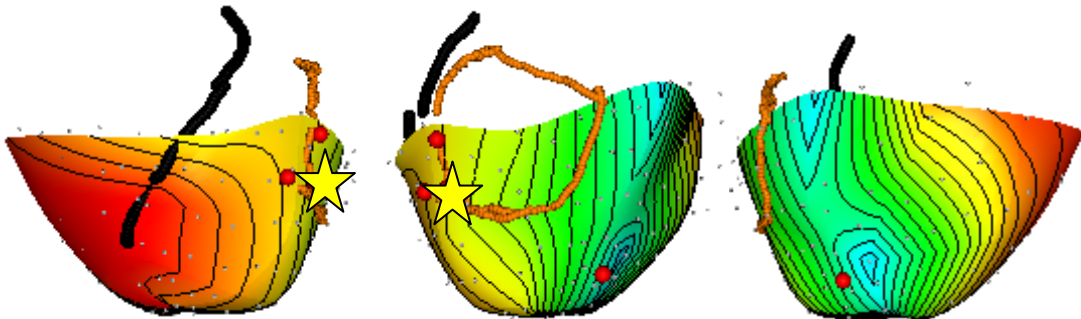


## Atrium + EPI Lateral Pacing

Anterior View

Lateral View

Posterior View



**Chronic Dog #1, OBI: 128-Electrode Sock, Bipolar  
Signals, Tachycardia-Induced Heart Failure with  
Myocardial Infarct**

---

**Atrial Pacing**

Anterior View

Lateral View

Posterior View



**Simulated LBBB (Atrium + RV Apex) Pacing**

Anterior View

Lateral View

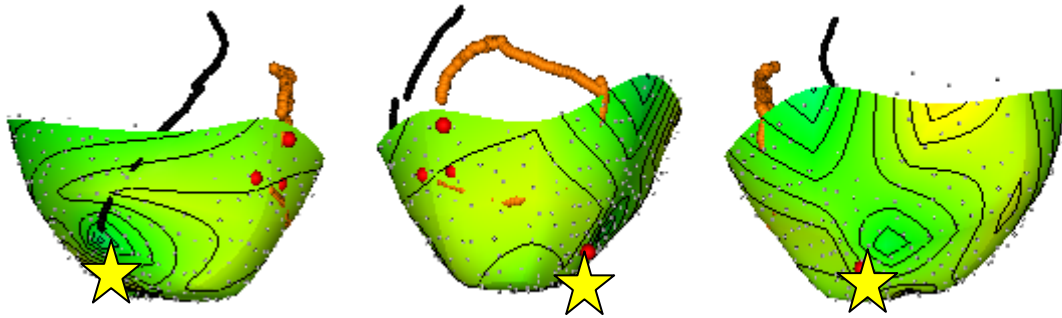
Posterior View



**Atrium + RV Apex + ENDO PCS Pacing**  
 Anterior View      Lateral View      Posterior View



**Atrium + RV Apex + EPI PCS Paing**  
 Anterior View      Lateral View      Posterior View



**Atrium + RV Apex + ENDO Lateral Pacing**  
 Anterior View      Lateral View      Posterior View



**Atrium + RV Apex + EPI Lateral Pacing**

Anterior View

Lateral View

Posterior View



### Atrium + RV Apex + ENDO Anterior Base Pacing

Anterior View

Lateral View

Posterior View



### Atrium + RV Apex + EPI Anterior Base Pacing

Anterior View

Lateral View

Posterior View



### Atrium + RV Apex + ENDO Anterior Mid-Ventricle Pacing

Anterior View

Lateral View

Posterior View





**Atrium + RV Apex + EPI Anterior Mid-Ventricle Pacing**

Anterior View

Lateral View

Posterior View



**Atrium + EPI Anterior Mid-Ventricle Pacing**

Anterior View

Lateral View

Posterior View



**Atrium + EPI PCS Pacing**

Anterior View

Lateral View

Posterior View



### Atrium + EPI Lateral

Anterior View

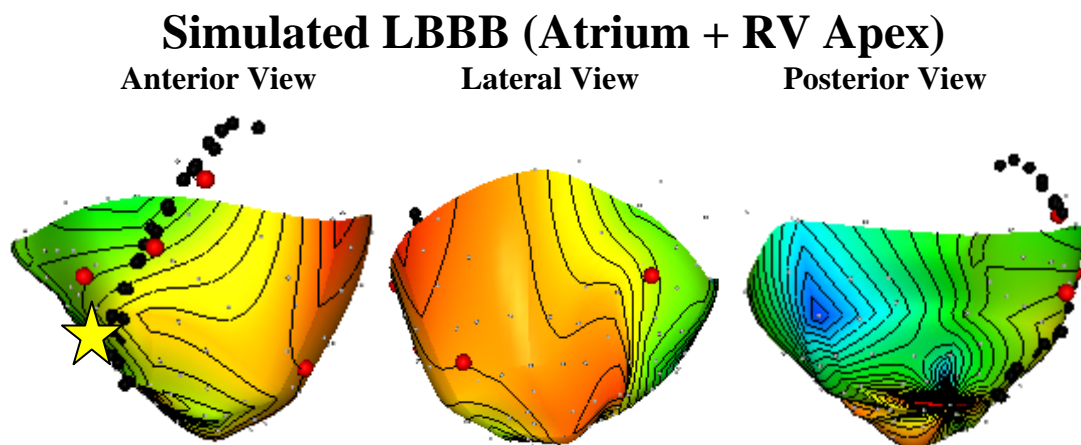
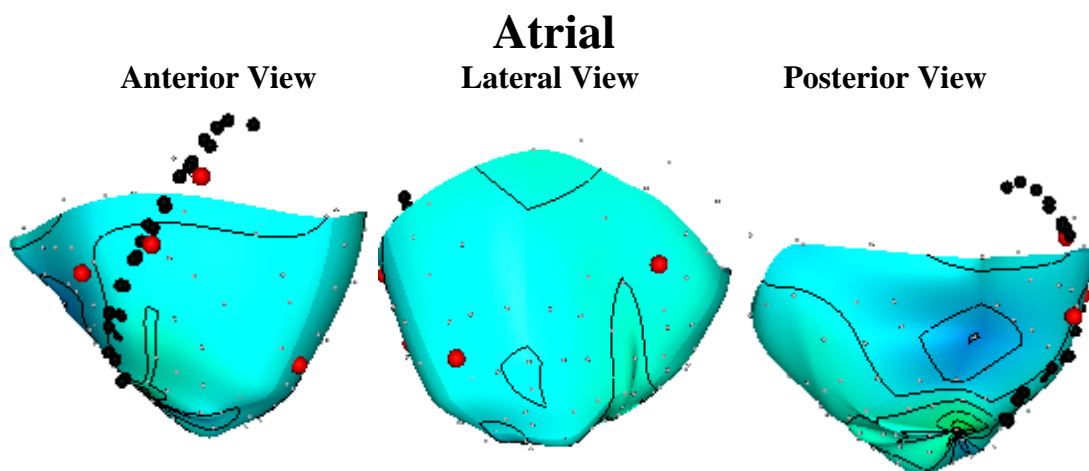
Lateral View

Posterior View



**Chronic Dog #2, RIPLEY: 128-Electrode Unipolar  
Sock, Tachycardia-Induced Heart Failure, No  
Myocardial Infarct**

---

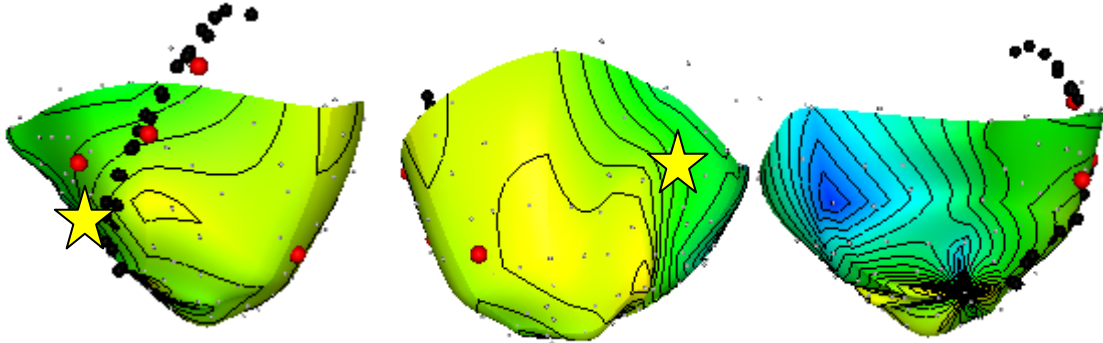


### Atrium + RV Apex + Endo PCS Pacing

Anterior View

Lateral View

Posterior View

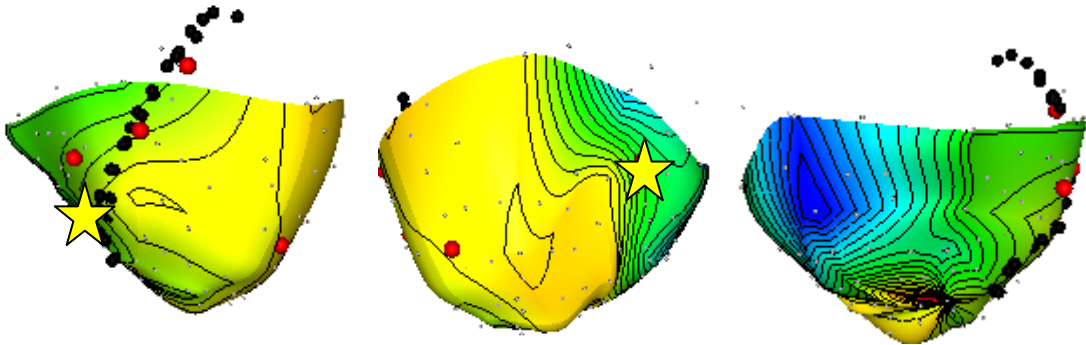


### Atrium + RV Apex + EPI PCS Pacing

Anterior View

Lateral View

Posterior View

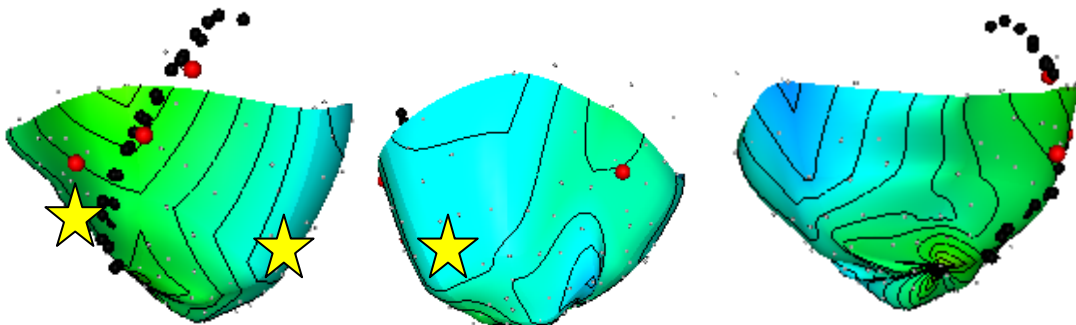


### Atrium + RV Apex + ENDO Lateral Pacing

Anterior View

Lateral View

Posterior View



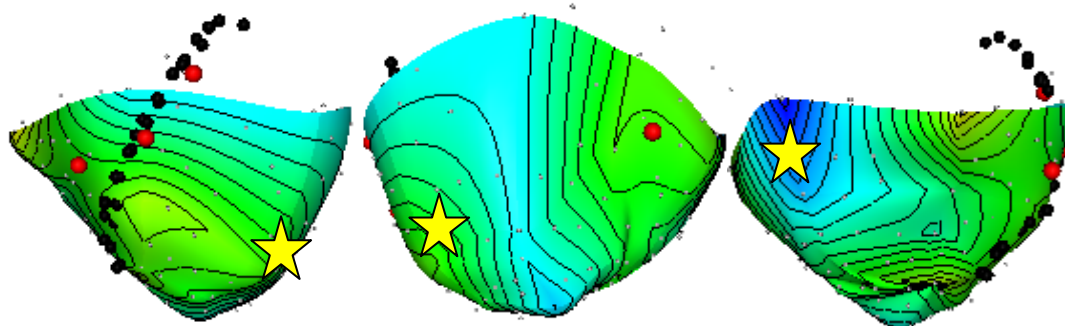


### Atrium + RV Apex + EPI Lateral Pacing

Anterior View

Lateral View

Posterior View

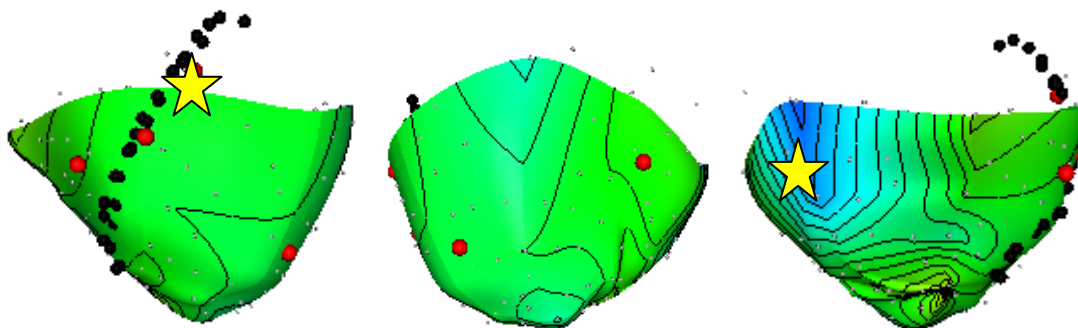


### Atrium + RV Apex + ENDO Anterior Base Pacing

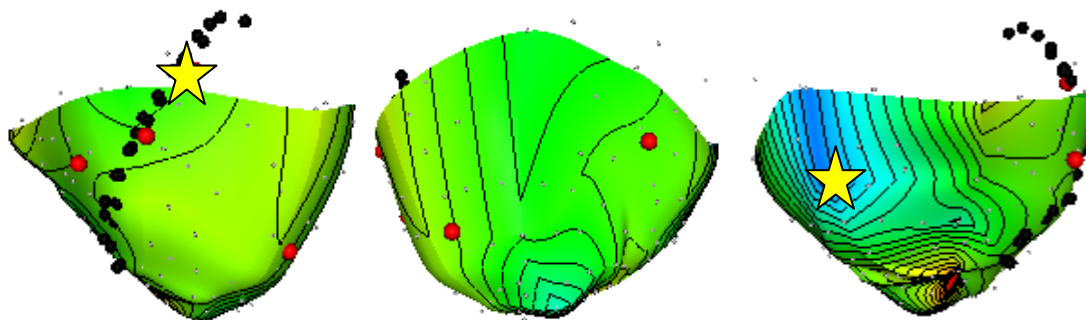
Anterior View

Lateral View

Posterior View



### Atrium + RV Apex + EPI Anterior Base Pacing

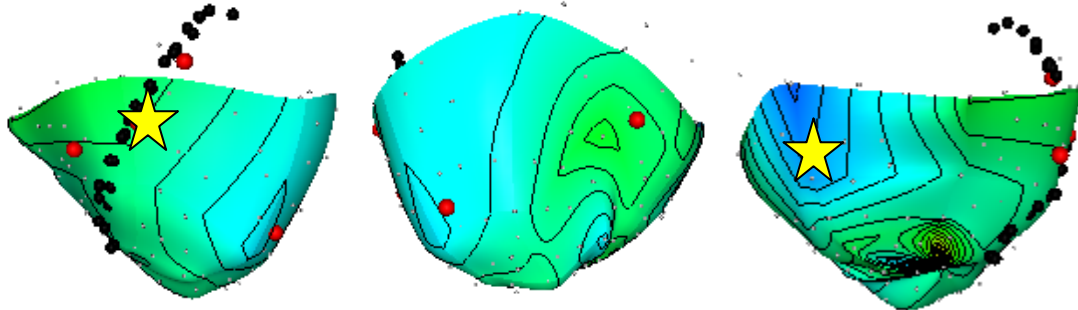


**Atrium + RV Apex + ENDO Anterior Mid-Ventricle Pacing**

Anterior View

Lateral View

Posterior View

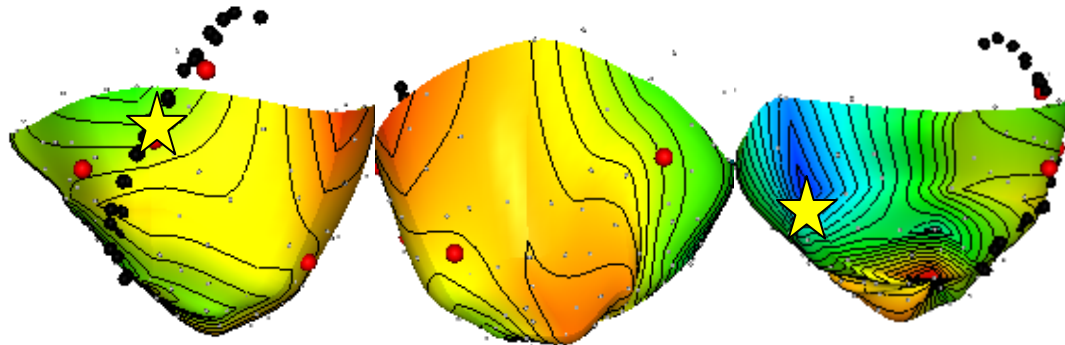


**Atrium + RV Apex + EPI Anterior Mid-Ventricle Pacing**

Anterior View

Lateral View

Posterior View

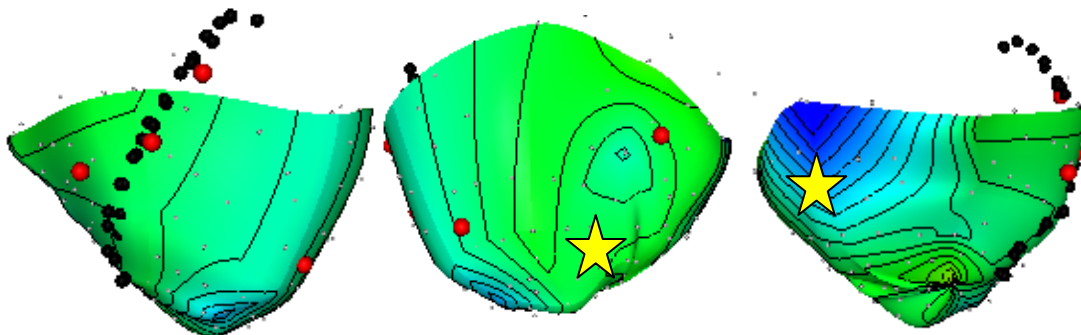


**Atrium + RV Apex + Endo BS**

Anterior View

Lateral View

Posterior View

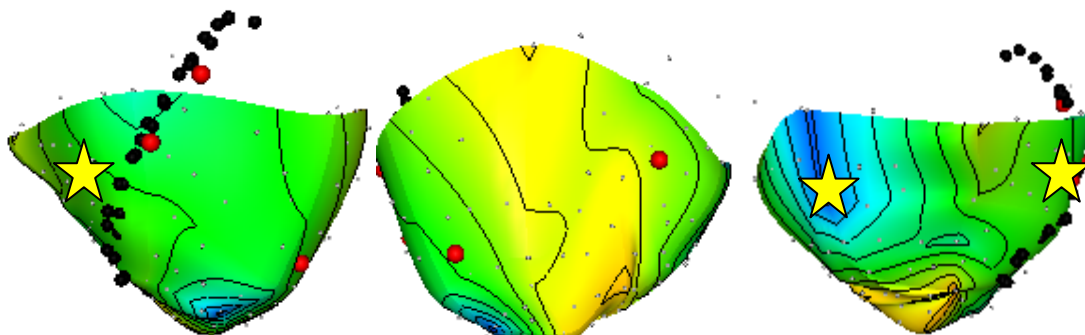


### Atrium + RV Apex + EPI BS

Anterior View

Lateral View

Posterior View

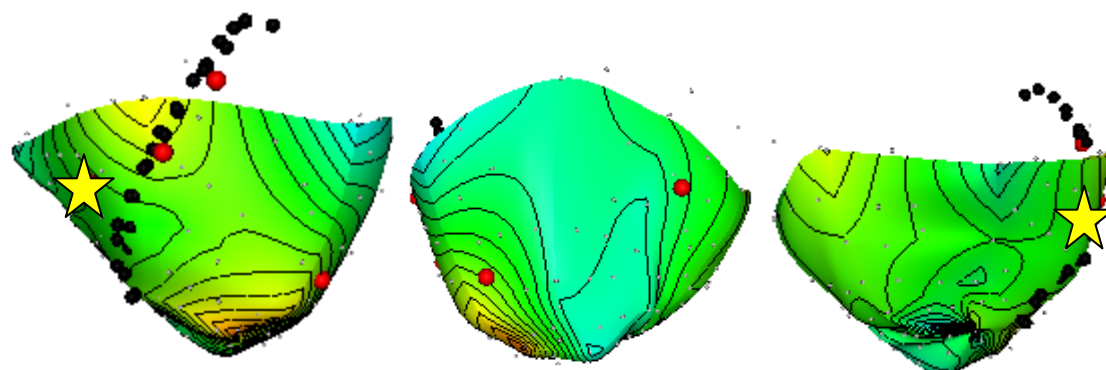


### Atrium + Epi BS

Anterior View

Lateral View

Posterior View

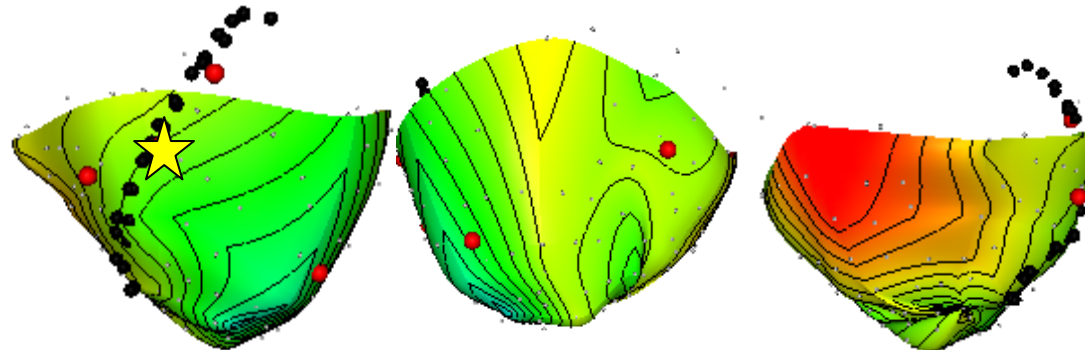


### Atrium + EPI Anterior Mid-Ventricle Pacing

Anterior View

Lateral View

Posterior View

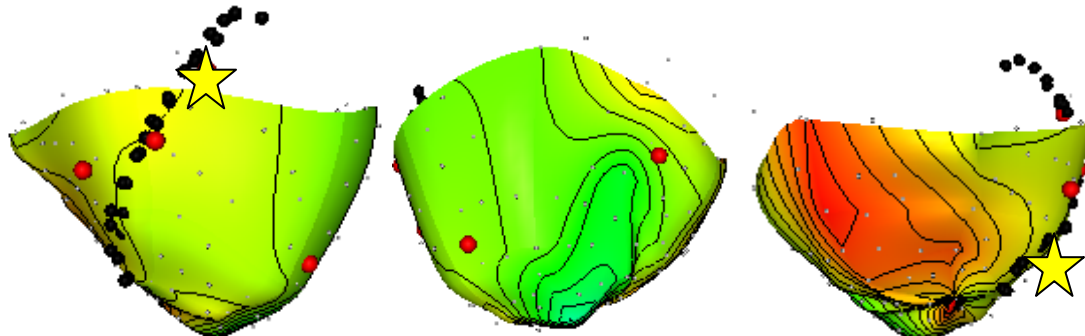


### Atrium + EPI Anterior Base Pacing

Anterior View

Lateral View

Posterior View

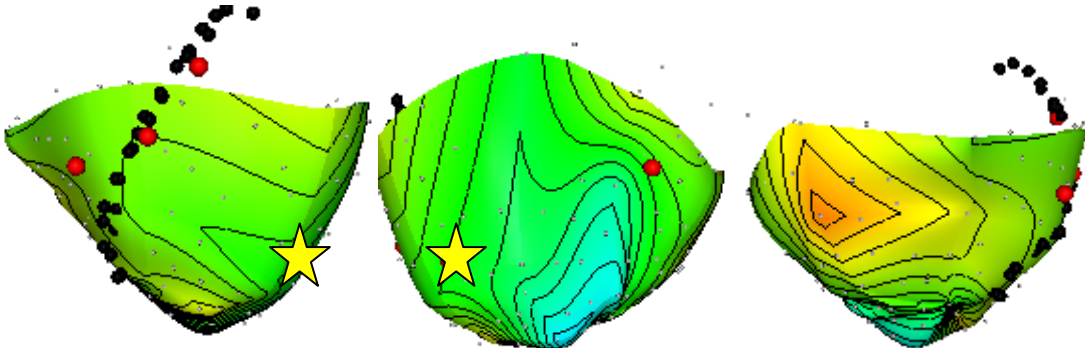


### Atrium + EPI Lateral Pacing

Anterior View

Lateral View

Posterior View

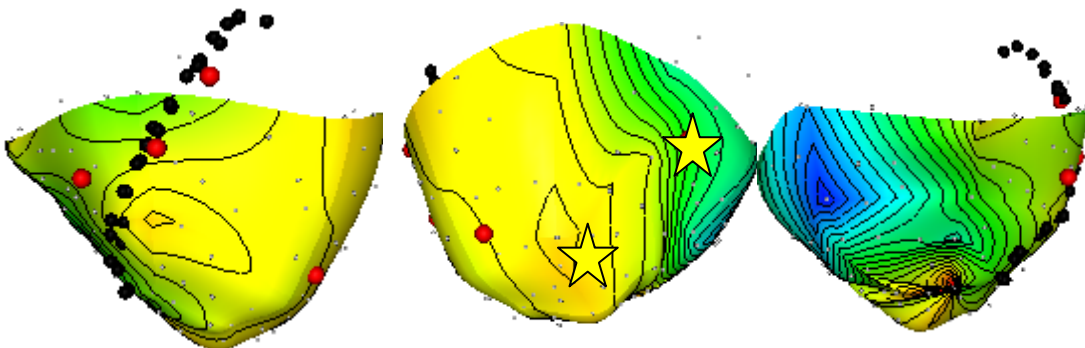


### Atrium + EPI PCS

Anterior View

Lateral View

Posterior View

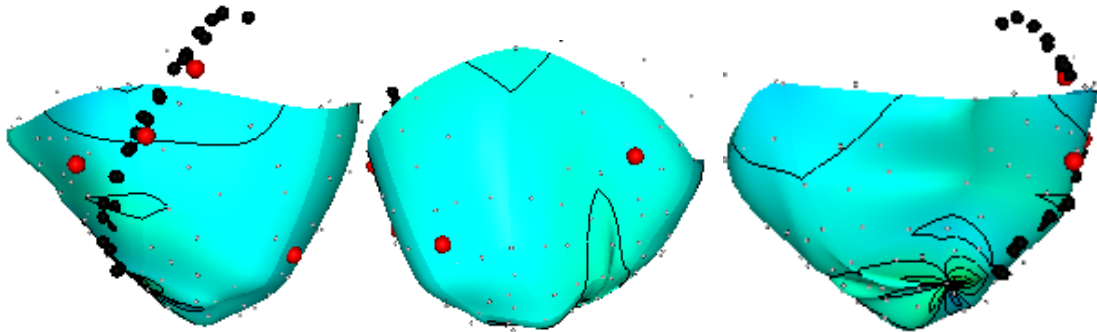


# Atrial Pacing

Anterior View

Lateral View

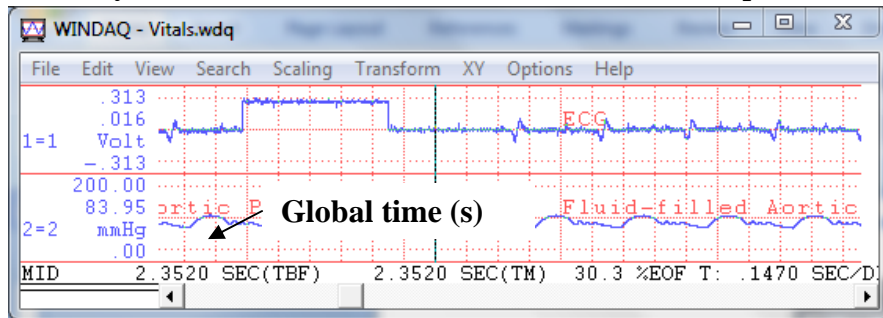
Posterior View



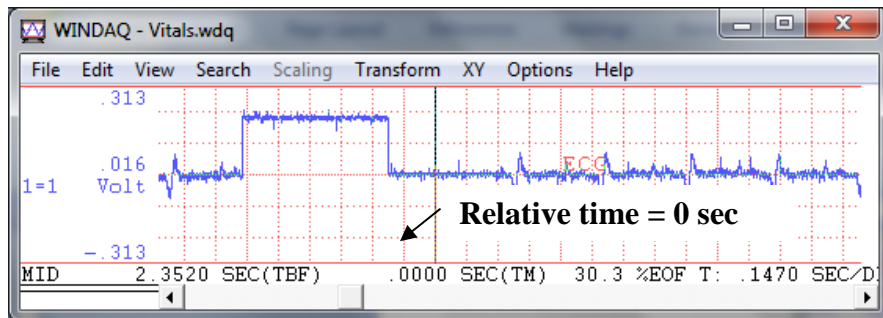
# APPENDIX B: ISOCHRONAL MAPS IN *CONTINUITY* INSTRUCTION MANUAL

## Part A: Save Raw Signals as .CVS files for input into Matlab

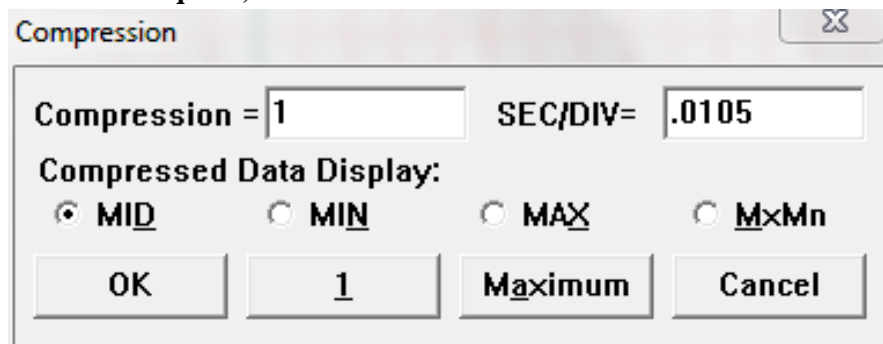
1. Open the Vitals files to select the beginning and end times.
  - a. Scroll to a time after the calibration mark. Note the global time as it is necessary to scroll to the same time in connectors 1-4 in step 2.



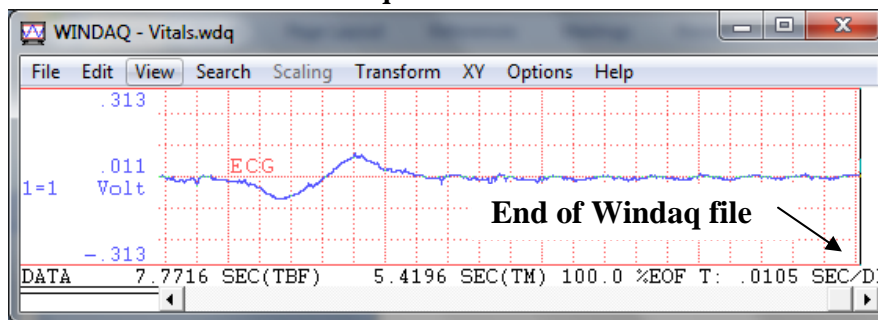
- b. Press F4 twice to make this the relative zero time.



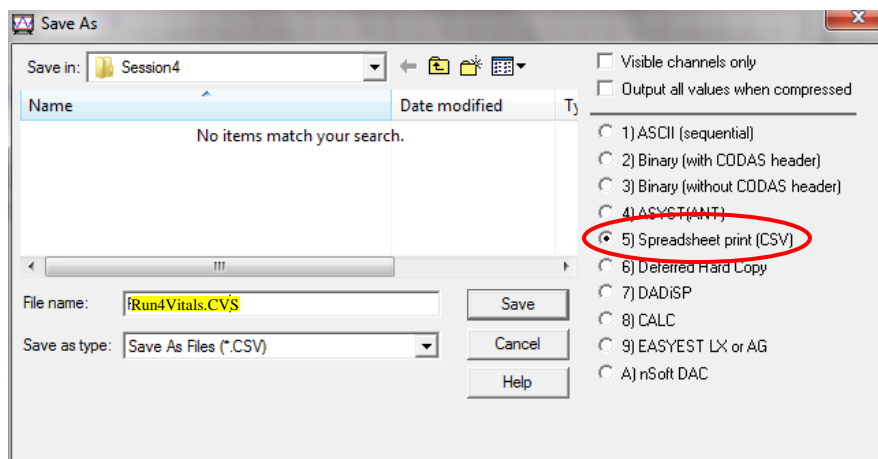
- c. Press F7 to change compression to 1 (to obtain maximum resolution from the .wdq files).



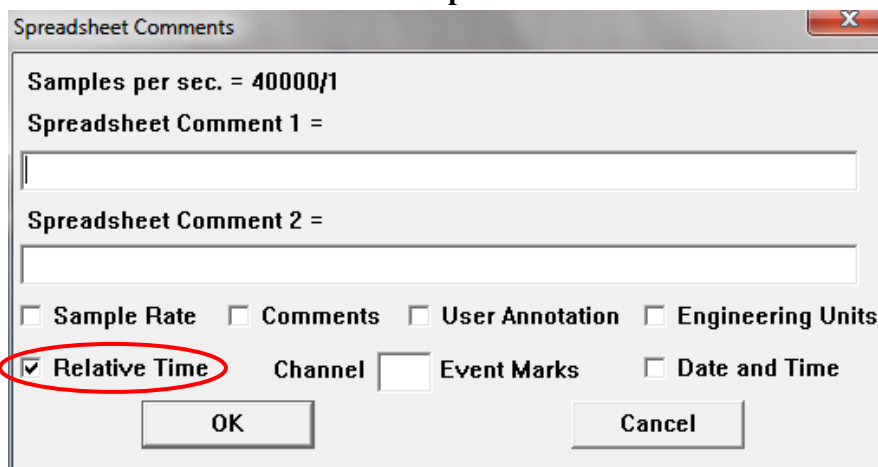
- d. Scroll to the end of the windaq file.



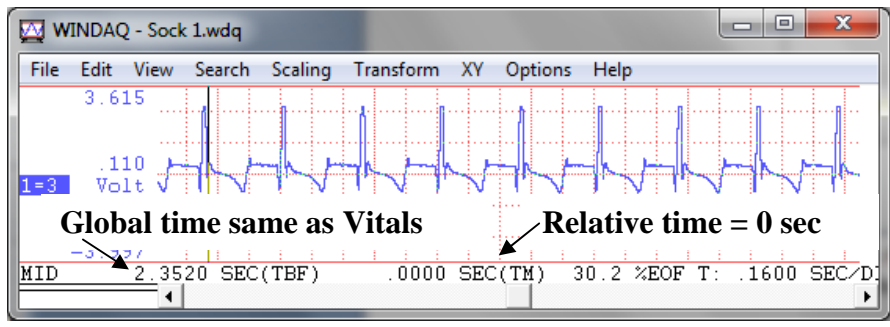
- e. Click on File → Save As... to save as a .CSV output. Rename the filename to be specific to the Run. Make sure that the output file type is .CSV. Click 'Save'.



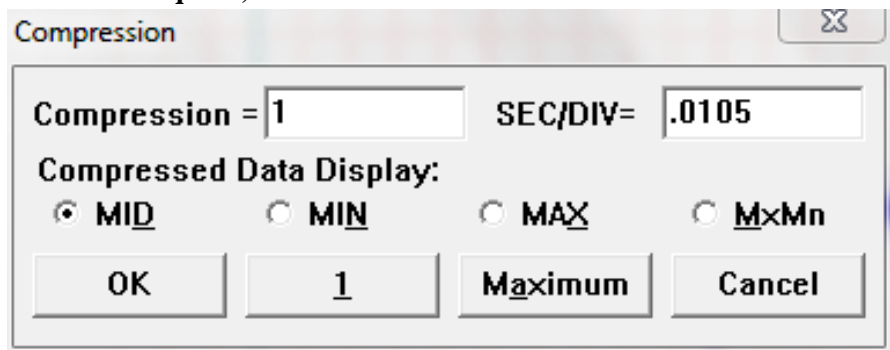
- f. Spreadsheet Comments window will pop up. Uncheck everything except 'Relative Time'. Click 'OK' to complete save.



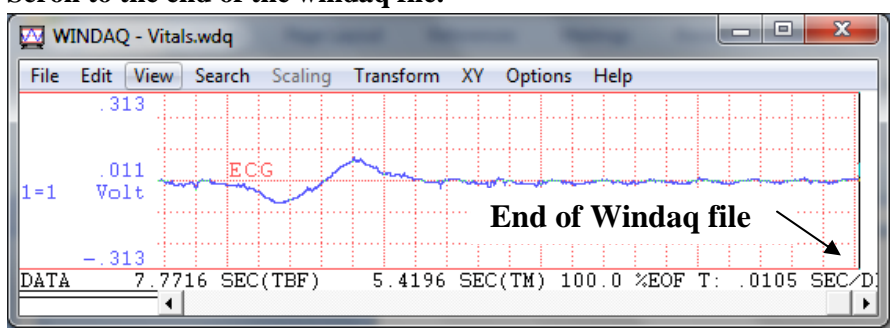
- 2. Open the Windaq .wdq connector files (1-4) and save output .CVS files. Repeat the following for connectors 1 through 4.
  - a. Scroll global time to time noted above. Press F4 twice to make relative time zero.



- b. Press F7 to change compression to 1 (to obtain maximum resolution from the .wdq files).

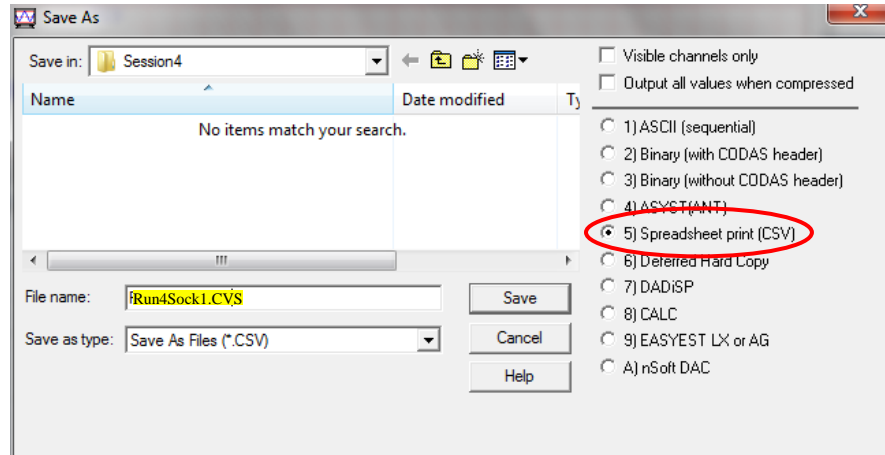


- c. Scroll to the end of the windaq file.

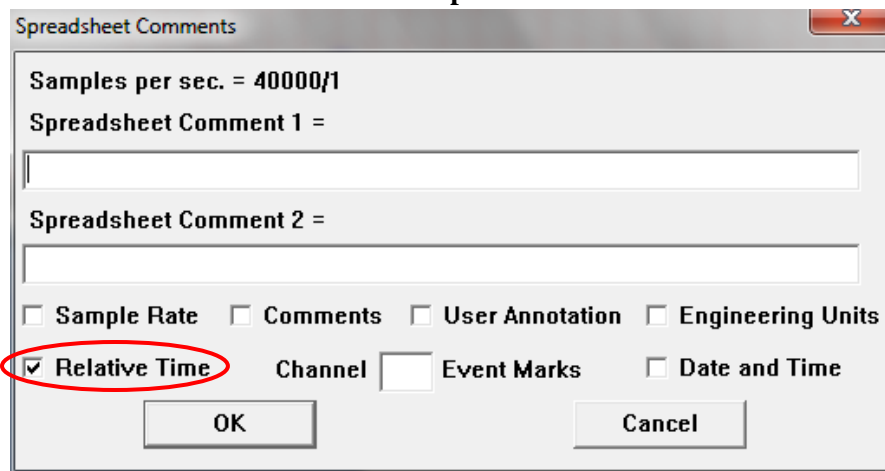


- d. Click on File → Save As... to save as a .CVS output. Rename the filename to be specific to the Run. Make sure that the output file type is .CVS.





- e. **Spreadsheet Comments window will pop up. Uncheck everything except 'Relative Time'. Click 'OK' to complete save.**



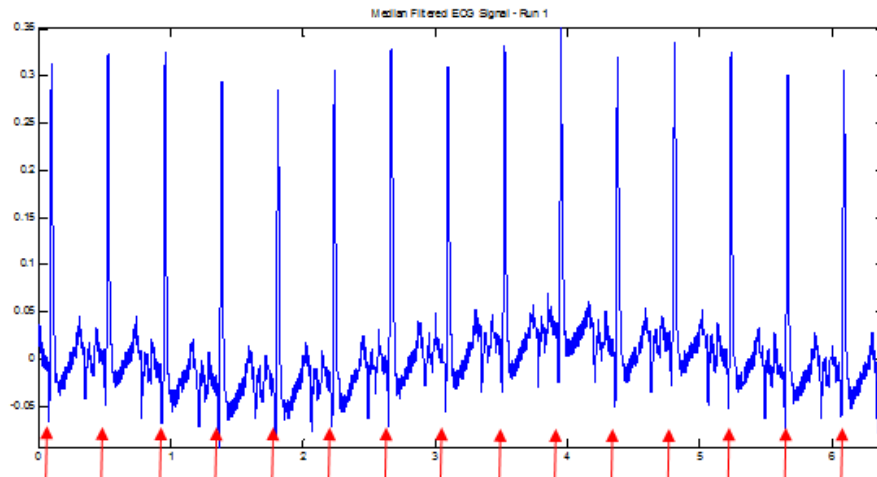
3. **At the completion of Part A, there should be 5 files named:**

- *RunXVitals.CVS*
- *RunXSock 1.CVS*
- *RunXSock 2.CVS*
- *RunXSock 3.CVS*
- *RunXSock 4.CVS*

## **Part B: Run *Matlab* Script to Calculate Local Activation Times**

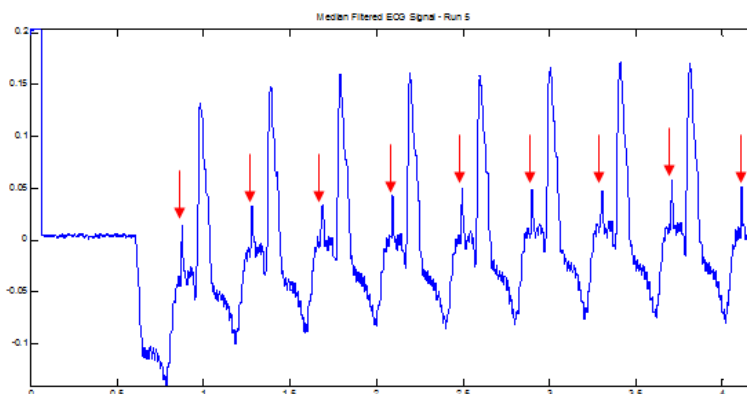
1. Open 'LOCAL\_ACTIVATION.M' in *Matlab*.
2. Before running the script, lines 14-21 should be edited.
  - dir: location of Matlab script, along with all the saved files.
  - save\_dir: folder within 'dir' folder to save all outputs
  - electpts: filename of 3D electrode positions, file should be Nx3 where N is the number of electrodes.
  - file\_1: filename of connector 1
  - file\_2: filename of connector 2
  - file\_3: filename of connector 3
  - file\_4: filename of connector 4
  - file\_ECG: filename of vitals file (which includes the ECG in channel 1)
3. Run Script.
4. Specify which runs are to be analyzed by answering the prompt that appears on the *Matlab* window.
  - **Q:** Which runs would you like to analyze?
  - **A:** The answer should be in [A, B, C, ...] format
5. Select the beat reference times for each run by answering the prompt that appears on the *Matlab* window.  
For atrial runs, select the beginning of each QRS complex in the selection window to be reference times.

**Atrial Run Sample Electrogram**



For the other paced runs (simulated LBBB, single LV pacing, and biventricular pacing), the reference time is the ventricular stimulus. The ventricular stimulus, however, is rarely visible on the local electrogram signals, thus, the atrial stimulus should be selected in the selection window. This time difference is compensated by entering in the AV delay in the next input. Press 'Enter' after all reference times have been selected.

### Paced Run Sample Electrogram



#### 6. Specify AV delay for each run by answering the prompt that appears on the *Matlab* window.

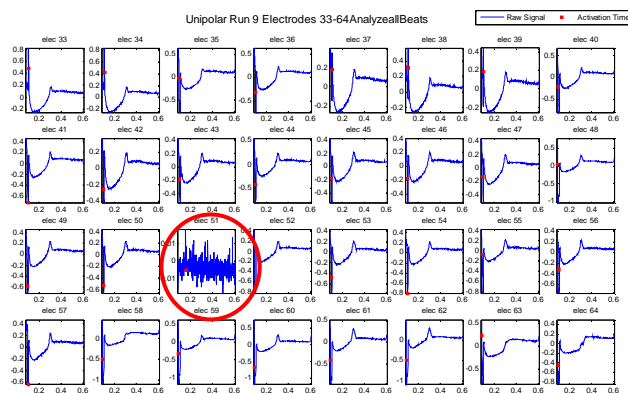
- Q: What's the AV delay?

A: The AV delay is 0 for atrial runs and 40 for other paced runs.

#### 7. Specify which electrodes are noisy and should be omitted by answering the prompt that appears on the *Matlab* window.

- Q: What electrodes are noisy?

A: Look at the visualization and enter in which electrodes are noisy. For example, in figure below, circled channel is noisy and should be omitted.



**8. Add a header to output activation time file.**

Matlab will compile 3D electrode positions and activation times into an output data .txt file. Add a header line should be added to this .txt file and the file is ready to be loaded into Continuity. Insert additional columns as necessary to accommodate for all runs analyzed. The size of the input should be  $(N+1) \times (7+(Runs*2))$  where  $N$  is the number of electrodes and  $Runs$  is the number of runs per dog.

Coord1_value	Coord1_weight	Coord2_value	Coord2_weight	Coord3_value	Coord3_weight	Run1_value	Run1_weight	Run2_value	Run2_weight	Data
11.338	1	-21.699	1	-2.408	1	26.083	1	53.167	1	1
3.6379	1	-27.324	1	2.0222	1	25.75	1	51.778	1	2
-20.662	1	-1.6742	1	-20.92	1	30.333	1	51.333	1	3
-26.937	1	10.951	1	-17.85	1	18.583	1	72.833	1	4
17.538	1	-17.349	1	4.7222	1	25.583	1	34.444	1	5
25.488	1	12.101	1	1.3222	1	21.333	1	76.833	1	6
-11.162	1	-29.724	1	16.147	1	13.083	1	61.167	1	7
23.663	1	-5.7742	1	8.2722	1	14.083	1	64.833	1	8
5.9379	1	-18.774	1	19.722	1	31.75	1	46.778	1	9
-9.5121	1	5.5758	1	-23.67	1	27.417	1	66.333	1	10

## Part C: Continuity Geometry and Activation Time Fitting

1. Load initial mesh. A pre-existing initial mesh can be used (option a) or a new initial mesh can be made (option b).
  - a. Load fitted geometry .cont6 files into *Continuity* to use a pre-existing initial mesh. If this is performed, user can skip to step b and move on to step 2.
  - b. Make a new initial mesh. This initial mesh should have 7 longitudinal and 3 apex-to-base elements with 28 nodes and 21 elements. This route requires user to edit 2 files: the nodes.txt file and the elements.txt file.
    - i. Edit the nodes.txt file so that coordinates 1, 2, and 3 (columns 1, 2, and 3 in the nodes.txt file) correspond to the 3D coordinates of the electrode number highlighted below.

Coords_1_val	Coords_2_val	Coords_3_val	Nodes #	Electrode #
2.6231	-39.4588	17.5045	1	5
-28.527	-7.6768	21.0655	2	36
3.1111	-46.8758	-4.3995	3	7
-30.931	9.0161	7.2985	4	46
20.188	-31.3218	22.4285	5	118
27.929	-38.9298	-3.8555	6	120
22.413	-4.3094	30.4875	7	93
41.165	-18.5648	-1.1595	8	113
23.837	8.935	27.7815	9	79
39.538	8.3278	-5.6353	10	102
12.888	25.7042	24.5095	11	67
14.715	33.4722	6.9705	12	75
-12.443	22.6242	26.5525	13	58
-13.444	26.0292	1.7535	14	55
-1.212	-23.6528	34.7755	15	3
-15.958	-16.6788	30.0275	16	22
6.5202	-16.6408	41.3755	17	103
12.014	-7.1812	41.3795	18	91
9.3234	1.8774	43.8045	19	85
5.2637	12.648	43.2645	20	60
-10.531	6.5224	40.9765	21	50
-7.4867	-8.0758	42.2575	22	15
-7.4867	-8.0758	42.2575	23	15
-7.4867	-8.0758	42.2575	24	15
-7.4867	-8.0758	42.2575	25	15
-7.4867	-8.0758	42.2575	26	15
-7.4867	-8.0758	42.2575	27	15
-7.4867	-8.0758	42.2575	28	15

ii. Load nodes file into Continuity.

1. Mesh → Edit → Nodes
2. In Continuity Node Form window, Click 'Import/Export/Graph'
3. In Continuity Table Manager window, File → Open
4. Select nodes.txt file (saved from step i above)
5. In Continuity Table Manager window, File → Close and update form
6. In Continuity Node Form, click 'OK'

c. Load elements.txt file. The elements file should look like this:

Node_0_Val	Node_1_Val	Node_2_Val	Node_3_Val	Label	Element
1	2	3	4	RV	1
5	1	6	3	RV	2
7	5	8	6	RV	3
9	7	10	8	LV	4
11	9	12	10	LV	5
13	11	14	12	LV	6
2	13	4	14	LV	7
15	16	1	2	RV	8
17	15	5	1	RV	9
18	17	7	5	RV	10
19	18	9	7	LV	11
20	19	11	9	LV	12
21	20	13	11	LV	13
16	21	2	13	LV	14
22	23	15	16	LV	15
24	22	17	15	LV	16
25	24	18	17	LV	17
26	25	19	18	LV	18
27	26	20	19	LV	19
28	27	21	20	LV	20
23	28	16	21	LV	21

1. Mesh → Edit → Elements
2. In Continuity Element Form window, Click 'Import/Export/Graph'
3. In Continuity Table Manager window, File → Open
4. Select elements.txt file (saved from step i above)
5. In Continuity Table Manager window, File → Close and update form

6. In Continuity Element Form window, click 'OK'

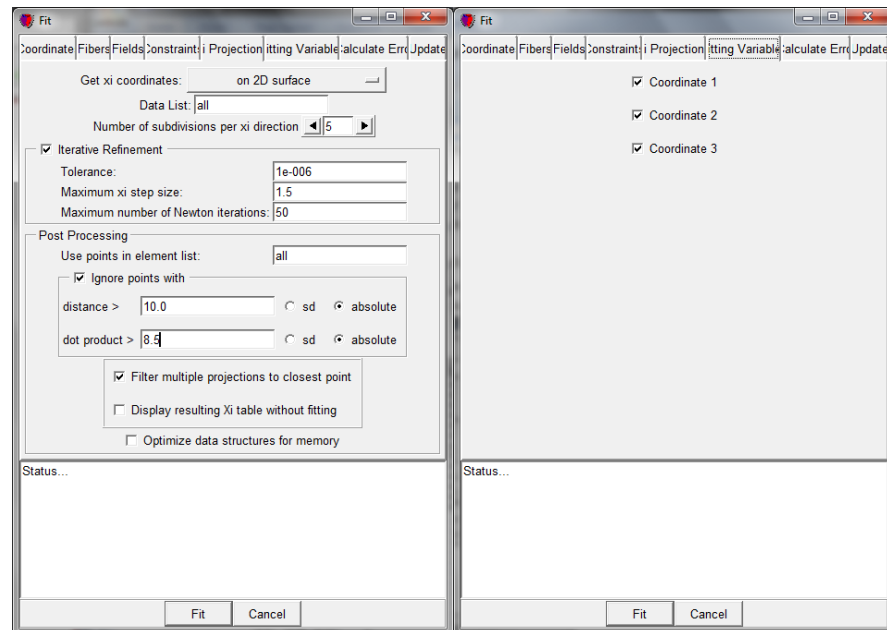
## 2. Edit data file

- Fitting → Edit → Data
- An Edit Data window will pop up. In this window, click 'Import/Export/Graph'
- A Continuity Table Manager window will pop up. In this window, Click File → Open
- Navigate to the location of the .txt continuity input file (Step 6 in part A) and click 'Open' to select file
- In the Continuity Table Manager window, click File → Close and Update Form
- In the Edit Data window, click 'OK'

3. Click  to calculate new data, nodes, and element inputs.

## 4. Fit geometry to initial mesh

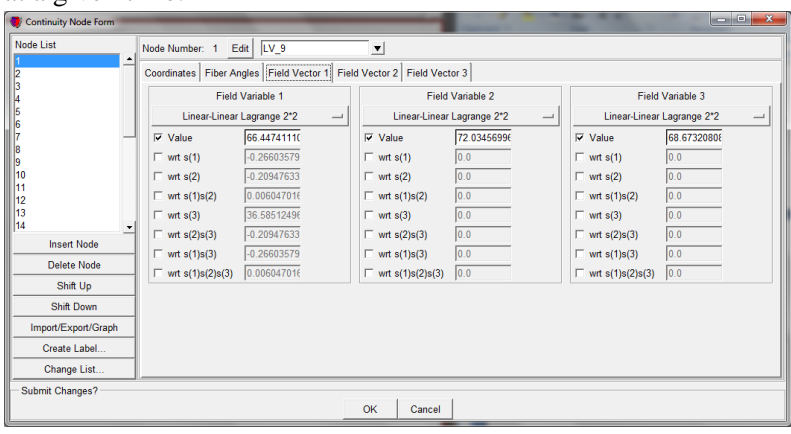
- Go to Fitting → Fit Data
- Under Xi Projection tab, edit distance > 10.0 (absolute value). Under Fitting variables tab, fit in coordinate 1, 2, and 3.



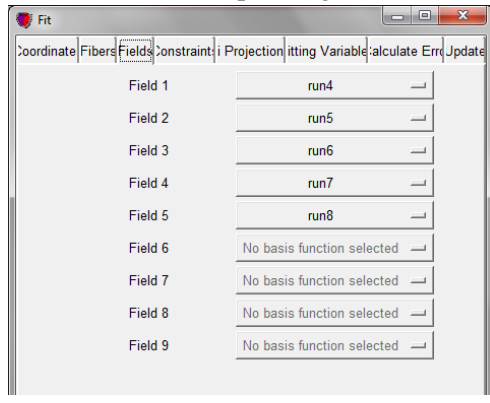
- Click 'Fit'

## 5. Fit activation time into field

- a. Indicate fitting conditions
  - i. Mesh → Edit → Nodes
  - ii. Under the field vector tabs, select basis number to ‘Linear-Linear Lagrange 2\*2’ for up to 9 variables. A maximum of 9 runs can be fit at a given time.

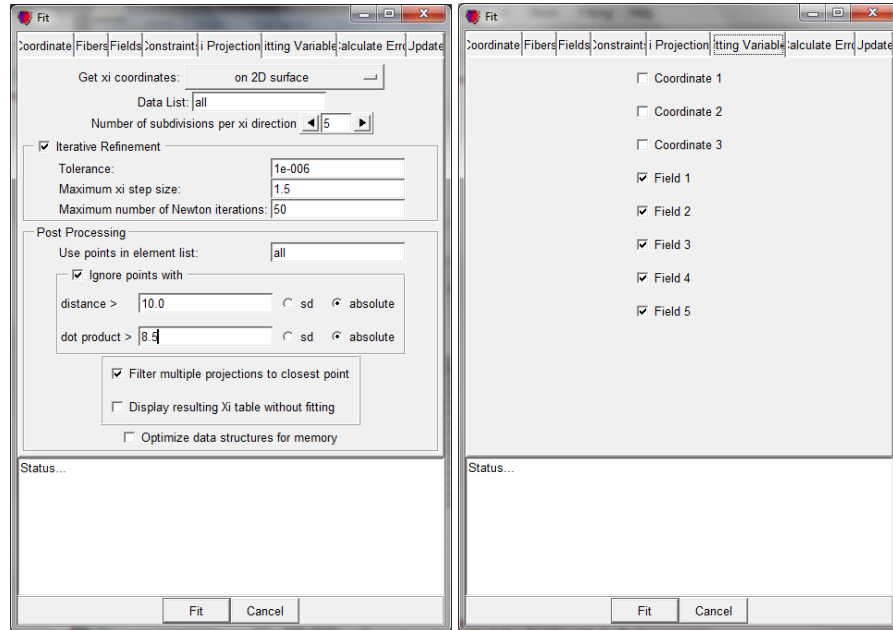


- iii. Click ‘OK’.
- b. Fitting -> Fit Data
- c. Under ‘Fields’ tab, select the corresponding run for each field.



- d. Under Xi Projection tab, edit distance > 10.0 (absolute value). Under Fitting variables tab, fit all fields.

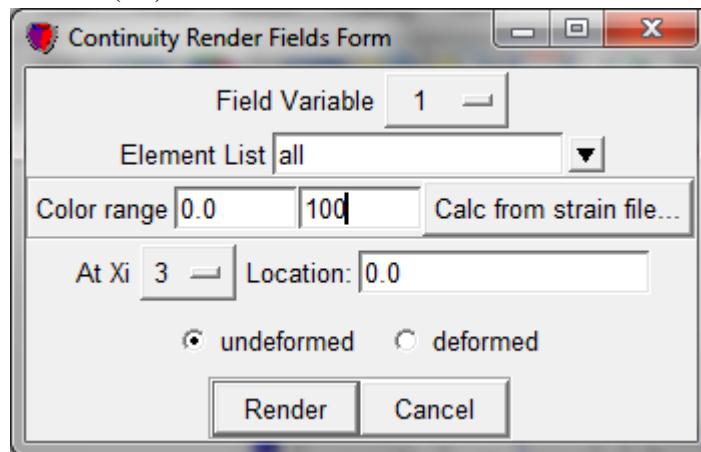




e. Click 'Fit'

**6. Render fit fields. This step must be repeated for each field variable (per run).**

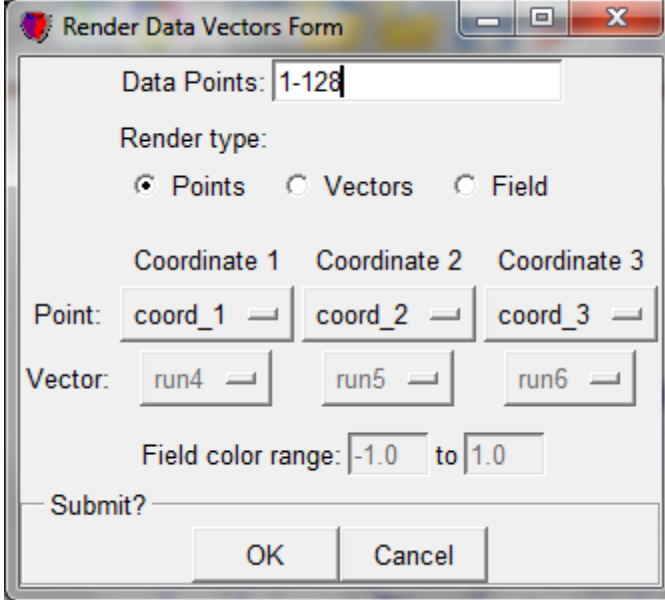
- a. Mesh → Render → Field
- b. Select field variable and specify color range, this can typically be between 0 and 100 (ms)



c. Click 'Render'

**7. Render fiducial markers.**

- a. Fitting → Render → Raw Data
- b. Enter in the points to be rendered



Render Data Vectors Form

Data Points: 1-128

Render type:

Points  Vectors  Field

Coordinate 1    Coordinate 2    Coordinate 3

Point: coord\_1    coord\_2    coord\_3

Vector: run4    run5    run6

Field color range: -1.0 to 1.0

Submit?

OK    Cancel

The image shows a dialog box titled "Render Data Vectors Form". It has a standard Windows-style title bar with minimize, maximize, and close buttons. The main content area contains several input fields and radio buttons. At the top, "Data Points" is set to "1-128". Below that, "Render type" has three radio buttons: "Points" (which is selected), "Vectors", and "Field". Under "Render type", there are three columns of input fields. The first column is labeled "Coordinate 1" and contains a "Point:" label followed by a text box with "coord\_1". The second column is labeled "Coordinate 2" and contains a text box with "coord\_2". The third column is labeled "Coordinate 3" and contains a text box with "coord\_3". Below these, there are three more text boxes labeled "run4", "run5", and "run6", which are grouped under a "Vector:" label. At the bottom of the form, there is a "Field color range:" label followed by two text boxes containing "-1.0" and "1.0". At the very bottom, there is a "Submit?" label and two buttons: "OK" and "Cancel".

c. Click 'OK'

# APPENDIX C: MATLAB SCRIPT FOR DETERMINING LOCAL ACTIVATION TIMES

```
close all
clear all

runs_to_analyze = input('What runs do you want to analyze? Use format [A,B,C,...]: ');
disp(['Runs to analyze: ' num2str(runs_to_analyze)]); disp(' ')
run_count=1;
for i=runs_to_analyze
    disp(['*****Run ' num2str(i) '*****'])
    % AVdelay=0
    omit=51;
    beats = 10;
    beats = 'all';
    %% COMPILE DATA from all four connectors
    dir='C:\Users\Owner\Documents\CMRG Lab Files\Dog2_Obi\';
    save_dir='C:\Users\Owner\Documents\CMRG Lab Files\Dog2_Obi\redid_single_LV_runs\';
    file_1=[ 'Run' num2str(i) 'Sock 1.CSV'];
    file_2=[ 'Run' num2str(i) 'Sock 2.CSV'];
    file_3=[ 'Run' num2str(i) 'Sock 3.CSV'];
    file_4=[ 'Run' num2str(i) 'Sock 4.CSV'];
    file_ECG=[ 'Run' num2str(i) 'Vitals.CSV'];
    data_1 = csvread([dir file_1]);
    data_2 = csvread([dir file_2]);
    data_3 = csvread([dir file_3]);
    data_4 = csvread([dir file_4]);
    ECG=csvread([dir file_ECG]);
    timeStep=data_1(2,1);
    time=min([size(data_1,1) size(data_2,1) size(data_3,1) size(data_4,1)]);
    for j=1:1:4
        data_all = ['data_' num2str(j)];
        data=eval(data_all);
        if j==1
            compiled=zeros(time,129);
            compiled(1:time,1:33)=data(1:time,1:33);
        end
        if j==2
            compiled(1:time,34:65)=data(1:time,2:33);
        end
        if j==3
            compiled(1:time,66:97)=data(1:time,2:33);
        end
        if j==4
            compiled(1:time,98:129)=data(1:time,2:33);
            compilefilename=[ 'Beagle Run' num2str(i) 'Compiled.txt'];
            dlmwrite([save_dir compilefilename], compiled,'delimiter','\t');
        end
        % disp(sprintf('<a href="matlab: winopen("%s%s")">%s</a>', dir, compilefilename, compilefilename));
    end
end

%% filter compiled
window = 15;
compiled_filtered = medfilt1(compiled, window);
```

```

%% load in electrode 3d points to prepare to convert unipolar to bipolar
if run_count==1
    electpts=['dog2_obi_3d_pts.xls'];
    data=xlsread([dir electpts]); % load in all data. this is a 198x4 matrix (electrode #, x, y, x)
    data=data(:,:);
    data(:,1)=data(:,1)-mean(data(:,1));
    data(:,2)=data(:,2)-mean(data(:,2));
    data(:,3)=data(:,3)-mean(data(:,3));
    % data(:,1)=-data(:,1)-mean(data(:,1))
    % data(:,2)=-data(:,2)-mean(data(:,2))
    % data(:,3)=-data(:,3)-mean(data(:,3))

    plot3(data(:,1),data(:,2),data(:,3),'bo', data(1:7,1),data(1:7,2),data(1:7,3),'r',data(8:13,1),data(8:13,2),data(8:13,3),'g.')
    axis equal

    % reply = input('Would you like to plot 3D rotation figures? y/n: ', 's');
    reply='n';
    % Plotting
    if reply=='y'
        figure(1)
        hold on;
        plot3(data(:,1),data(:,2),data(:,3),'bo');
        grid on;xlabel('X');ylabel('Y');zlabel('Z');title('Original(From segmented images)');
        box on;
        plot3(0,0,0,'ko');
    else
    end

    % Align the data points along coordinates in Continuity.
    % The angle angy, angz is found estimated.

    angx = 180;
    angy = 90;

    roty = [cosd(angy) 0 -sind(angy);
            0 1 0;
            sind(angy) 0 cosd(angy)];

    rotx = [1 0 0
            0 cosd(angx) -sind(angx);
            0 sind(angx) cosd(angx)];

    data = roty*rotx*data';
    data = data';

    if reply=='y'
        figure(2)
        hold on;
        plot3(data(:,1),data(:,2),data(:,3),'bo');

        grid on;xlabel('X');ylabel('Y');zlabel('Z');title('Original(From segmented images)');
        box on;
        plot3(0,0,0,'k*');
        grid on;xlabel('X');ylabel('Y');zlabel('Z');title('Rotated to be

```

```

    approximately aligned with z-axis');
else
end

% Find the apex of the heart(blunt extremity formed by the LV) and move the
origin to the apex of the heart
% Find the apex:

[apex_x, entry_no] = max(data(:,1));
apex_y = data(entry_no,2);
apex_z = data(entry_no,3);

datanew_LV(:,1) = data(:,1)- apex_x;
datanew_LV(:,2) = data(:,2)- apex_y;
datanew_LV(:,3) = data(:,3)- apex_z;

% Plotting
if reply=='y'
    xaxis = [1 0 0]';
    yaxis = [0 1 0]';
    zaxis = [0 0 1]';

    figure(3)
    hold on;
    plot3(datanew_LV(:,1),datanew_LV(:,2),datanew_LV(:,3),'bo');
    plot3(0,0,0,'r');

    grid on;xlabel('X');ylabel('Y');zlabel('Z');title('Origin moved to
    apex');
    box on;
else
end

% Sample every other point of 'LVcoordnew' since there's too many data pts
for SVD
datasmall_LV(:,1) = datanew_LV(1:1:end,1);
datasmall_LV(:,2) = datanew_LV(1:1:end,2);
datasmall_LV(:,3) = datanew_LV(1:1:end,3);

% Tilt the data points to align
% Singular Value Decomposition (svd) to get the vector we want to orient
% the x-coordinate along with. The eigenvector that corresponds to the
largest
% (dominant) eigenvalue is the vector we want.

[U,S,V] = svd(datasmall_LV');

% Flip the sign of U(:,1)
U_mod(:,1) = U(:,1);
U_mod(1,1) = -U(1,1);
U_mod(3,1) = -U(3,1);

```

```

if reply=='y'
    figure(4)
    hold on;
    t = -30*pi:pi/50:5*pi;
    plot3(U_mod(1,1)*t,U_mod(2,1)*t,U_mod(3,1)*t,'r*')
    plot3(U(1,2)*t,U(2,2)*t,U(3,2)*t,'g*')
    plot3(U(1,3)*t,U(2,3)*t,U(3,3)*t,'k*')
    grid on;
    plot3(datanew_LV(:,1),datanew_LV(:,2),datanew_LV(:,3),'*');
    title('LV before tilting with vector from SVD');
    xlabel('X');
    ylabel('Y');
    zlabel('Z');
else
end

% Rotation matrix calculation
x_vector = U_mod(:,1);
newx = U_mod(2)/ U_mod(1);
y_vector = [0;1;0];
y_vector(3) = newx;

% Normalizing the y-vector.
length_y = norm(y_vector);
y_vector = y_vector ./ length_y;

% Fourth, need to find the z-axis which is the cross product of the x-axis
and the y-axis.
z_vector = cross(x_vector, y_vector);

% Finally, once all the three axes are determined, we need to just
transform the data to match the model's axes.
M(:,1) = x_vector;
M(:,2) = y_vector;
M(:,3) = z_vector;

M_old = [1 0 0;0 1 0;0 0 1]; % Initial vectors that x, y, z axes are lined
with.
x = M_old \ M; % To compute the rotation matrix that transforms the
coordinate system from M_old to M.(solution to x* M_old = M)

datanew_LV = datanew_LV';

clear datanew_LV2
for b =1:length(datanew_LV)
    datanew_LV2(:,b) = inv(x) * datanew_LV(:,b); % inv(x) is used
instead of x because inv(x) is the transformation from M to M_old
end

datanew_LV = datanew_LV';

datanew_LV2 = datanew_LV2';

if reply=='y'

```

```

figure(5)
hold on;
tt = [1 0 0]';
t = -40*pi:pi/5:10*pi;
plot3(M(1,1)*t,M(2,1)*t,M(3,1)*t,'ro');
plot3(datanew_LV(:,1),datanew_LV(:,2),datanew_LV(:,3),'yo');
plot3(datanew_LV2(:,1),datanew_LV2(:,2),datanew_LV2(:,3),'k*');
plot3(tt(1)*t,tt(2)*t,tt(3)*t,'b*');
grid on;xlabel('X');ylabel('Y');zlabel('Z');
title('Comparison between untilted LV and tilted LV');
legend('vector','before','after');
else
end

% Move the origin to the 2/3 base-apex length of the LV
datanew_LV2(:,1) = datanew_LV2(:,1) + (2/3)*(max(datanew_LV2(:,1))-
min(datanew_LV2(:,1)));

% Plotting
if reply=='y'
figure(6)
t = -20*pi:pi/5:30*pi;
hold on;
plot3(xaxis(1,1)*t,xaxis(2,1)*t,xaxis(3,1)*t,'k*');
plot3(yaxis(1,1)*t,yaxis(2,1)*t,yaxis(3,1)*t,'k*');

plot3(datanew_LV2(:,1),datanew_LV2(:,2),datanew_LV2(:,3),'ro');

grid on;xlabel('X');ylabel('Y');zlabel('Z');
title('Whole Heart(tilted)');
else
end

% Write to txt file
coordallnew = [datanew_LV2];
coord_weights = 1 * ones(1,length(coordallnew));

% load continuitydatainput_wat.mat
% coord_AT_val=coord_AT_val(:,7);

% Label = [20*ones(1,length(datanew_LV2))];
% count = 1:length(coordallnew);
% data = [coordallnew(:,1),coord_weights',coordallnew(:,2),coord_weights',
coordallnew(:,3),coord_weights',coord_AT_val,coord_weights', count' ];
rotatedData=data;
savedfile='rotatedElectPts_data-NEW-subtractMeanFirst.txt';
dlmwrite([save_dir savedfile], rotatedData, 'delimiter','\t',
'newline','pc');
disp(sprintf('<a href="matlab: winopen("%s%s")">%s</a>', save_dir,
savedfile, savedfile));
end

%% convert unipolar to bipolar
% reply = input('Would you like to plot bipolarize figures? y/n: ', 's');
reply='n';

```

```

% load unipolar electrode positions in variable elecsh
if run_count==1
    elecsh=rotatedData(1:128,:);
end
% disp(['Dimensions of elecsh: ' num2str(size(elecsh))])
% filename=['Run' num2str(i) 'compiled.mat'];
% load(filename) % compiled is 7001x129
average_signal=transpose(compiled(:,2:129)); % 129x7001 (first column is
time)
% disp(['Dimensions of average_signal: ' num2str(size(average_signal))])

% Create traingular tessellation for uni leads
if run_count==1
    trin = tess3d_data(elecsh(:,1),elecsh(:,2),elecsh(:,3),30); % Change
the last variable(=90 in this case) to optimize the tessellation in
individual cases)
end

% plot unipolar results
if reply=='y'
    figure; trisurf(trin,elecsh(:,1),elecsh(:,2),elecsh(:,3)); axis equal;
% uni lead locations
figure; plot(average_signal(10,:)); % sample uni electrogram (noisy)
else
end

% Bipolarize unipolar electrode locations and electrograms
[elecbi,ecgbi]= unip2bip(trin,elecsh,average_signal);

% Create traingular tessellation for bi leads
if run_count==1
    trib = tess3d_data(elecbi(:,1),elecbi(:,2),elecbi(:,3),30); % Change
the last variable(=90 in this case) to optimize the tessellation in
individual cases)
end

if reply=='y'
% plot bipolar results
figure; trisurf(trib,elecbi(:,1),elecbi(:,2),elecbi(:,3)); axis equal;
% uni lead locations
figure; plot(ecgbi(10,:)); % sample bi electrogram (less noisy)
else
end
ecgbi=transpose(ecgbi) ;
ecgbi(:,1)=compiled(:,1);

%% TAKE DERIVATIVE
Derivative = diff(compiled); % don't divide by timestep because timestep is
constant so this is just a scaling factor
Derivative_filtered=diff(compiled_filtered);

%% filter ECG for easier beat selection
[min_difference, timeindex_ecg] = min(abs(ECG(:,1) - (time*timeStep) ));
timestep_ecg=ECG(2,1);

```



```

frame = 15;
degree = 0;
ECG_filtered = sgolayfilt(ECG(:,2), degree, frame);
x_ecg=ECG(1:timeindex_ecg-1,2);
window = 15;
y_ecg = medfilt1(x_ecg, window);

%% SELECT BEAT REFERENCE TIMES
% For atrial runs, the reference time is the BEGINNING OF THE QRS complex.
% For paced runs, the reference time is the atrial stimulus which is designated by a large stimulus artifact peak.

fullscreen = get(0,'ScreenSize');
figure('Position',[0 100 fullscreen(3) fullscreen(4)-200])
plot(ECG(1:timeindex_ecg-1,1), y_ecg)
axis tight
title(['Median Filtered ECG Signal - Run ' num2str(i)])

if beats=='all'
    [xclick_ecg,yclick] = ginput();
else
    [xclick_ecg,yclick] = ginput(beats+1);
end

cycleStartTimes=xclick_ecg;
[dataRows, dataColumns] = size(compiled);
close

AVdelay = input('What the AVdelay for this run? ');
if AVdelay == 0;
    noATzone = 150;
else
    noATzone = AVdelay;
end

%% CALCULATE LOCAL ACTIVATION TIMES of unfiltered, filtered, and bipolar
(unfiltered) signals (over multiple beats)
clear index
for c=2:size(compiled,2)      % number of electrodes
    for k = 1:size(cycleStartTimes)-1
        [min_difference, t1ecg(k)] = min(abs(ECG(:,1) -
            cycleStartTimes(k)));
        [min_difference, t2ecg(k)] = min(abs(ECG(:,1) -
            cycleStartTimes(k+1)));
        [min_difference, t1(k)] = min(abs(compiled(:,1) - ECG(t1ecg(k))));
        [min_difference, t2(k)] = min(abs(compiled(:,1) - ECG(t2ecg(k))));
        index(c-1,k)= min( find( Derivative(t1(k)+AVdelay:t2(k)-noATzone,c)
            ==min(Derivative(t1(k)+AVdelay:t2(k)-noATzone,c) ) ) ); % subtract
            1 from the t2(k) because when you take the derivative, it tkes
            differences
        AT=index.*timeStep.*1000;

        index_filtered(c-1,k)= min( find( Derivative_filtered(t1(k)+AVdelay:t2(k)-noATzone,c) ==...
            min(Derivative_filtered(t1(k)+AVdelay:t2(k)-noATzone,c) ) ) ); % subtract 1 from the
            t2(k) because when you take the derivative, it tkes differences
        AT_filtered=index_filtered.*timeStep.*1000;
    end
end

```

```

end

for c=2:size(ecgbi,2) % number of electrodes
    for k = 1:size(cycleStartTimes)-1
        [min_difference, t1ecg(k)] = min(abs(ECG(:,1) -
            cycleStartTimes(k)));
        [min_difference, t2ecg(k)] = min(abs(ECG(:,1) -
            cycleStartTimes(k+1)));
        [min_difference, t1(k)] = min(abs(compiled(:,1) - ECG(t1ecg(k))));
        [min_difference, t2(k)] = min(abs(compiled(:,1) - ECG(t2ecg(k))));
        index_bi(c-1,k)= min( find( abs(ecgbi(t1(k)+AVdelay:t2(k)-
            noATzone,c))==max(abs(ecgbi(t1(k)+AVdelay:t2(k)-noATzone,c))
            ) ); % subtract 1 from the t2(k) because when you take the
            derivative, it tkes differences
        AT_bi=index_bi.*timeStep.*1000;
    end
end

output_unipolar = [AT, mean(AT,2), zeros(size(AT),1), AT_filtered,
    mean(AT_filtered,2)];
savedfile=['run' num2str(i) 'combined_AT.txt'];
dlmwrite([save_dir savedfile], output_unipolar, 'delimiter','t',
    'newline','pc');

output_bipolar = [zeros(size(AT_bi),1),AT_bi, mean(AT_bi,2)];
dlmwrite([save_dir savedfile], output_bipolar, 'delimiter','t',
    'newline','pc', 'coffset', size(output_unipolar,2), '-
    append');

disp(sprintf('<a href="matlab: winopen("%s%s")">%s</a>', save_dir,
    savedfile, savedfile));

%% PLOT ACTIVATION TIMES WITH A RED DOT
k=1;
c = 1;
ecguni=compiled(:,2:129);
uniDerivative=Derivative(:,2:129);
for b = 1:size(ecguni,2)
    if mod(b,32)==0
        c = 32;
        subplot(4,8,c)
        plot(compiled(t1(k):t2(k)-1,1), ecguni(t1(k):t2(k)-1,b),'b-')
        hold on
        plot(
            ((AVdelay+index(b,k)+t1(k))*timeStep),ecguni((index(b,k)+AVdelay+t1(k))
            ,b),'rs',...
            'MarkerEdgeColor','r',...
            'MarkerFaceColor','r',...
            'MarkerSize',3)
        axis tight
        title(['elec ' num2str(b)])
        suptitle(filename)
        legend ('Raw Signal','Activation Time',...
            'orientation','horizontal', 'location',[.8 .94 .05 .03])
        c=1;
        filename = [num2str(date) '_' filename '.bmp'];
        saveas(gcf,filename,'bmp')
    end
end

```

```

elseif mod(b,32)==1
    filename=[ 'Unipolar Run ' num2str(i) ' Electrodes ' num2str(b) ' '
num2str(b+31) 'Analyze' num2str(beats) 'Beats'];
    figure('name',filename,'NumberTitle','off','Position',[0 0
fullscreen(3) fullscreen(4)])
    subplot(4,8,c)
    plot(compiled(t1(k):t2(k)-1,1), ecguni(t1(k):t2(k)-1,b),'b-')
    hold on
    plot(((AVdelay+index(b,k)+t1(k))*timeStep),ecguni((index(b,k)+
AVdelay+t1(k)),b),'rs',...
        'MarkerEdgeColor','r',...
        'MarkerFaceColor','r',...
        'MarkerSize',3)
    axis tight
    title(['elec ' num2str(b)])
    c=c+1;
else
    subplot(4,8,c)
    plot(compiled(t1(k):t2(k)-1,1), ecguni(t1(k):t2(k)-1,b),'b-')
    hold on
    plot(((AVdelay+index(b,k)+t1(k))*timeStep),ecguni((index(b,k)+
AVdelay+ t1(k)),b),'rs',...
        'MarkerEdgeColor','r',...
        'MarkerFaceColor','r',...
        'MarkerSize',3)
    axis tight
    title(['elec ' num2str(b)])
    c=c+1;
end
end
filename = [num2str(date) ' ' filename '.bmp'];
saveas(gcf,filename,'bmp')

%% omit electrodes that are noisy to make 2D contour plot
omit = input('What electrodes are noisy? (Format [A,B,C,...]): ');
new_at=zeros(size(AT,1)-size(omit,2),1);
if size(omit,2)==1
    new_at(1:omit(1)-1,1)=AT(1:omit(1)-1,1);
    new_at(omit(1):end,1)=AT(omit(1)+1:end,1);
elseif size(omit,2)==2
    new_at(1:omit(1)-1,1)=AT(1:omit(1)-1,1);
    new_at(omit(1):omit(2)-2,1)=AT(omit(1)+1:omit(2)-1,1);
    new_at(omit(2)-1:end,1)=AT(omit(1)+1:end,1);
elseif size(omit,2)==3
    new_at(1:omit(1)-1,1)=AT(1:omit(1)-1,1);
    new_at(omit(1):omit(2)-2,1)=AT(omit(1)+1:omit(2)-1,1);
    new_at(omit(2)-1:omit(3)-3,1)=AT(omit(2)+1:omit(3)-1,1);
    new_at(omit(3)-2:end)=AT(omit(3)+1:end,1);
end

%% 2D CONTOUR PLOT OF LOCAL ACTIVATION

eval(['Run' num2str(i) 'AT_one = AT(:,1);']);
eval(['Run' num2str(i) 'AT_mean=mean(AT,2);']);
eval(['Run' num2str(i) 'AT_filtered_one=AT_filtered(:,1);']);
eval(['Run' num2str(i) 'AT_filtered_mean=mean(AT_filtered,2);']);
eval(['Run' num2str(i) 'AT_bi_one=AT_bi(:,1);']);
eval(['Run' num2str(i) 'AT_bi_mean=mean(AT_bi,2);']);

```

```

AT_one=AT(:,1);
AT_mean=mean(AT,2);
AT_filtered_one=AT_filtered(:,1);
AT_filtered_mean=mean(AT_filtered,2);
AT_bi_one=AT_bi(:,1);
AT_bi_mean=mean(AT_bi,2);

for om=1:size(omit,1)
    AT_one(omit(om))=mean(AT_one);
    AT_mean(omit(om))=mean(AT_mean);
    AT_filtered_one(omit(om))=mean(AT_filtered_one);
    AT_filtered_mean(omit(om))=mean(AT_filtered_mean);
    AT_bi_one(omit(om))=mean(AT_bi_one);
    AT_bi_mean(omit(om))=mean(AT_bi_mean);
end

count=1;
for AT=[AT_one, AT_mean, AT_filtered_one, AT_filtered_mean];
    ATmatrix=zeros(6, 21);

    elements=[AT(39) AT(43) AT(46) AT(47)]; ATmatrix(6,1)=mean(elements);
    ATmatrix(5,1)=AT(39);
    ATmatrix(4,1)=AT(38);
    ATmatrix(3,1)=AT(35);
    ATmatrix(2,1)=AT(37);
    elements=[AT(31) AT(35) AT(36)]; ATmatrix(1,1)=mean(elements);

    ATmatrix(6,2)=AT(47);
    elements=[AT(43) AT(46)]; ATmatrix(5,2)=mean(elements);
    elements=[AT(42) AT(45)]; ATmatrix(4,2)=mean(elements);
    ATmatrix(3,2)=AT(41);
    ATmatrix(2,2)=AT(36);
    ATmatrix(1,2)=AT(35);

    elements=[AT(49) AT(54)]; ATmatrix(6,3)=mean(elements);
    ATmatrix(5,3)=AT(50);
    ATmatrix(4,3)=AT(51);
    ATmatrix(3,3)=AT(44);
    ATmatrix(2,3)=AT(40);
    ATmatrix(1,3)=AT(63);

    elements=[AT(56) AT(57)]; ATmatrix(6,4)=mean(elements);
    elements=[AT(53) AT(55)]; ATmatrix(5,4)=mean(elements);
    ATmatrix(4,4)=AT(52);
    ATmatrix(3,4)=AT(48);
    ATmatrix(2,4)=AT(58);
    elements=[AT(40) AT(58) AT(63)]; ATmatrix(1,4)=mean(elements);

    ATmatrix(6,5)=AT(60);
    ATmatrix(5,5)=AT(61);
    ATmatrix(4,5)=AT(62);
    ATmatrix(3,5)=AT(59);
    ATmatrix(2,5)=AT(64);
    elements=[AT(58) AT(64) AT(65) ATmatrix(1,4)];

```

```

ATmatrix(1,5)=mean(elements);

elements=[AT(60) AT(61) AT(70) AT(71) AT(72) AT(80)];
ATmatrix(6,6)=mean(elements);
elements=[AT(70) AT(71)]; ATmatrix(5,6)=mean(elements);
ATmatrix(4,6)=AT(69);
ATmatrix(3,6)=AT(68);
ATmatrix(2,6)=AT(65);
elements=[AT(64) AT(65) AT(67) AT(75) ATmatrix(1,5)];
ATmatrix(1,6)=mean(elements);

ATmatrix(6,7)=AT(72);
ATmatrix(5,7)=AT(80);
ATmatrix(4,7)=AT(79);
ATmatrix(3,7)=AT(78);
ATmatrix(2,7)=AT(75);
ATmatrix(1,7)=AT(67);

ATmatrix(6,8)=AT(87);
ATmatrix(5,8)=AT(86);
elements=[AT(83) AT(85)]; ATmatrix(4,8)=mean(elements);
elements=[AT(77) AT(82)]; ATmatrix(3,8)=mean(elements);
elements=[AT(74) AT(76)]; ATmatrix(2,8)=mean(elements);
ATmatrix(1,8)=AT(66);

ATmatrix(6,9)=AT(93);
ATmatrix(5,9)=AT(92);
ATmatrix(4,9)=AT(91);
ATmatrix(3,9)=AT(84);
ATmatrix(2,9)=AT(81);
ATmatrix(1,9)=AT(73);

ATmatrix(6,10)=AT(96);
ATmatrix(5,10)=AT(95);
ATmatrix(4,10)=AT(94);
ATmatrix(3,10)=AT(90);
ATmatrix(2,10)=AT(89);
ATmatrix(1,10)=AT(88);

ATmatrix(6,11)=AT(101);
ATmatrix(5,11)=AT(100);
ATmatrix(4,11)=AT(99);
ATmatrix(3,11)=AT(98);
ATmatrix(2,11)=AT(97);
ATmatrix(1,11)=AT(123);

ATmatrix(6,12)=AT(105);
ATmatrix(5,12)=AT(104);
ATmatrix(4,12)=AT(103);
ATmatrix(3,12)=AT(102);
elements=[AT(97) AT(98) AT(102) AT(106) AT(111) AT(112) AT(123)];
ATmatrix(2,12)=mean(elements);
elements=[ATmatrix(2,12) AT(97) AT(111) AT(123)];
ATmatrix(1,12)=mean(elements);

```

```

ATmatrix(6,13)=AT(109);
elements=[AT(108) AT(114)]; ATmatrix(5,13)=mean(elements);
elements=[AT(107) AT(113)]; ATmatrix(4,13)=mean(elements);
elements=[AT(106) AT(112)]; ATmatrix(3,13)=mean(elements);
ATmatrix(2,13)=AT(111);
elements=[ATmatrix(1,12) ATmatrix(2,12) AT(111)];
ATmatrix(1,13)=mean(elements);

```

```

ATmatrix(6,14)=AT(119);
ATmatrix(5,14)=AT(118);
ATmatrix(4,14)=AT(117);
ATmatrix(3,14)=AT(116);
elements=[ATmatrix(1,13) AT(110) AT(111) AT(115) AT(106) AT(112)
AT(116)]; ATmatrix(2,14)=mean(elements);
elements=[ATmatrix(1,13) ATmatrix(2,14) AT(110) AT(110) AT(111)];
ATmatrix(1,14)=mean(elements);

```

```

ATmatrix(6,15)=AT(122);
ATmatrix(5,15)=AT(121);
ATmatrix(4,15)=AT(120);
ATmatrix(3,15)=AT(115);
ATmatrix(2,15)=AT(110);
elements=[ATmatrix(1,14) ATmatrix(2,14) AT(110) AT(124)];
ATmatrix(1,15)=mean(elements);

```

```

ATmatrix(6,16)=AT(128);
ATmatrix(5,16)=AT(127);
ATmatrix(4,16)=AT(126);
ATmatrix(3,16)=AT(125);
ATmatrix(2,16)=AT(124);
elements=[AT(1) AT(2) AT(110) AT(124)]; ATmatrix(1,16)=mean(elements);

```

```

ATmatrix(6,17)=AT(7);
ATmatrix(5,17)=AT(6);
elements=[AT(4) AT(5)]; ATmatrix(4,17)=mean(elements);
ATmatrix(3,17)=AT(3);
ATmatrix(2,17)=AT(2);
ATmatrix(1,17)=AT(1);

```

```

ATmatrix(6,18)=AT(13);
ATmatrix(5,18)=AT(12);
ATmatrix(4,18)=AT(11);
ATmatrix(3,18)=AT(10);
ATmatrix(2,18)=AT(9);
ATmatrix(1,18)=AT(8);

```

```

elements=[AT(18) AT(19)]; ATmatrix(6,19)=mean(elements);
ATmatrix(5,19)=AT(17);
ATmatrix(4,19)=AT(16);
ATmatrix(3,19)=AT(15);
ATmatrix(2,19)=AT(14);
ATmatrix(1,19)=AT(20);

```

```

ATmatrix(6,20)=AT(25);

```

```

ATmatrix(5,20)=AT(24);
ATmatrix(4,20)=AT(23);
ATmatrix(3,20)=AT(22);
ATmatrix(2,20)=AT(21);
elements=[AT(14) AT(20) AT(21) AT(26)]; ATmatrix(1,20)=mean(elements);

ATmatrix(6,21)=AT(30);
elements=[AT(29) AT(34)]; ATmatrix(5,21)=mean(elements);
elements=[AT(28) AT(33)]; ATmatrix(4,21)=mean(elements);
elements=[AT(27) AT(32)]; ATmatrix(3,21)=mean(elements);
ATmatrix(2,21)=AT(26);
elements=[AT(21) AT(26) ATmatrix(1,20)]; ATmatrix(1,21)=mean(elements);

if count==1
    filename=['Run ' num2str(i) ' - AT one beat.bmp'];
elseif count==2
    filename=['Run ' num2str(i) ' - AT multiple beats.bmp'];
elseif count==3
    filename=['Run ' num2str(i) ' - AT filtered one beat.bmp'];
else
    filename=['Run ' num2str(i) ' - AT filtered multiple beats.bmp'];
end
figure('name',filename(1:end-4),'NumberTitle','off')
[C,h]=contourf(ATmatrix);
set(h,'ShowText','on','TextStep',get(h,'LevelStep')*1)
title(filename)
axis equal
axis tight
colorbar
caxis([0 100])
saveas(gcf,[save_dir filename], 'bmp')
count=count+1;
end

figure; trisurf(trin,elecsh(:,1),elecsh(:,2),elecsh(:,3),[AT_one])
title(['Run ' num2str(i) 'Unipolar Activation Times One Beat'])
colorbar
caxis([0 100])
axis equal
hold on
plot3(rotatedData(138:142,1), rotatedData(138:142,2),
rotatedData(138:142,3), 'k','LineWidth',20,...
'MarkerEdgeColor','k',...
'MarkerFaceColor','k',...
'MarkerSize',50)
text(rotatedData(138,1),rotatedData(138,2),rotatedData(138,3),'Pos CS')
text(rotatedData(139,1),rotatedData(139,2),rotatedData(139,3),'Ant. Near Infarct')
text(rotatedData(140,1),rotatedData(140,2),rotatedData(140,3),'Ant. 50% Remote')
text(rotatedData(141,1),rotatedData(141,2),rotatedData(141,3),'Ant. Remote')
text(rotatedData(142,1),rotatedData(142,2),rotatedData(142,3),'Bead Set')
plot3(rotatedData(305:380,1), rotatedData(305:380,2),
rotatedData(305:380,3), 'k','LineWidth',20,...
'MarkerEdgeColor','k',...
'MarkerFaceColor','k',...
'MarkerSize',20);
text(rotatedData(380,1),rotatedData(380,2),rotatedData(380,3),'LAD')

```

```

figure; trisurf(trin,elecsh(:,1),elecsh(:,2),elecsh(:,3),[AT_mean])
title(['Run ' num2str(i) 'Unipolar Activation Times Multiple Beats'])
colorbar
caxis([0 100])
axis equal
hold on
plot3(rotatedData(138:142,1), rotatedData(138:142,2),
rotatedData(138:142,3), 'k','LineWidth',20,...
'MarkerEdgeColor','k',...
'MarkerFaceColor','k',...
'MarkerSize',50)
text(rotatedData(138,1),rotatedData(138,2),rotatedData(138,3),'Pos CS')
text(rotatedData(139,1),rotatedData(139,2),rotatedData(139,3),'Ant. Near
Infarct')
text(rotatedData(140,1),rotatedData(140,2),rotatedData(140,3),'Ant. 50%
Remote')
text(rotatedData(141,1),rotatedData(141,2),rotatedData(141,3),'Ant.
Remote')
text(rotatedData(142,1),rotatedData(142,2),rotatedData(142,3),'Bead Set')
plot3(rotatedData(305:380,1), rotatedData(305:380,2),
rotatedData(305:380,3), 'k','LineWidth',20,...
'MarkerEdgeColor','k',...
'MarkerFaceColor','k',...
'MarkerSize',20);
text(rotatedData(380,1),rotatedData(380,2),rotatedData(380,3),'LAD')

```

```

figure; trisurf(trib,elecbi(:,1),elecbi(:,2),elecbi(:,3),[0; AT_bi_one])
title(['Run ' num2str(i) 'Bipolar Activation Times One Beat'])
colorbar
caxis([0 100])
axis equal
hold on
plot3(rotatedData(138:142,1), rotatedData(138:142,2),
rotatedData(138:142,3), 'k','LineWidth',20,...
'MarkerEdgeColor','k',...
'MarkerFaceColor','k',...
'MarkerSize',50)
text(rotatedData(138,1),rotatedData(138,2),rotatedData(138,3),'Pos CS')
text(rotatedData(139,1),rotatedData(139,2),rotatedData(139,3),'Ant. Near
Infarct')
text(rotatedData(140,1),rotatedData(140,2),rotatedData(140,3),'Ant. 50%
Remote')
text(rotatedData(141,1),rotatedData(141,2),rotatedData(141,3),'Ant.
Remote')
text(rotatedData(142,1),rotatedData(142,2),rotatedData(142,3),'Bead Set')
plot3(rotatedData(305:380,1), rotatedData(305:380,2),
rotatedData(305:380,3), 'k','LineWidth',20,...
'MarkerEdgeColor','k',...
'MarkerFaceColor','k',...
'MarkerSize',20);
text(rotatedData(380,1),rotatedData(380,2),rotatedData(380,3),'LAD')

```

```

figure; trisurf(trib,elecbi(:,1),elecbi(:,2),elecbi(:,3),[0; AT_bi_mean])
title(['Run ' num2str(i) 'Bipolar Activation Times Multiple Beats'])
colorbar
caxis([0 100])
axis equal
hold on
plot3(rotatedData(138:142,1), rotatedData(138:142,2),

```



```

rotatedData(138:142,3), 'k','LineWidth',20,...
    'MarkerEdgeColor','k',...
    'MarkerFaceColor','k',...
    'MarkerSize',50)
text(rotatedData(138,1),rotatedData(138,2),rotatedData(138,3),'Pos CS')
text(rotatedData(139,1),rotatedData(139,2),rotatedData(139,3),'Ant. Near
Infarct')
text(rotatedData(140,1),rotatedData(140,2),rotatedData(140,3),'Ant. 50%
Remote')
text(rotatedData(141,1),rotatedData(141,2),rotatedData(141,3),'Ant.
Remote')
text(rotatedData(142,1),rotatedData(142,2),rotatedData(142,3),'Bead Set')
plot3(rotatedData(305:380,1), rotatedData(305:380,2),
rotatedData(305:380,3), 'k','LineWidth',20,...
    'MarkerEdgeColor','k',...
    'MarkerFaceColor','k',...
    'MarkerSize',20);
text(rotatedData(380,1),rotatedData(380,2),rotatedData(380,3),'LAD')

run_count=run_count+1;
end

disp(sprintf('Location of saved files: <a href="matlab: winopen("%s")">%s</a>', save_dir,save_dir))
coord_weights = 1 * ones(length(rotatedData),1);

AT='AT_one';
clear continuity_output
continuity_output = [rotatedData(:,1), coord_weights, rotatedData(:,1), coord_weights, rotatedData(:,1),
coord_weights];
for i=runs_to_analyze
continuity_output = [continuity_output, ...
    [eval(['Run' num2str(i) AT]); mean(eval(['Run' num2str(i) AT])) *
    ones(length(rotatedData)-length(eval(AT)),1) ], ...
    [1 * ones(length(eval(AT)),1); 0.001 * ones(length(rotatedData)-
length(eval(AT)),1) ]];
end
filename=[AT '.txt'];
dlmwrite([save_dir filename], continuity_output, 'delimiter','\t', 'newline','pc')
disp(sprintf('<a href="matlab: winopen("%s%s")">%s</a>', save_dir, filename, filename));

AT='AT_mean';
clear continuity_output
continuity_output = [rotatedData(:,1), coord_weights, rotatedData(:,1), coord_weights, rotatedData(:,1),
coord_weights];
for i=runs_to_analyze
    continuity_output = [continuity_output, ...
    [eval(['Run' num2str(i) AT]); mean(eval(['Run' num2str(i) AT])) *
    ones(length(rotatedData)-length(eval(AT)),1) ], ...
    [1 * ones(length(eval(AT)),1); 0.001 * ones(length(rotatedData)-
length(eval(AT)),1) ]];
end
filename=[AT '.txt'];
dlmwrite([save_dir filename], continuity_output, 'delimiter','\t', 'newline','pc')
disp(sprintf('<a href="matlab: winopen("%s%s")">%s</a>', save_dir, filename, filename));

AT='AT_filtered_one';
clear continuity_output

```

```

continuity_output = [rotatedData(:,1), coord_weights, rotatedData(:,1), coord_weights, rotatedData(:,1),
coord_weights];
for i=runs_to_analyze
    continuity_output = [continuity_output, ...
    [eval(['Run' num2str(i) AT]); mean(eval(['Run' num2str(i) AT])) *
    ones(length(rotatedData)-length(eval(AT)),1) ], ...
    [1 * ones(length(eval(AT)),1); 0.001 * ones(length(rotatedData)-
length(eval(AT)),1) ]];
end
filename=[AT '.txt'];
dlmwrite([save_dir filename], continuity_output, 'delimiter','\t', 'newline','pc')
disp(sprintf('<a href="matlab: winopen("%s%s")">%s</a>', save_dir, filename, filename));

AT='AT_filtered_mean';
clear continuity_output
continuity_output = [rotatedData(:,1), coord_weights, rotatedData(:,1), coord_weights, rotatedData(:,1),
coord_weights];
for i=runs_to_analyze
    continuity_output = [continuity_output, ...
    [eval(['Run' num2str(i) AT]); mean(eval(['Run' num2str(i) AT])) *
    ones(length(rotatedData)-length(eval(AT)),1) ], ...
    [1 * ones(length(eval(AT)),1); 0.001 * ones(length(rotatedData)-
length(eval(AT)),1) ]];
end
filename=[AT '.txt'];
dlmwrite([save_dir filename], continuity_output, 'delimiter','\t', 'newline','pc')
disp(sprintf('<a href="matlab: winopen("%s%s")">%s</a>', save_dir, filename, filename)

```

## REFERENCES

1. Katz, A.M., *Physiology of the heart*. 2001, Lippincott Williams & Wilkins: Philadelphia, PA.
2. LeGrice, I.J., B.H. Smaill, L.Z. Chai, S.G. Edgar, J.B. Gavin, and P.J. Hunter, *Laminar structure of the heart: ventricular myocyte arrangement and connective tissue architecture in the dog*. *Am J Physiol*, 1995. **269**(2 Pt 2): p. H571-82.
3. Scollan, D.F., A. Holmes, J. Zhang, and R.L. Winslow, *Reconstruction of cardiac ventricular geometry and fiber orientation using magnetic resonance imaging*. *Ann Biomed Eng*, 2000. **28**(8): p. 934-44.
4. Streeter, D.D., Jr., R.N. Vaishnav, D.J. Patel, H.M. Spotnitz, J. Ross, Jr., and E.H. Sonnenblick, *Stress distribution in the canine left ventricle during diastole and systole*. *Biophys J*, 1970. **10**(4): p. 345-63.
5. Streeter, D.D., Jr. and W.T. Hanna, *Engineering mechanics for successive states in canine left ventricular myocardium. II. Fiber angle and sarcomere length*. *Circ Res*, 1973. **33**(6): p. 656-64.
6. Ross, A.A. and D.D. Streeter, Jr., *Myocardial fiber disarray*. *Circulation*, 1979. **60**(6): p. 1425-6.
7. Lloyd-Jones, D., R. Adams, M. Carnethon, G. De Simone, T.B. Ferguson, K. Flegal, E. Ford, K. Furie, A. Go, K. Greenlund, N. Haase, S. Hailpern, M. Ho, V. Howard, B. Kissela, S. Kittner, D. Lackland, L. Lisabeth, A. Marelli, M. McDermott, J. Meigs, D. Mozaffarian, G. Nichol, C. O'Donnell, V. Roger, W. Rosamond, R. Sacco, P. Sorlie, R. Stafford, J. Steinberger, T. Thom, S. Wasserthiel-Smoller, N. Wong, J. Wylie-Rosett, and Y. Hong, *Heart disease and stroke statistics--2009 update: a report from the American Heart Association Statistics Committee and Stroke Statistics Subcommittee*. *Circulation*, 2009. **119**(3): p. 480-6.
8. Lloyd-Jones, D.M., M.G. Larson, E.P. Leip, A. Beiser, R.B. D'Agostino, W.B. Kannel, J.M. Murabito, R.S. Vasan, E.J. Benjamin, and D. Levy, *Lifetime risk for developing congestive heart failure: the Framingham Heart Study*. *Circulation*, 2002. **106**(24): p. 3068-72.

9. Lloyd-Jones, D., R.J. Adams, T.M. Brown, M. Carnethon, S. Dai, G. De Simone, T.B. Ferguson, E. Ford, K. Furie, C. Gillespie, A. Go, K. Greenlund, N. Haase, S. Hailpern, P.M. Ho, V. Howard, B. Kissela, S. Kittner, D. Lackland, L. Lisabeth, A. Marelli, M.M. McDermott, J. Meigs, D. Mozaffarian, M. Mussolino, G. Nichol, V.L. Roger, W. Rosamond, R. Sacco, P. Sorlie, T. Thom, S. Wasserthiel-Smoller, N.D. Wong, and J. Wylie-Rosett, *Heart disease and stroke statistics--2010 update: a report from the American Heart Association*. *Circulation*, 2010. **121**(7): p. e46-e215.
10. McMurray, J.J. and M.A. Pfeffer, *Heart failure*. *Lancet*, 2005. **365**(9474): p. 1877-89.
11. Athanasopoulos, L.V., A. Dritsas, H.A. Doll, and D.V. Cokkinos, *Comparative value of NYHA functional class and quality-of-life questionnaire scores in assessing heart failure*. *J Cardiopulm Rehabil Prev*, 2010. **30**(2): p. 101-5.
12. Rose, E.A., A.C. Gelijns, A.J. Moskowitz, D.F. Heitjan, L.W. Stevenson, W. Dembitsky, J.W. Long, D.D. Ascheim, A.R. Tierney, R.G. Levitan, J.T. Watson, P. Meier, N.S. Ronan, P.A. Shapiro, R.M. Lazar, L.W. Miller, L. Gupta, O.H. Frazier, P. Desvigne-Nickens, M.C. Oz, and V.L. Poirier, *Long-term mechanical left ventricular assistance for end-stage heart failure*. *N Engl J Med*, 2001. **345**(20): p. 1435-43.
13. Buxton, A.E., K.L. Lee, J.D. Fisher, M.E. Josephson, E.N. Prystowsky, and G. Hafley, *A randomized study of the prevention of sudden death in patients with coronary artery disease. Multicenter Unsustained Tachycardia Trial Investigators*. *N Engl J Med*, 1999. **341**(25): p. 1882-90.
14. Moss, A.J., W. Zareba, W.J. Hall, H. Klein, D.J. Wilber, D.S. Cannom, J.P. Daubert, S.L. Higgins, M.W. Brown, and M.L. Andrews, *Prophylactic implantation of a defibrillator in patients with myocardial infarction and reduced ejection fraction*. *N Engl J Med*, 2002. **346**(12): p. 877-83.
15. McMurray, J., A. Cohen-Solal, R. Dietz, E. Eichhorn, L. Erhardt, F.D. Hobbs, H. Krum, A. Maggioni, R.S. McKelvie, I.L. Pina, J. Soler-Soler, and K. Swedberg, *Practical recommendations for the use of ACE inhibitors, beta-blockers, aldosterone antagonists and angiotensin receptor blockers in heart failure: putting guidelines into practice*. *Eur J Heart Fail*, 2005. **7**(5): p. 710-21.
16. *Effects of enalapril on mortality in severe congestive heart failure. Results of the Cooperative North Scandinavian Enalapril Survival Study (CONSENSUS). The CONSENSUS Trial Study Group*. *N Engl J Med*, 1987. **316**(23): p. 1429-35.

17. *Effect of enalapril on survival in patients with reduced left ventricular ejection fractions and congestive heart failure. The SOLVD Investigators.* N Engl J Med, 1991. **325**(5): p. 293-302.
18. Auricchio, A., C. Stellbrink, S. Sack, M. Block, J. Vogt, P. Bakker, C. Huth, F. Schondube, U. Wolfhard, D. Bocker, O. Krahnfeld, and H. Kirkels, *Long-term clinical effect of hemodynamically optimized cardiac resynchronization therapy in patients with heart failure and ventricular conduction delay.* J Am Coll Cardiol, 2002. **39**(12): p. 2026-33.
19. Abraham, W.T., W.G. Fisher, A.L. Smith, D.B. Delurgio, A.R. Leon, E. Loh, D.Z. Kocovic, M. Packer, A.L. Clavell, D.L. Hayes, M. Ellestad, R.J. Trupp, J. Underwood, F. Pickering, C. Truex, P. McAtee, and J. Messenger, *Cardiac resynchronization in chronic heart failure.* N Engl J Med, 2002. **346**(24): p. 1845-53.
20. Cazeau, S., C. Leclercq, T. Lavergne, S. Walker, C. Varma, C. Linde, S. Garrigue, L. Kappenberger, G.A. Haywood, M. Santini, C. Bailleul, and J.C. Daubert, *Effects of multisite biventricular pacing in patients with heart failure and intraventricular conduction delay.* N Engl J Med, 2001. **344**(12): p. 873-80.
21. Abraham, W.T., *Cardiac resynchronization therapy for the management of chronic heart failure.* Am Heart Hosp J, 2003. **1**(1): p. 55-61.
22. Young, J.B., W.T. Abraham, A.L. Smith, A.R. Leon, R. Lieberman, B. Wilkoff, R.C. Canby, J.S. Schroeder, L.B. Liem, S. Hall, and K. Wheelan, *Combined cardiac resynchronization and implantable cardioversion defibrillation in advanced chronic heart failure: the MIRACLE ICD Trial.* JAMA, 2003. **289**(20): p. 2685-94.
23. Bax, J.J., E.E. Van der Wall, and M.J. Schalij, *Cardiac resynchronization therapy for heart failure.* N Engl J Med, 2002. **347**(22): p. 1803-4; author reply 1803-4.
24. Bax, J.J., G.B. Bleeker, T.H. Marwick, S.G. Molhoek, E. Boersma, P. Steendijk, E.E. van der Wall, and M.J. Schalij, *Left ventricular dyssynchrony predicts response and prognosis after cardiac resynchronization therapy.* J Am Coll Cardiol, 2004. **44**(9): p. 1834-40.
25. Achilli, A., M. Sassara, S. Ficili, D. Pontillo, P. Achilli, C. Alessi, S. De Spirito, R. Guerra, N. Patruno, and F. Serra, *Long-term effectiveness of cardiac resynchronization therapy in patients with refractory heart failure and "narrow" QRS.* J Am Coll Cardiol, 2003. **42**(12): p. 2117-24.

26. Mollema, S.A., G.B. Bleeker, E.E. van der Wall, M.J. Schalij, and J.J. Bax, *Usefulness of QRS duration to predict response to cardiac resynchronization therapy in patients with end-stage heart failure*. Am J Cardiol, 2007. **100**(11): p. 1665-70.
27. Lambiase, P.D., A. Rinaldi, J. Hauck, M. Mobb, D. Elliott, S. Mohammad, J.S. Gill, and C.A. Bucknall, *Non-contact left ventricular endocardial mapping in cardiac resynchronisation therapy*. Heart, 2004. **90**(1): p. 44-51.
28. Garrigue, S., P. Jais, G. Espil, J.N. Labeque, M. Hocini, D.C. Shah, M. Haissaguerre, and J. Clementy, *Comparison of chronic biventricular pacing between epicardial and endocardial left ventricular stimulation using Doppler tissue imaging in patients with heart failure*. Am J Cardiol, 2001. **88**(8): p. 858-62.
29. Abendroth, R.R., J. Ostermeyer, G. Breithardt, L. Seipel, and W. Bircks, *Reproducibility of local activation times during intraoperative epicardial mapping*. Circulation, 1980. **62**(1): p. 75-9.
30. Durrer, D. and L.H. Van Der Tweel, *Spread of activation in the left ventricular wall of the dog. II. Activation conditions at the epicardial surface*. Am Heart J, 1954. **47**(2): p. 192-203.
31. Durrer, D. and L.H. Van Der Tweel, *Excitation of the left ventricular wall of the dog and goat*. Ann N Y Acad Sci, 1957. **65**(6): p. 779-803.
32. Paul, T., J.P. Moak, C. Morris, and A. Garson, Jr., *Epicardial mapping: how to measure local activation?* Pacing Clin Electrophysiol, 1990. **13**(3): p. 285-92.
33. Spach, M.S. and R.C. Barr, *Ventricular intramural and epicardial potential distributions during ventricular activation and repolarization in the intact dog*. Circ Res, 1975. **37**(2): p. 243-57.
34. Koor, P., M. Daly, J. Pouliopoulos, V. Eipper, B. Dewsnap, and D.L. Ross, *Comparison of unipolar versus bipolar ablation and single electrode control versus simultaneous multielectrode temperature control*. J Interv Card Electrophysiol, 2007. **19**(2): p. 85-93.
35. Taccardi, B., B.B. Punske, E. Macchi, R.S. Macleod, and P.R. Ershler, *Epicardial and intramural excitation during ventricular pacing: effect of myocardial structure*. Am J Physiol Heart Circ Physiol, 2008. **294**(4): p. H1753-66.

36. Ndrepepa, G., E.B. Caref, H. Yin, N. el-Sherif, and M. Restivo, *Activation time determination by high-resolution unipolar and bipolar extracellular electrograms in the canine heart*. J Cardiovasc Electrophysiol, 1995. **6**(3): p. 174-88.
37. Ideker, R.E., W.M. Smith, S.M. Blanchard, S.L. Reiser, E.V. Simpson, P.D. Wolf, and N.D. Danieleley, *The assumptions of isochronal cardiac mapping*. Pacing Clin Electrophysiol, 1989. **12**(3): p. 456-78.
38. Sevaptisidis, E., S. Masse, I.D. Parson, E. Downar, and S. Kimber, *Simultaneous unipolar and bipolar recording of cardiac electrical activity*. Pacing Clin Electrophysiol, 1992. **15**(1): p. 45-51.
39. Gallagher, J.J., J. Kasell, W.C. Sealy, E.L. Pritchett, and A.G. Wallace, *Epicardial mapping in the Wolff-Parkinson-White syndrome*. Circulation, 1978. **57**(5): p. 854-66.
40. de Bakker, J.M., M.J. Janse, F.J. van Capelle, and D. Durrer, *An interactive computer system for guiding the surgical treatment of life-threatening ventricular tachycardias*. IEEE Trans Biomed Eng, 1984. **31**(4): p. 362-8.
41. Downar, E., L. Harris, L.L. Mickleborough, N. Shaikh, and I.D. Parson, *Endocardial mapping of ventricular tachycardia in the intact human ventricle: evidence for reentrant mechanisms*. J Am Coll Cardiol, 1988. **11**(4): p. 783-91.
42. de Bakker, J.M., F.J. van Capelle, M.J. Janse, A.A. Wilde, R. Coronel, A.E. Becker, K.P. Dingemans, N.M. van Hemel, and R.N. Hauer, *Reentry as a cause of ventricular tachycardia in patients with chronic ischemic heart disease: electrophysiologic and anatomic correlation*. Circulation, 1988. **77**(3): p. 589-606.
43. Janse, M.J., F.J. van Capelle, H. Morsink, A.G. Kleber, F. Wilms-Schopman, R. Cardinal, C.N. d'Alnoncourt, and D. Durrer, *Flow of "injury" current and patterns of excitation during early ventricular arrhythmias in acute regional myocardial ischemia in isolated porcine and canine hearts. Evidence for two different arrhythmogenic mechanisms*. Circ Res, 1980. **47**(2): p. 151-65.
44. El-Sherif, N., R.A. Smith, and K. Evans, *Canine ventricular arrhythmias in the late myocardial infarction period. 8. Epicardial mapping of reentrant circuits*. Circ Res, 1981. **49**(1): p. 255-65.
45. Restivo, M., W.B. Gough, and N. el-Sherif, *Ventricular arrhythmias in the subacute myocardial infarction period. High-resolution activation and refractory patterns of reentrant rhythms*. Circ Res, 1990. **66**(5): p. 1310-27.
46. Chen, P.S., P.D. Wolf, S.D. Melnick, N.D. Danieleley, W.M. Smith, and R.E. Ideker, *Comparison of activation during ventricular fibrillation and following*

- unsuccessful defibrillation shocks in open-chest dogs.* Circ Res, 1990. **66**(6): p. 1544-60.
47. Boineau, J.P., E.N. Moore, W.C. Sealy, and J.H. Kasell, *Epicardial mapping in Wolff-Parkinson-White syndrome.* Arch Intern Med, 1975. **135**(3): p. 422-31.
  48. Lin, G., N.S. Anavekar, T.L. Webster, R.F. Rea, D.L. Hayes, and P.A. Brady, *Long-term stability of endocardial left ventricular pacing leads placed via the coronary sinus.* Pacing Clin Electrophysiol, 2009. **32**(9): p. 1117-22.
  49. Bracke, F.A., P. Houthuizen, B.M. Rahel, and B.M. van Gelder, *Left ventricular endocardial pacing improves the clinical efficacy in a non-responder to cardiac resynchronization therapy: role of acute haemodynamic testing.* Europace, 2010.
  50. van Deursen, C., I.E. van Geldorp, L.M. Rademakers, A. van Hunnik, M. Kuiper, C. Klersy, A. Auricchio, and F.W. Prinzen, *Left ventricular endocardial pacing improves resynchronization therapy in canine left bundle-branch hearts.* Circ Arrhythm Electrophysiol, 2009. **2**(5): p. 580-7.
  51. Morina-Vazquez, P., R. Barba-Pichardo, J.V. Gamero, and J.M. Fernandez-Gomez, *Implantation via the femoral vein of a biventricular defibrillator with transseptal endocardial left ventricular pacing.* Rev Esp Cardiol, 2009. **62**(12): p. 1503-5.
  52. Igor R. Efimov, M.W.K., Patrick J. Tchou, *Cardiac Bioelectric Therapy: Mechanisms and Practical Implications* 2009: Springer Science + Business Media, LLC.
  53. Fenoglio, J.J., Jr., H.S. Karagueuzian, P.L. Friedman, A. Albala, and A.L. Wit, *Time course of infarct growth toward the endocardium after coronary occlusion.* Am J Physiol, 1979. **236**(2): p. H356-70.